

Three-dimensional surface imaging in pectus excavatum

Citation for published version (APA):

Daemen, J. H. T. (2023). *Three-dimensional surface imaging in pectus excavatum*. [Doctoral Thesis, Maastricht University]. Maastricht University. <https://doi.org/10.26481/dis.20230512jd>

Document status and date:

Published: 01/01/2023

DOI:

[10.26481/dis.20230512jd](https://doi.org/10.26481/dis.20230512jd)

Document Version:

Publisher's PDF, also known as Version of record

Please check the document version of this publication:

- A submitted manuscript is the version of the article upon submission and before peer-review. There can be important differences between the submitted version and the official published version of record. People interested in the research are advised to contact the author for the final version of the publication, or visit the DOI to the publisher's website.
- The final author version and the galley proof are versions of the publication after peer review.
- The final published version features the final layout of the paper including the volume, issue and page numbers.

[Link to publication](#)

General rights

Copyright and moral rights for the publications made accessible in the public portal are retained by the authors and/or other copyright owners and it is a condition of accessing publications that users recognise and abide by the legal requirements associated with these rights.

- Users may download and print one copy of any publication from the public portal for the purpose of private study or research.
- You may not further distribute the material or use it for any profit-making activity or commercial gain
- You may freely distribute the URL identifying the publication in the public portal.

If the publication is distributed under the terms of Article 25fa of the Dutch Copyright Act, indicated by the "Taverne" license above, please follow below link for the End User Agreement:

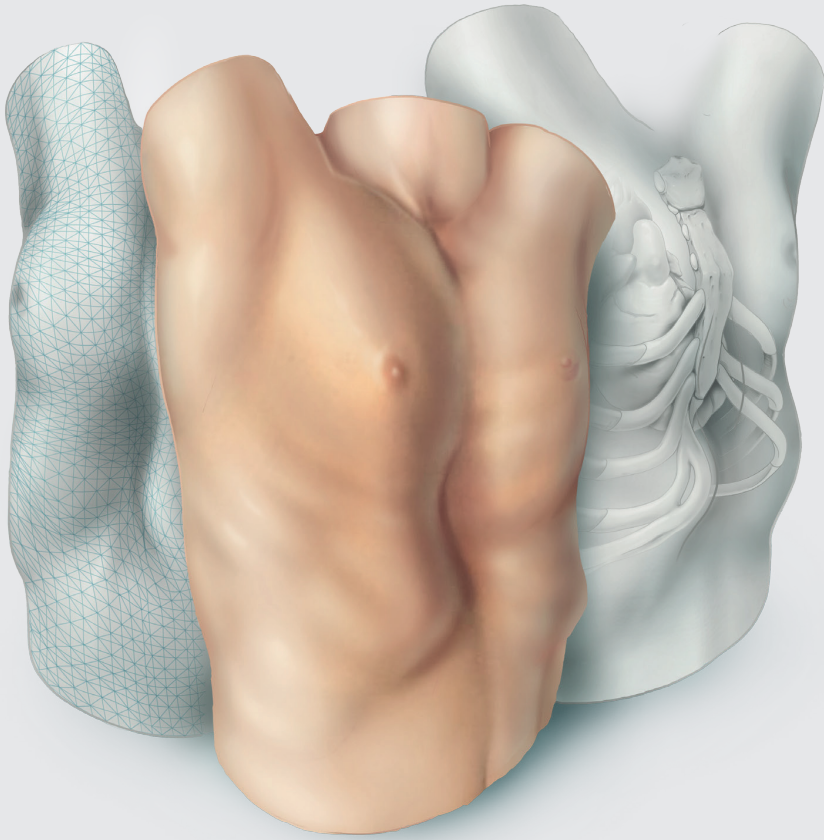
www.umlib.nl/taverne-license

Take down policy

If you believe that this document breaches copyright please contact us at:

repository@maastrichtuniversity.nl

providing details and we will investigate your claim.



THREE-DIMENSIONAL SURFACE IMAGING IN PECTUS EXCAVATUM

Jean H.T. Daemen

THREE-DIMENSIONAL SURFACE IMAGING IN PECTUS EXCAVATUM

- Jean H.T. Daemen -

Publication of this thesis was financially supported by:



© Jean Hubertus Theresia Daemen, Maastricht, the Netherlands, 2023

Three-dimensional Surface Imaging in Pectus Excavatum

Thesis, Maastricht University, the Netherlands

No part of this book may be reproduced or transmitted in any form or by any means, without prior permission in writing by the author, or when appropriate, by the publishers of the publications.

Cover design:

Stephanie Philippaerts | Medical-illustration

Lay-out:

Publiss | www.publiss.nl

Print:

Ridderprint | www.ridderprint.nl

ISBN:

978-94-6483-063-7

Three-dimensional Surface Imaging in Pectus Excavatum

Proefschrift

Ter verkrijging van de graad van doctor aan de Universiteit Maastricht,
op gezag van Rector Magnificus, Prof. dr. Pamela Habibović,
volgens besluit van het College van Decanen,
in het openbaar te verdedigen op vrijdag 12 mei 2023 om 13:00 uur.

Door

Jean Hubertus Theresia Daemen

Geboren op 18 april 1992 te Puth

Promotor:

Prof. dr. J.G. Maessen

Co-promotoren:

Dr. E.R. de Loos (Zuyderland Medisch Centrum)

Dr. Y.L.J. Vissers (Zuyderland Medisch Centrum)

Beoordelingscommissie:

Prof. dr. L.P.S. Stassen (voorzitter)

Prof. dr. W. Morshuis (Radboud Universitair Medisch Centrum)

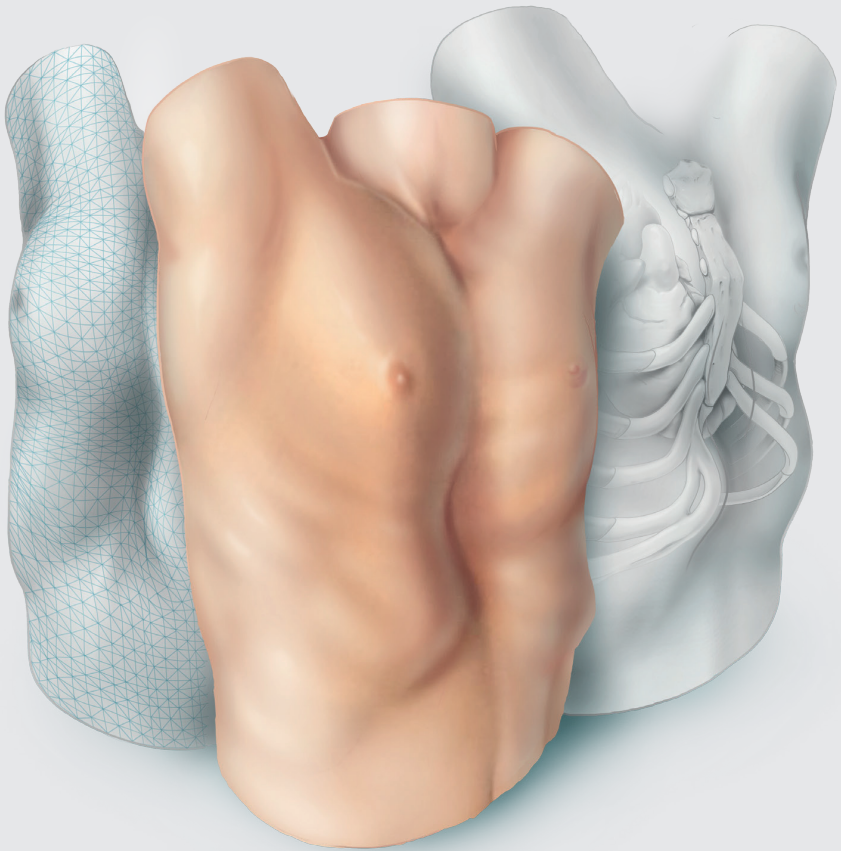
Prof. dr. S.G.F. Robben

Prof. dr. C. Slump (Universiteit Twente)

Dr. P. Sardari Nia

Contents

Chapter 1	Introduction	7
Chapter 2	Optical imaging versus CT and plain radiography to quantify pectus severity: a systematic review and meta-analysis	23
Chapter 3	Photographic documentation and severity quantification of pectus excavatum through three-dimensional optical surface imaging	53
Chapter 4	Three-dimensional imaging of the chest wall: a comparison between three different imaging systems	69
Chapter 5	Three-dimensional surface imaging for clinical decision making in pectus excavatum	89
Chapter 6	Development of a prediction model for cardiac compression in pectus excavatum based on three-dimensional surface images	111
Chapter 7	Visual diagnosis of pectus excavatum: an inter-observer and intra-observer agreement analysis	135
Chapter 8	General discussion	155
Chapter 9	Summary Samenvatting	168 171
Chapter 10	Impact paragraph	175
Chapter 11	Dankwoord	181
Chapter 12	Curriculum vitae List of publications	194 196





Introduction

General introduction

Pectus excavatum is considered the most common congenital anterior chest wall deformity, comprising 90% of all morphological chest wall abnormalities [1]. The characterizing posterior displacement of the sternum and adjacent costal cartilage affects 1 in 400 newborns (i.e., birth prevalence) [2] with an estimated worldwide incidence of 1 to 8 per 1000 persons [3]. Pectus excavatum predominantly affects the male sex with a male-female ratio ranging from 2:1 to 9:1 [3] and is less common among African Americans, Hispanics, and Asians than Caucasians [4, 5]. Yet, there is no direct racial predisposition. The exact etiopathogenetic mechanism is still unknown. The current leading hypotheses focus on two etiologies, namely: growth disturbances of sternocostal cartilage or costae [6-9] and metabolic chondrocyte abnormalities of the sternocostal cartilage, resulting in biomechanical weakness [10, 11]. Next to the developmental and metabolic theory there is the genetic theory. A positive family history is present in approximately 45% of patients [12, 13] and several potential genes such as GAL3ST4, ADGRG6 and those on chromosome 18q have been identified [14-16], however, no direct genetic linkage has yet been found.

Despite generally being considered congenital, pectus excavatum is only present in one-third of patients during infancy [17] and becomes apparent prior to puberty in the rest. In addition, the deformity becomes more pronounced in one-third of patients during the growth spurt, while the remaining two-thirds show no progression [18, 19].

The clinical presentation of pectus excavatum is diverse, ranging from no symptoms to physical and psychological distress. The most frequently perceived physical complaints include exercise intolerance, exertional dyspnea and chest pain or tightness [20-23]. Associated diseases include scoliosis [24, 25] and connective tissue disorders, such as Marfan syndrome [26, 27]. Up to 90% suffer from an impaired body image [20, 28].

The morphology of pectus excavatum is as diverse as its symptomatology and differs from case to case. The most common phenotype is a right-sided localized symmetric (i.e., cup-shaped; see Figure 1A) depression involving the mid to lower sternum and adjoining costal cartilage. Morphological variants include an asymmetrical form, anterior protrusion of the inferior costal cartilage (also known as winging or flaring; see Figure 1B), a long trench-like depression (see Figure 1C), a diffuse saucer-like depression (see Figure 1D), or a combination of the aforementioned [29, 30].

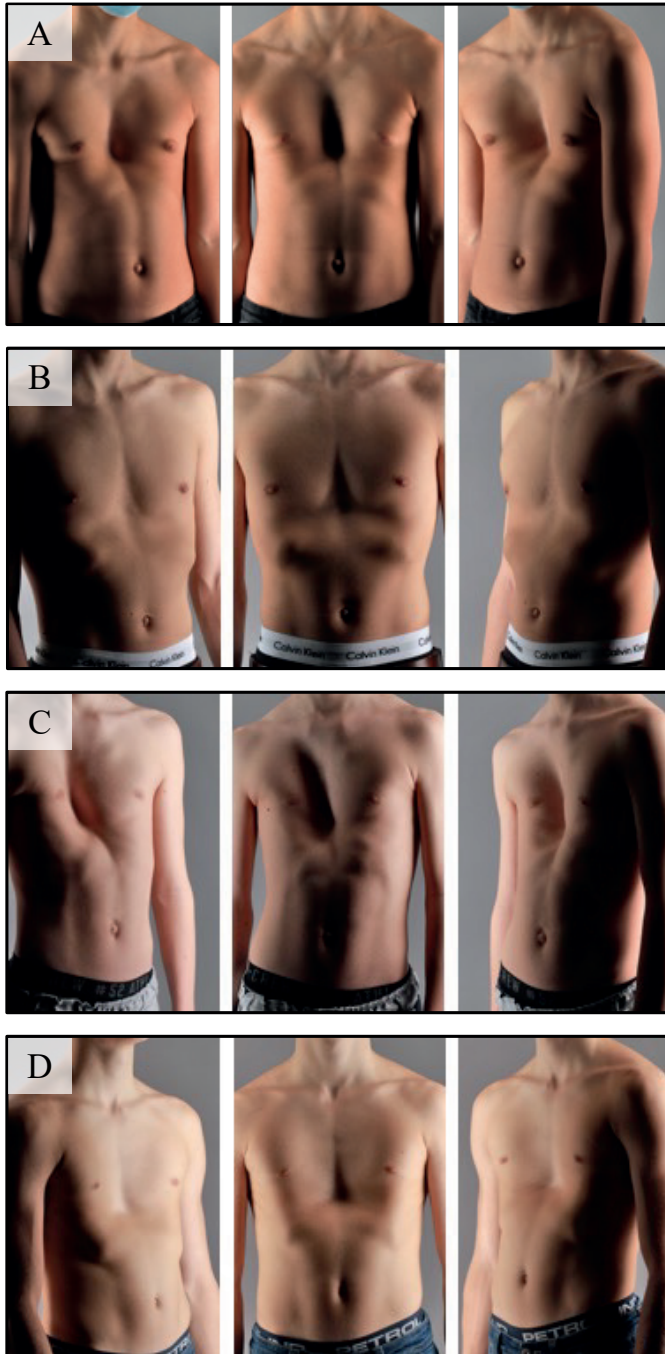


Figure 1: Different phenotypes of pectus excavatum. (A) Cup-shaped. (B) Pectus excavatum with flaring. (C) Trench-like depression. (D) Saucer-shaped.

A brief review of history

The first relief of a man with as it would appear pectus excavatum originates from the Old Kingdom of Egypt, dating back to 2400 Before Christ [31]. Pectus excavatum was also discovered in portraits made by famous painters like Leonardo da Vinci as early as 1510 [32]. Yet, the first documented writing of pectus excavatum originates from 1594 [33] and was not described as a medical condition until 1870 by Eggel. He published a case report describing a male suffering from a funnel-formed thoracic depression, referred to as *miraculum naturae*. It was at the time assumed to be caused by abnormal sternal weakness and flexibility due to developmental or nutritional disturbances [34]. Early treatment was limited to lying in the lateral position, fresh air, breathing exercises and aerobic activities [35]. In 1911, the first surgical correction was attempted by Meyer, resecting the costal cartilage of costae two and three. However, no improvement of the deformity was observed [36]. Sauerbruch was the first one to perform repair through bilateral costal cartilage resection and sternal osteotomy where-after external traction was applied for 6 weeks [37]. This technique was later popularized by Ravitch who advocated more radical sternal mobilization (i.e., transection of all sternal attachments, encompassing the rectus abdominus muscles, intercostal neurovascular bundles, diaphragmatic attachments, and resection of the xiphoid process) without external traction [38]. Over time, the technique proposed by Ravitch was modified by many surgeons and became the most common treatment option for pectus excavatum, currently known as the modified Ravitch procedure. In 1986, Nuss was struck by the flexibility and malleability of the costochondral structures and subsequently attempted to correct the deformity by a substernal titanium bar. The bar instantaneously corrected the deformity, however, its effect lessened over time due to poor mechanical bar characteristics [39]. With time, many modifications have been made (e.g., thoroscopic guidance and stabilizers) [40, 41] and the technique, known as the Nuss procedure, rapidly gained wide acceptance. In our institution (Zuyderland Medical Center, Heerlen, the Netherlands) the ratio between the Nuss and modified Ravitch procedure is 5:1 (based on unpublished data of all surgical corrections between 2007 and 2018) while Zuidema and colleagues reported a ratio of approximately 1:2 in 2013 in the Netherlands [42].

Preoperative evaluation

Pectus excavatum is a clinical diagnosis without general consensus on its definition. Indications for surgical chest wall reconstruction differ per country and region and

are not always standardized. In the United States of America (USA), indications seem more narrowly defined than in European countries because reimbursement rates are dependent on the severity of deformity. To be eligible for corrective surgery, according to the available literature that is predominantly USA-based, two of the following criteria must be present: (I) a Haller index equal to or greater than 3.25 with associated pulmonary or cardiac compression on computed tomography (CT), (II) restrictive or obstructive pulmonary impairment indicated by pulmonary function tests, (III) cardiologic evaluation demonstrating cardiac displacement, compression, conduction abnormalities, mitral valve prolapse or murmurs, (IV) objective progression of the pectus deformity with advancing age in association with worsening or development of physiologic symptoms [17, 43]. In for example the Netherlands, there is more emphasis on the entire biopsychosocial status and associated burden of disease. Thus, indications for surgical chest wall reconstruction in the Netherlands also consider cosmetics, psychological complaints, and patient preference, next to the aforementioned physical abnormalities and complaints.

After or prior to consultation and physical examination, conventionally a chest CT is acquired to determine the (gold standard) Haller index [44]. The resulting CT is, moreover, used to assess the presence of pulmonary or cardiac compression and other intrathoracic anomalies. Yet, significant anomalies are scarce and only found in less than 1% of patients [45]. The correction index is often determined as an adjunct measure of severity, depicting the percentage of chest depth to be corrected [46]. Its use is anticipated to intensify in the future whereas the correction index is better able to distinguish between the diseased and healthy population [47]. Some authors advocate for the use of two-view plain chest radiographs instead of CT to limit exposure to ionizing radiation [48-51], that is especially harmful for the pediatric pectus population due to their long life-time risk to develop associated pathologies [52, 53]. Some even promote the use of magnetic resonance imaging (MRI) for primary evaluation. However, MRI is limited by high costs, reduced availability, lengthy acquisition time, its sensitivity to motion requiring sedation in young patients and it is not suitable for claustrophobic patients [54, 55]. In several centers, additional photographic documentation is performed to objectively assess chest wall changes over time without repeated exposure to ionizing radiation. Acquired photographs are also often used for preoperative planning purposes, create insight into the patients' own disease and assess aesthetic improvement following surgery [56].

After primary severity evaluation, more profound assessment of cardiorespiratory function is performed based on clinical symptomatology and imaging results. If indicated, an electrocardiogram, echocardiography or cardiac MRI is performed to assess cardiac function, may reveal right-sided cardiac dysfunction [57-61] due to cardiac compression that is present in up to 90% of cases [62, 63], while in a large series of 1215 patients mitral valve prolapse and dysrhythmias were observed in 18 and 16%, respectively [64]. Pulmonary function at rest is analyzed by spirometry or plethysmography, where an average 10 to 20% less than expected forced vital capacity, forced expiratory volume in one second and forced expiratory is found in the pectus excavatum population [22, 64, 65]. Yet, the main problem seems to be impaired cardiovascular performance [66]. Cycle ergometry can be used for exercise capacity testing [67, 68], however, merely used in daily clinical practice.

Psychosocial burden can be objectified through checklists and questionnaires like the Achenbach Child Behavior Checklist [69] and Pectus Excavatum Evaluation Questionnaire [70], however, scarcely employed because their added clinical value over anamnestic complaints is undetermined for the process of clinical decision making.

Treatment

Current therapeutic options for pectus excavatum encompass surgical and conservative treatments. The latter includes, among others, the vacuum bell; a cup-shaped device that utilizes a vacuum-like state to create sternal lift [71] and should be applied for at least two 30-minute cycles per day [72]. Albeit its position in the pectus treatment algorithm is still undetermined due to varying short- and lack of long-term results [72-74]. Exercise programs and braces have also been used. Still, surgical interventions remain the only effective and evidence-based treatment with improvement or even disappearance of complaints in up to 96% of initially symptomatic patients [75-77]. The most established surgical treatment options encompass the Nuss [39] and modified Ravitch procedure [38]. The Nuss procedure is currently considered the treatment of choice among adolescents [22, 23, 42, 78-81] due to its minimal invasive character (i.e., small incision, minimal blood loss and short operation time) [82]. Though, its use in adults has also been described to be feasible despite higher chest wall rigidity [83-85]. The Nuss procedure is, moreover, regarded to as a safe procedure to learn with acceptable complication rates from

the first procedure onward [86]. The metal bar remains in situ for three years where-after good to excellent anatomic results are achieved in up to 96% of cases [64]. Though, the open modified Ravitch procedure is still considered depending on the patients' age, severity of deformity and experience of the surgical team. The major drawbacks of the modified Ravitch procedure comprise of its invasiveness and extent. This results from the need for chondrocostal resection and sternal osteotomy with fixation that may on its turn lead to Jeune syndrome (i.e., acquired restrictive thoracic dystrophy) when intervened at a young age [87-89]. Yet, the Ravitch procedure appears to be associated with fewer complications among adults [90].

Three-dimensional imaging and outline of thesis

The principle of three-dimensional (3D) surface imaging is to digitize real-world objects by obtaining its geometry and texture information. In 1944, Thalman was one of the first who captured the 3D surface of two patients with facial abnormalities using stereophotogrammetry to construct contour maps [91]. In the decades thereafter, the primary goal was to improve resulting images and explore the potential of other imaging techniques, such as moiré photography [92, 93]. Since the 21st century, the clinical use of 3D imaging developed exponentially whereby structured light and stereophotogrammetry techniques gained prominence [94]. As these methods became more and more established, emphasis shifted from improvement to validation of 3D imaging. Surface imaging is currently being deployed for analysis, planning, follow-up, and research purposes where the majority of applications are historically and still nowadays found in plastic and reconstructive surgery. Though, applications are gradually being extrapolated to other specialisms among which thoracic surgery to evaluate anterior chest wall anomalies like pectus excavatum [95]. Three-dimensional imaging methods can potentially be used in the preoperative evaluation of pectus excavatum to circumvent the exposure to ionizing radiation from CT scans and plain radiographs that is especially harmful for pediatric patients due to their relatively long life-time risk to develop associated pathologies [52, 53]. Therefore, the main objective of this thesis is to eliminate the exposure to ionizing radiation in the preoperative evaluation of pectus excavatum by introduction of 3D surface imaging. It was hypothesized that 3D surface images can be used interchangeably with CT scans and plain radiographs as a valid and accurate diagnostic tool in the preoperative

work-up of patients suffering from pectus excavatum. To test this hypothesis, individual chapters can be distinguished forming the basis of this thesis.

Aiming to introduce novel diagnostic procedures it is crucial to identify what is already known and determine which aspects require further investigation before the distinct procedure can be implemented. **Chapter 2** evaluates the current role of three-dimensional imaging as a diagnostic tool to determine pectus severity compared to CT scans and plain radiographs by systematic review of all available literature. Based on this chapter, the objectives of the succeeding chapters were established.

Reproducibility, as investigated later on, is not just dependent on the employed imaging system, but also whether a standardized protocol is utilized. **Chapter 3** describes a comprehensive imaging and processing protocol, to visually document pectus excavatum through three-dimensional surface imaging and, moreover, evaluates whether three-dimensional imaging can be used interchangeably with conventional photography. The protocol was built using information from previous studies described in **Chapter 2**.

One of the basic conditions for the introduction of novel diagnostic imaging procedures is that they should be accurate and reproducible to establish their validity. **Chapter 4** investigates the accuracy and reproducibility of three commercially available three-dimensional imaging systems that are used to obtain images of the anterior chest wall. Evaluating the validity of these imaging systems it was, moreover, investigated whether they can be used interchangeably.

The conventional Haller index and correction index, derived from CT and/or plain radiographs, are routinely used as objective measures in the multi-factorial to determine surgical candidacy for pectus excavatum repair. However, as both measures are based on internal dimensions they cannot be derived from three-dimensional images. Utilizing the optimal imaging system in conjunction with a dedicated protocol, **Chapter 5** aims to determine novel cut-off values for the three-dimensional image based external Haller and external correction index and assess their accuracy as diagnostic instrument to facilitate clinical decision making in patients with pectus excavatum. Surgical candidacy based on the conventional CT and/or radiograph derived Haller index and correction index was used as reference.

The main disadvantage of three-dimensional imaging compared to cross-sectional imaging is that it does not allow for cardiac evaluation due to the lack

of intrathoracic information. **Chapter 6** aims to overcome this limitation by development of a three-dimensional image based prediction model for cardiac compression in patients evaluated for pectus excavatum.

Pectus excavatum is a clinical diagnosis without general consensus on its definition. Consequently, work-up and treatment strategy may differ among experts and upon repeated evaluation. **Chapter 7** evaluates the inter-observer and intra-observer agreement of visual examination and diagnosis of pectus excavatum among experts through three-dimensional images.

The present thesis ends with a general discussion in **Chapter 8**. This discussion does not intend to reiterate the discussion points and limitations of the various chapters, but to put their rationale and findings into a broader perspective, address their implications, reflect on the lessons learned and choices made, as well as provide direction for future perspectives.

References

1. Fokin AA, Steuerwald NM, Ahrens WA, Allen KE. Anatomical, histologic, and genetic characteristics of congenital chest wall deformities. *Semin Thorac Cardiovasc Surg* 2009;21:44-57.
2. Chung CS, Myriantopoulos NC. Factors affecting risks of congenital malformations. I. Analysis of epidemiologic factors in congenital malformations. Report from the Collaborative Perinatal Project. *Birth Defects Orig Artic Ser* 1975;11:1-22.
3. Brochhausen C, Turial S, Müller FK, Schmitt VH, Coerdts W, Wihlm JM et al. Pectus excavatum: history, hypotheses and treatment options. *Interact Cardiovasc Thorac Surg* 2012;14:801-6.
4. Koumbourlis AC, Stolar CJ. Lung growth and function in children and adolescents with idiopathic pectus excavatum. *Pediatr Pulmonol* 2004;38:339-43.
5. Fonkalsrud EW. Current management of pectus excavatum. *World J Surg* 2003;27:502-8.
6. Nakaoka T, Uemura S, Yano T, Nakagawa Y, Tanimoto T, Suehiro S. Does overgrowth of costal cartilage cause pectus excavatum? A study on the lengths of ribs and costal cartilages in asymmetric patients. *J Pediatr Surg* 2009;44:1333-6.
7. Nakaoka T, Uemura S, Yoshida T, Tanimoto T, Miyake H. Overgrowth of costal cartilage is not the etiology of pectus excavatum. *J Pediatr Surg* 2010;45:2015-8.
8. Eisinger RS, Harris T, Rajderkar DA, Islam S. Against the Overgrowth Hypothesis: Shorter Costal Cartilage Lengths in Pectus Excavatum. *J Surg Res* 2019;235:93-7.
9. Park CH, Kim TH, Haam SJ, Lee S. Rib overgrowth may be a contributing factor for pectus excavatum: Evaluation of prepubertal patients younger than 10 years old. *J Pediatr Surg* 2015;50:1945-8.
10. Feng J, Hu T, Liu W, Zhang S, Tang Y, Chen R et al. The biomechanical, morphologic, and histochemical properties of the costal cartilages in children with pectus excavatum. *J Pediatr Surg* 2001;36:1770-6.
11. Rupperecht H, Hümmer HP, Stöss H, Waldherr T. [Pathogenesis of chest wall abnormalities - electron microscopy studies and trace element analysis of rib cartilage]. *Z Kinderchir* 1987;42:228-9.
12. Goretsky MJ, Kelly RE, Jr., Croitoru D, Nuss D. Chest wall anomalies: pectus excavatum and pectus carinatum. *Adolesc Med Clin* 2004;15:455-71.
13. Kuru P, Cakiroglu A, Er A, Ozbakir H, Cinel AE, Cangut B et al. Pectus Excavatum and Pectus Carinatum: Associated Conditions, Family History, and Postoperative Patient Satisfaction. *Korean J Thorac Cardiovasc Surg* 2016;49:29-34.
14. Gurnett CA, Alaei F, Bowcock A, Kruse L, Lenke LG, Bridwell KH et al. Genetic linkage localizes an adolescent idiopathic scoliosis and pectus excavatum gene to chromosome 18q. *Spine* 2009;34:E94-E100.
15. Wu S, Sun X, Zhu W, Huang Y, Mou L, Liu M et al. Evidence for GAL3ST4 mutation as the potential cause of pectus excavatum. *Cell Res* 2012;22:1712-5.
16. Karner CM, Long F, Solnica-Krezel L, Monk KR, Gray RS. Gpr126/Adgrg6 deletion in cartilage models idiopathic scoliosis and pectus excavatum in mice. *Hum Mol Genet* 2015;24:4365-73.
17. Kelly RE, Jr. Pectus excavatum: historical background, clinical picture, preoperative evaluation and criteria for operation. *Semin Pediatr Surg* 2008;17:181-93.

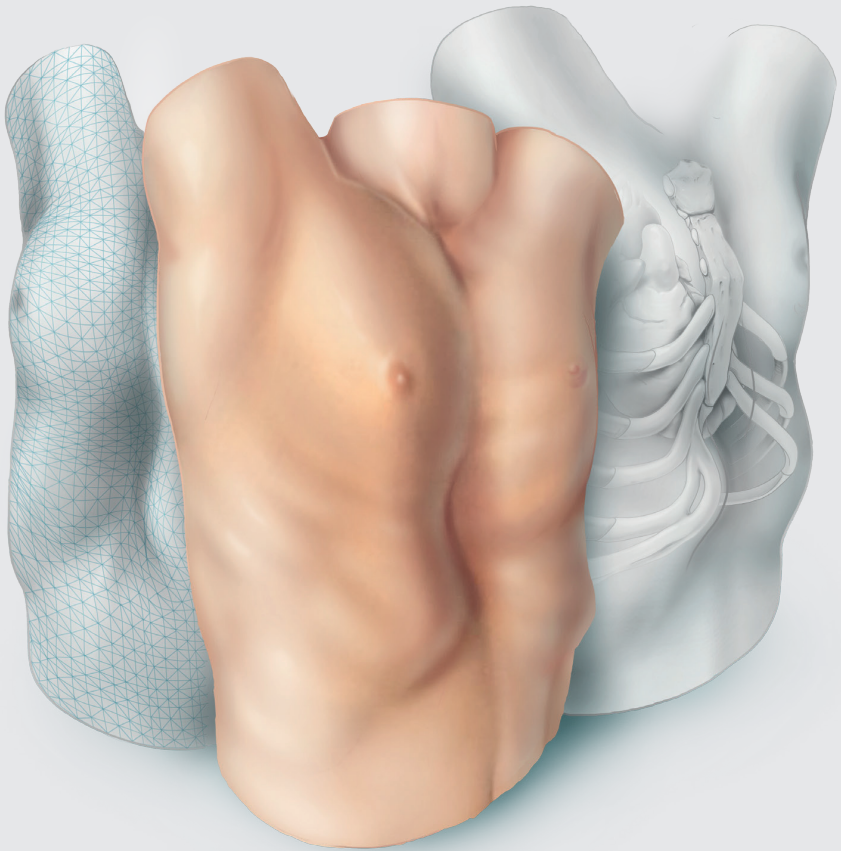
18. Humphreys GH, 2nd, Jaretzki A, 3rd. Pectus excavatum. Late results with and without operation. *J Thorac Cardiovasc Surg* 1980;80:686-95.
19. Lacquet LK, Morshuis WJ, Folgering HT. Long-term results after correction of anterior chest wall deformities. *J Cardiovasc Surg (Torino)* 1998;39:683-8.
20. Ewert F, Syed J, Kern S, Besendörfer M, Carbon RT, Schulz-Drost S. Symptoms in Pectus Deformities: A Scoring System for Subjective Physical Complaints. *Thorac Cardiovasc Surg* 2017;65:43-9.
21. Fonkalsrud EW, Dunn JC, Atkinson JB. Repair of pectus excavatum deformities: 30 years of experience with 375 patients. *Ann Surg* 2000;231:443-8.
22. Kelly RE, Jr., Shamberger RC, Mellins RB, Mitchell KK, Lawson ML, Oldham K et al. Prospective multicenter study of surgical correction of pectus excavatum: design, perioperative complications, pain, and baseline pulmonary function facilitated by internet-based data collection. *J Am Coll Surg* 2007;205:205-16.
23. Miller KA, Woods RK, Sharp RJ, Gittes GK, Wade K, Ashcraft KW et al. Minimally invasive repair of pectus excavatum: A single institution's experience. *Surgery* 2001;130:652-9.
24. Hong JY, Suh SW, Park HJ, Kim YH, Park JH, Park SY. Correlations of adolescent idiopathic scoliosis and pectus excavatum. *J Pediatr Orthop* 2011;31:870-4.
25. Waters P, Welch K, Micheli LJ, Shamberger R, Hall JE. Scoliosis in children with pectus excavatum and pectus carinatum. *J Pediatr Orthop* 1989;9:551-6.
26. Golladay ES, Char F, Mollitt DL. Children with Marfan's syndrome and pectus excavatum. *South Med J* 1985;78:1319-23.
27. Kotzot D, Schwabegger AH. Etiology of chest wall deformities--a genetic review for the treating physician. *J Pediatr Surg* 2009;44:2004-11.
28. Steinmann C, Krille S, Mueller A, Weber P, Reingruber B, Martin A. Pectus excavatum and pectus carinatum patients suffer from lower quality of life and impaired body image: a control group comparison of psychological characteristics prior to surgical correction. *Eur J Cardiothorac Surg* 2011;40:1138-45.
29. Kelly RE, Quinn A, Varela P, Redlinger RE, Nuss D. Dymorphology of Chest Wall Deformities: Frequency Distribution of Subtypes of Typical Pectus Excavatum and Rare Subtypes. *Arch Bronconeumol* 2013;49:196-200.
30. Cartoski MJ, Nuss D, Goretsky MJ, Proud VK, Croitoru DP, Gustin T et al. Classification of the dymorphology of pectus excavatum. *J Pediatr Surg* 2006;41:1573-81.
31. Bialas AJ, Kaczmarek J, Kozak J, Kempinska-Mirowska B. Pectus excavatum in relief from Ancient Egypt (dating back to circa 2400 BC). *Interact Cardiovasc Thorac Surg* 2015;20:556-7.
32. Ashrafian H. Leonardo da Vinci and the first portrayal of pectus excavatum. *Thorax* 2013;68:1081.
33. Bauhinus J, Schenck von Grafenberg J. *Observationum medicarum, rararum, novarum, admirabilium, et monstrosarum, liber secundus. Departibus vitalibus, thorace contentis.* Observation 1594;264-516.
34. Eggel. Eine seltene missbildung des thorax. *Virchows Arch Path Anat* 1870;49:230.
35. Ebstein W. *Über die trichterburst.* *Arch Klin Med* 1882;30:411-23.
36. Meyer L. *Zurchirurgischen behandlung der augeborenen trichterburst.* *Verh Bel Med Gest* 1911;42:364.

37. Sauerbruch F. Operative beseitigung der angeborenen trichterburst. *Deutsche Zeitschr Chir* 1931;234:760.
38. Ravitch MM. The Operative Treatment of Pectus Excavatum. *Ann Surg* 1949;129:429-44.
39. Nuss D, Kelly RE, Croitoru DP, Katz ME. A 10-year review of a minimally invasive technique for the correction of pectus excavatum. *J Pediatr Surg* 1998;33:545-52.
40. Croitoru DP, Kelly RE, Jr., Goretsky MJ, Lawson ML, Swoveland B, Nuss D. Experience and modification update for the minimally invasive Nuss technique for pectus excavatum repair in 303 patients. *J Pediatr Surg* 2002;37:437-45.
41. Park HJ, Lee SY, Lee CS, Youm W, Lee KR. The Nuss procedure for pectus excavatum: evolution of techniques and early results on 322 patients. *Ann Thorac Surg* 2004;77:289-95.
42. Zuidema WP, van der Steeg AFW, Oosterhuis JWA, van Heurn E. Trends in the Treatment of Pectus Excavatum in the Netherlands. *Eur J Pediatr Surg* 2020.
43. Nuss D, Kelly RE, Jr. Indications and technique of Nuss procedure for pectus excavatum. *Thorac Surg Clin* 2010;20:583-97.
44. Haller JA, Jr., Kramer SS, Lietman SA. Use of CT scans in selection of patients for pectus excavatum surgery: a preliminary report. *J Pediatr Surg* 1987;22:904-6.
45. Rattan AS, Laor T, Ryckman FC, Brody AS. Pectus excavatum imaging: enough but not too much. *Pediatr Radiol* 2010;40:168-72.
46. Poston PM, Patel SS, Rajput M, Rossi NO, Ghanamah MS, Davis JE et al. The correction index: setting the standard for recommending operative repair of pectus excavatum. *Ann Thorac Surg* 2014;97:1176-9; discussion 9-80.
47. St Peter SD, Juang D, Garey CL, Laituri CA, Ostlie DJ, Sharp RJ et al. A novel measure for pectus excavatum: the correction index. *J Pediatr Surg* 2011;46:2270-3.
48. Khanna G, Jaju A, Don S, Keys T, Hildebolt CF. Comparison of Haller index values calculated with chest radiographs versus CT for pectus excavatum evaluation. *Pediatr Radiol* 2010;40:1763-7.
49. Mueller C, Saint-Vil D, Bouchard S. Chest x-ray as a primary modality for preoperative imaging of pectus excavatum. *J Pediatr Surg* 2008;43:71-3.
50. Poston PM, Patel SS, Rajput M, Rossi NO, Davis JE, Turek JW. Defining the role of chest radiography in determining candidacy for pectus excavatum repair. *Innovations (Phila)* 2014;9:117-21; discussion 21.
51. Poston PM, McHugh MA, Rossi NO, Patel SS, Rajput M, Turek JW. The case for using the correction index obtained from chest radiography for evaluation of pectus excavatum. *J Pediatr Surg* 2015;50:1940-4.
52. Don S. Radiosensitivity of children: potential for overexposure in CR and DR and magnitude of doses in ordinary radiographic examinations. *Pediatr Radiol* 2004;34 Suppl 3:S167-72; discussion S234-41.
53. Miglioretti DL, Johnson E, Williams A, Greenlee RT, Weinmann S, Solberg LI et al. The use of computed tomography in pediatrics and the associated radiation exposure and estimated cancer risk. *JAMA Pediatr* 2013;167:700-7.
54. Birkemeier KL, Podberesky DJ, Salisbury S, Serai S. Limited, fast magnetic resonance imaging as an alternative for preoperative evaluation of pectus excavatum: a feasibility study. *J Thorac Imaging* 2012;27:393-7.

55. Lo Piccolo R, Bongini U, Basile M, Savelli S, Morelli C, Cerra C et al. Chest fast MRI: an imaging alternative on pre-operative evaluation of Pectus Excavatum. *J Pediatr Surg* 2012;47:485-9.
56. van Dijk H, Höppener PF, Siebenga J, Kragten HA. Medical photography: a reliable and objective method for documenting the results of reconstructive surgery of pectus excavatum. *J Vis Commun Med* 2011;34:14-21.
57. Huang PM, Liu CM, Cheng YJ, Kuo SW, Wu ET, Lee YC. Evaluation of intraoperative cardiovascular responses to closed repair for pectus excavatum. *Thorac Cardiovasc Surg* 2008;56:353-8.
58. Mocchegiani R, Badano L, Lestuzzi C, Nicolosi GL, Zanuttini D. Relation of right ventricular morphology and function in pectus excavatum to the severity of the chest wall deformity. *Am J Cardiol* 1995;76:941-6.
59. Töpfer A, Polleichtner S, Zagrosek A, Prothmann M, Traber J, Schwenke C et al. Impact of surgical correction of pectus excavatum on cardiac function: insights on the right ventricle. A cardiovascular magnetic resonance study†. *Interact Cardiovasc Thorac Surg* 2016;22:38-46.
60. Malek MH, Berger DE, Housh TJ, Marelich WD, Coburn JW, Beck TW. Cardiovascular Function Following Surgical Repair of Pectus Excavatum. *Chest* 2006;130:506-16.
61. Kowalewski J, Brocki M, Dryjanski T, Zolyński K, Koktysz R. Pectus excavatum: Increase of right ventricular systolic, diastolic, and stroke volumes after surgical repair. *J Thorac Cardiovasc Surg* 1999;118:87-92.
62. Nuss D, Croitoru DP, Kelly RE, Jr., Goretsky MJ, Nuss KJ, Gustin TS. Review and discussion of the complications of minimally invasive pectus excavatum repair. *Eur J Pediatr Surg* 2002;12:230-4.
63. Rodriguez-Granillo GA, Raggio IM, Deviggiano A, Bellia-Munzon G, Capunay C, Nazar M et al. Impact of pectus excavatum on cardiac morphology and function according to the site of maximum compression: effect of physical exertion and respiratory cycle. *Eur Heart J Cardiovasc Imaging* 2019;21:77-84.
64. Kelly RE, Goretsky MJ, Obermeyer R, Kuhn MA, Redlinger R, Haney TS et al. Twenty-one years of experience with minimally invasive repair of pectus excavatum by the Nuss procedure in 1215 patients. *Ann Surg* 2010;252:1072-81.
65. Lawson ML, Mellins RB, Tabangin M, Kelly RE, Jr., Croitoru DP, Goretsky MJ et al. Impact of pectus excavatum on pulmonary function before and after repair with the Nuss procedure. *J Pediatr Surg* 2005;40:174-80.
66. Malek MH, Fonkalsrud EW, Cooper CB. Ventilatory and cardiovascular responses to exercise in patients with pectus excavatum. *Chest* 2003;124:870-82.
67. Tang M, Nielsen HH, Lesbo M, Frøkiær J, Maagaard M, Pilegaard HK et al. Improved cardiopulmonary exercise function after modified Nuss operation for pectus excavatum. *Eur J Cardiothorac Surg* 2012;41:1063-7.
68. Maagaard M, Heiberg J. Improved cardiac function and exercise capacity following correction of pectus excavatum: a review of current literature. *Ann Cardiothorac Surg* 2016;5:485-92.
69. Ji Y, Liu W, Chen S, Xu B, Tang Y, Wang X et al. Assessment of psychosocial functioning and its risk factors in children with pectus excavatum. *Health Qual Life Outcomes* 2011;9:28.

70. Lawson ML, Cash TF, Akers R, Vasser E, Burke B, Tabangin M et al. A pilot study of the impact of surgical repair on disease-specific quality of life among patients with pectus excavatum. *J Pediatr Surg* 2003;38:916-8.
71. Schier F, Bahr M, Klobe E. The vacuum chest wall lifter: an innovative, nonsurgical addition to the management of pectus excavatum. *J Pediatr Surg* 2005;40:496-500.
72. Haecker F-M, Mayr J. The vacuum bell for treatment of pectus excavatum: an alternative to surgical correction? *Eur J Cardiothorac Surg* 2006;29:557-61.
73. Haecker FM. The vacuum bell for conservative treatment of pectus excavatum: the Basle experience. *Pediatr Surg Int* 2011;27:623-7.
74. Obermeyer RJ, Cohen NS, Kelly RE, Ann Kuhn M, Frantz FW, McGuire MM et al. Nonoperative management of pectus excavatum with vacuum bell therapy: A single center study. *J Pediatr Surg* 2018;53:1221-5.
75. Fonkalsrud EW. 912 open pectus excavatum repairs: changing trends, lessons learned: one surgeon's experience. *World J Surg* 2009;33:180-90.
76. Huddleston CB. Pectus excavatum. *Semin Thorac Cardiovasc Surg* 2004;16:225-32.
77. Kelly RE, Jr., Cash TF, Shamberger RC, Mitchell KK, Mellins RB, Lawson ML et al. Surgical repair of pectus excavatum markedly improves body image and perceived ability for physical activity: multicenter study. *Pediatrics* 2008;122:1218-22.
78. Hebra A, Swoveland B, Egbert M, Tagge EP, Georgeson K, Othersen HB, Jr. et al. Outcome analysis of minimally invasive repair of pectus excavatum: review of 251 cases. *J Pediatr Surg* 2000;35:252-7; discussion 7-8.
79. Hosie S, Sitkiewicz T, Petersen C, Göbel P, Schaarschmidt K, Till H et al. Minimally invasive repair of pectus excavatum--the Nuss procedure. A European multicentre experience. *Eur J Pediatr Surg* 2002;12:235-8.
80. Park HJ, Lee SY, Lee CS. Complications associated with the nuss procedure: analysis of risk factors and suggested measures for prevention of complications. *J Pediatr Surg* 2004;39:391-5.
81. Pilegaard HK. Nuss technique in pectus excavatum: a mono-institutional experience. *J Thorac Dis* 2015;7:S172-S6.
82. Mao YZ, Tang S, Li S. Comparison of the Nuss versus Ravitch procedure for pectus excavatum repair: an updated meta-analysis. *J Pediatr Surg* 2017;52:1545-52.
83. Hanna WC, Ko MA, Blitz M, Shargall Y, Compeau CG. Thoracoscopic Nuss procedure for young adults with pectus excavatum: excellent midterm results and patient satisfaction. *Ann Thorac Surg* 2013;96:1033-6.
84. Pilegaard HK. Extending the use of Nuss procedure in patients older than 30 years. *Eur J Cardiothorac Surg* 2011;40:334-7.
85. de Loos ER, Pennings AJ, van Roozendaal LM, Daemen JHT, van Gool MH, Lenderink T et al. Nuss procedure for pectus excavatum: a comparison of complications between young and adult patients. *Ann Thorac Surg* 2020.
86. de Loos ER, Daemen JHT, Pennings AJ, Heuts S, Maessen JG, Hulsewé KWE et al. Minimally invasive repair of pectus excavatum by the Nuss procedure: The learning curve. *J Thorac Cardiovasc Surg* 2020.
87. Haller JA, Colombani PM, Humphries CT, Azizkhan RG, Loughlin GM. Chest wall constriction after too extensive and too early operations for pectus excavatum. *Ann Thorac Surg* 1996;61:1618-25.

88. Robicsek F, Fokin AA. How not to do it: restrictive thoracic dystrophy after pectus excavatum repair. *Interact Cardiovasc Thorac Surg* 2004;3:566-8.
89. Martinez D, Juame J, Stein T, Peña A. The effect of costal cartilage resection on chest wall development. *Pediatr Surg Int* 1990;5:170-3.
90. Kanagaratnam A, Phan S, Tchantchaleishvili V, Phan K. Ravitch versus Nuss procedure for pectus excavatum: systematic review and meta-analysis. *Ann Cardiothorac Surg* 2016;5:409-21.
91. Thalmaan D. Diastereogrammetrie: ein diagnostisches Hilfsmittel in der Kieferorthopaedie [Stereophotogrammetry: a diagnostic device in orthodontology]. Zurich (Switzerland): University Zurich, Switzerland 1944.
92. Hajeer MY, Ayoub AF, Millett DT, Bock M, Siebert JP. Three-dimensional imaging in orthognathic surgery: the clinical application of a new method. *Int J Adult Orthodon Orthognath Surg* 2002;17:318-30.
93. Karlan MS. Contour analysis in plastic and reconstructive surgery. *Arch Otolaryngol* 1979;105:670-9.
94. Chang JB, Small KH, Choi M, Karp NS. Three-dimensional surface imaging in plastic surgery: foundation, practical applications, and beyond. *Plast Reconstr Surg* 2015;135:1295-304.
95. Poncet P, Kravarusic D, Richart T, Evison R, Ronsky JL, Alassiri A et al. Clinical impact of optical imaging with 3-D reconstruction of torso topography in common anterior chest wall anomalies. *J Pediatr Surg* 2007;42:898-903.





Optical imaging versus CT and plain radiography to quantify pectus severity: a systematic review and meta-analysis

Jean H.T. Daemen, Pieter W.J. Lozekoot, Jos G. Maessen, Thomas J.J. Maal, Karel W.E. Hulstewé, Yvonne L.J. Vissers, Erik R. de Loos

Adapted from: J Thorac Dis 2020;12:1475-87.

Abstract

Background

Computed tomography (CT) and two-view chest radiographies are the most commonly used imaging techniques to quantify the severity of pectus excavatum (PE) and pectus carinatum (PC). Both modalities expose patients to ionizing radiation that should ideally be avoided, especially in pediatric patients. In an effort to diminish this exposure, three-dimensional (3D) optical surface imaging has recently been proposed as an alternative method. To assess its clinical value as a tool to determine pectus severity we conducted a systematic review in which we assessed all studies that compared 3D scan-based pectus severity measurements with those derived from CT-scans and radiographies.

Methods

Six scientific databases and three registries were searched through April 30th, 2019. Data regarding the correlation between severity measures was extracted and submitted to meta-analysis using the random-effects model and I^2 -test for heterogeneity.

Results

Five observational studies were included, enrolling 75 participants in total. Pooled analysis of participants with PE demonstrated a high positive correlation coefficient of 0.89 [95% confidence interval (CI): 0.81 to 0.93; $P < 0.001$] between the CT-derived Haller index (HI) and its 3D scan equivalent based on external measures. No heterogeneity was detected ($I^2 = 0.00\%$; $P = 0.834$).

Conclusions

3D optical surface scanning is an attractive and promising imaging technique to determine the severity of PE without exposure to ionizing radiation. However, further research is needed to determine novel cut-off values for 3D scans to facilitate clinical decision making and help determine surgical candidacy. No evidence was found that supports nor discards the use of 3D scans to determine PC severity.

Introduction

Pectus excavatum (PE) and pectus carinatum (PC) are the most common congenital chest wall deformities. The latter is characterized by an outward protrusion of the sternum, while PE is characterized by an inward depression. PE occurs in 1:400 of live births [1], in comparison to PC which is reported to occur 2–4 times less frequent [2]. PE and PC may be associated with impaired body image perception and result in lowered self-esteem, psychological stress and diminished quality of life. Next to these psychological effects, PE may be associated with impaired cardiopulmonary function [3, 4]. The current gold standard to evaluate the extent of pectus deformities is computed tomography (CT). In patients with PE, CT is generally used to calculate the Haller index (HI) [5]. The resulting HI is subsequently used in the process of decision making to determine surgical candidacy. In PC no such standard metric exists. Despite CT being the current gold standard, it inescapably implies exposure to ionizing radiation. Two-view chest radiographies may be used alternatively to CT, resulting in dose reduction. However, according to the doctrine of radiation hygiene, every effort should be made to avoid, or if not possible, limit radiation exposure, especially in pediatric patients with a long lifetime risk to develop radiation related pathologies [6, 7]. In an effort to diminish radiation exposure, alternative methods are being explored to quantify the extent of chest wall deformities, among which three-dimensional (3D) optical surface imaging shows great potential [8]. This technology has been widely used to map the chest surface in scoliosis patients and may serve as a safe and non-invasive severity measurement tool that utilizes non-ionizing light illumination. Optical imaging produced trunk topographies have already been demonstrated to be clinically feasible and accurate [9, 10]. However, as stressed by Sarwar and colleagues [8], the exact clinical value (e.g., in the process of decision making, follow-up, et cetera) of this novel severity measurement technique in PE and PC is yet to be investigated. Consequently, the following research question was formulated: can the evaluation of pectus excavatum and carinatum severity through chest CTs and radiographies be replaced by 3D optical scans? To answer this question, we conducted a systematic review and pooled analysis of the currently available literature in which we assessed all studies that compared 3D optical scan-based severity measurements with those derived from CT-scans or chest radiographies in patients with PE and PC. To our knowledge no such comprehensive review has been conducted to date.

Materials and methods

Protocol and registration

Prior to start, the review protocol was registered to the PROSPERO registry (Record ID: CRD42019122860). In addition, this review was written in compliance with the PRISMA statements to ensure quality and transparency throughout [11].

Eligibility criteria

Types of participants

Patients of any race, sex and age with PE or PC were considered for inclusion.

Types of intervention

Papers that performed pectus severity quantification based on 3D optical imaging and compared its performance to severity measurements based on chest radiographies or CT-scans were examined for eligibility. All optical surface imaging techniques, such as laser and structured (white) light, were considered for inclusion. Contact 3D scanners that probe the subject through physical touch were not considered.

Primary outcome measure(s)

Comparison of pectus severity measurements based on 3D optical surface scanning and the study's comparative measurement method (i.e., CT-scans or chest radiographies).

Types of studies

All observational and randomized studies adhering to the aforementioned criteria were assessed for eligibility. Studies reporting combined data on PE and PC severity measurements were considered only if data were presented separately.

Search and study selection

Potentially eligible papers were identified by searching electronic scientific databases and trial registries. Solely articles reported in English were considered. No publication date restrictions were imposed. The search strategy was first applied to the PubMed database and subsequently adapted for EMBASE, Web of Science,

the Cochrane Library, and CINAHL. In addition, the PROSPERO, WHO-ICTRP, and Clinicaltrials.gov registries were searched. See Supplementary Data S1-S5 for the complete scientific database search queries. Identical queries were used to search the aforementioned registries. An additional manual cross-reference and related-articles search was conducted to identify articles that were not found through the prior search. This additional

step also functioned as an indicator of the quality and integrity of the database search strategy. All searches were performed by a certified librarian. The last search was run on April 30th, 2019. Articles resulting from the searches were judged for eligibility based on their title and abstract. Thereafter, full text of potentially eligible articles was read and assessed according to the predefined eligibility criteria. Papers meeting these criteria were included for systematic review, and if applicable, meta-analysis. Article selection was performed in a standardized, unblinded manner by two independent reviewers (Jean H. T. Daemen & Tom G. J. Loonen). Inter-reviewer disagreements were resolved by consultation of Erik R. de Loos.

Data collection and data items

Data was extracted by one independent reviewer (Jean H. T. Daemen) and validated by a second reviewer (Tom G. J. Loonen). Inter-reviewer disagreements were resolved by consultation of Erik R. de Loos. To structure data extraction and presentation, an extraction sheet was developed and pilot-tested on two randomly selected included studies. The sheet was adopted accordingly. Data was extracted from each included paper on: (I) general study characteristics: study design, country and enrolment period; (II) characteristics of participants: number of included participants, gender, age, and the thoracic wall deformity that was studied (i.e., PE or PC); (III) characteristics of the optical scan(ner): scanner brand/type, scanning method, static or handheld, accuracy, acquisition and/or processing time, used software, patient position, and pectus severity measurement method; (IV) characteristics of the comparison: comparative technique (e.g., CT-scans or radiographies), and severity measurement method; (V) primary outcome measure: comparison of 3D optical surface scan- and radiography- or CT-based severity measurements. Continuous variables were denoted as mean, standard deviation (SD) and range. Continuous variables reported as median and interquartile range or standard error were converted. The primary outcome measure was extracted as reported. For studies that solely reported raw severity measurement data, Pearson's correlation coefficients (r) were calculated

using SPSS statistics (IBM Corp. Released 2017. IBM SPSS statistics for MacOS, version 25.0, Armonk, NY, USA). The Pearson's correlation coefficient was chosen as this was the most used metric to compare severity indices as found during the preliminary search. Missing P values were, if possible, calculated from the available data. $P \leq 0.05$ was considered to be statistically significant. To interpret the size of reported correlation coefficients, we used cut-off values as described by Mukaka [12]. Correlation sizes that ranged from 0 to 0.30 were judged to be negligible, while correlations that ranged from 0.30 to 0.50, 0.50 to 0.70, 0.70 to 0.90, and 0.90 to 1.00 were interpreted as either low, moderate, high and very high.

Risk of bias in individual studies

No validated tools exist that assess quality of correlation studies. Therefore, a tool was constructed (See Figure 1). This tool was adapted from the National Heart, Lung, and Blood Institute Quality Assessment Tool for Observational Cohort and Cross-Sectional Studies [13] and pilot tested on two randomly selected included studies. The tool was adopted accordingly. Questions were answered by Yes, No, not applicable (NA), or not reported (NR). Studies were, subsequently, given an overall quality judgement (Good, Fair, or Poor). This judgement was not based on simple summation of answers but based on the ability of studies to draw associative conclusions about the effect of the imaging techniques being studied on outcomes. Quality assessment was performed by two reviewers (Jean H. T. Daemen & Tom G. J. Loonen). Inter-reviewer disagreements were resolved by consultation of Erik R. de Loos.

Summary measures and synthesis of results

Quantitative synthesis of the primary outcome measure was only performed if studies were sufficiently homogeneous, otherwise, data was reported as such. For quantitative synthesis, correlation coefficients were converted into Z-scores using the Fisher Z-transformation method. Resulting Z-scores were pooled using the random-effects model. Pooled Z-scores and their corresponding 95% confidence interval (95% CI) were converted back into pooled correlation coefficients to allow easy interpretation. No additional analyses were performed. The I^2 -test for statistical heterogeneity was used as a measure of consistency. I^2 values greater than 50%, with a P value ≤ 0.10 indicated the presence of substantial heterogeneity. Meta-analyses were performed by ProMeta 3.0 software for MacOS (based on ProMeta 2.1, deployed by Internovi, Cesena, Italy).

1. Research question						
A.	The research question, objective(s) and/or hypotheses were clearly stated	Yes	Yes	Yes	Yes	Yes
2. Study population						
A.	The source population was clearly defined	No	Yes	Yes	Yes	Yes
B.	All subjects were selected or recruited from the same or similar population(s)	NR	NR	Yes	Yes	Yes
C.	Inclusion and/or exclusion criteria were clearly defined	No	No	Yes	Yes	Yes
3. Study design						
A.	The study design was stated to be prospective	NR	Yes	Yes	Yes	Yes
B.	The participation rate of eligible persons was at least 50%	NR	NR	Yes	NR	NR
4. Measurements, analyses and outcomes						
A.	Method(s) of measurement(s) were clearly defined	Yes	Yes	Yes	Yes	Yes
B.	Used soft- and hardware were clearly described	Yes	Yes	Yes	Yes	Yes
C.	Measurements were performed in a valid, blinded, and/or standardized manner	Yes	Yes	Yes	Yes	Yes
D.	Methods of statistical analyses were clearly described and appropriate	Yes	Yes	Yes	Yes	No
E.	Data presentation included measures of precision (e.g. SD or range)	NR	Yes	Yes	Yes	Yes
F.	Outcome data were available for (nearly) all participants (max. loss = 20% after baseline)	Yes	Yes	Yes	Yes	No
5. Overall quality judgement						
		Fair	Good	Good	Good	Fair
		Bliss et al.	Glinkowski et al.	Hebal et al.	Poncet et al.	Ucheddu et al.

Figure 1: Risk of bias per individual study.
NR, not reported.

Risk of bias across studies

Publication bias was assessed both visually by a funnel plot (a standard error by Z-score plot of the primary outcome measure), and statistically with Egger's linear regression, and Begg's and Mazumdar's rank correlation tests. A P value ≤ 0.10 was considered statistically significant. Publication bias analyses were performed by ProMeta 3.0 software for MacOS (based on ProMeta 2.1, deployed by Internovi, Cesena, Italy).

Results

Study selection

See flow diagram, Figure 2. The PubMed (n=721), EMBASE (n=1,061), Web of Science (n=2,290), Cochrane Library (n=142), CINAHL (n=98), PROSPERO (n=87), WHO-ICTRP (n=53), and Clinicaltrials.gov (n=42) databases and registries provided a total number of 4,494 citations. No citations were obtained through the related-articles and cross-reference searches. No unpublished data was obtained. Of the 4,494 citations, 1,130 duplicates were discarded using the Mendeley find duplicates function (Mendeley Desktop v1.19.4 for MacOS, Mendeley Ltd., Elsevier). An additional 3,345 studies were discarded because their title and/or abstract did not comply with the predetermined eligibility criteria. Full texts of the remaining 19 papers were read, whereupon another 14 papers were excluded for systematic review. Reasons for exclusion were: lack of a comparative method (n=6); the full text was NR in the English language (n=3); only a conference abstract was available (n=2); the fact that only inter-user reliability was assessed (n=1); PE and PC data were not presented separately (n=1) or the use of correlation data from another article (n=1). Eventually, 5 papers were considered eligible for systematic review and qualitative synthesis, while 4 papers were also included for quantitative synthesis (i.e., meta-analysis).

Study characteristics

Methods

See Table 1. All included papers conducted an observational study, of which 4 were stated to be prospective [14-17]. No randomized controlled trials were included. Studies were conducted in Canada, Italy, Poland, Spain or the USA, participants were enrolled between 2005 and 2017.

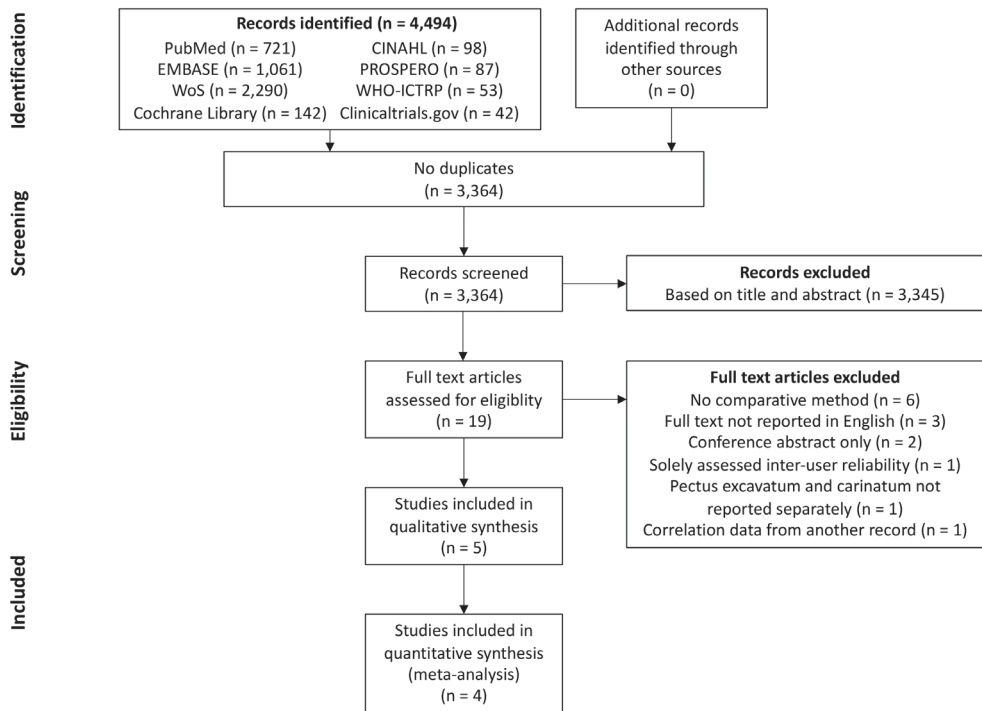


Figure 2: A PRISMA flow diagram of the study selection procedure.

PRISMA, Preferred Reporting Items for Systematic Reviews and Meta-Analysis; WoS, Web of Science; CINAHL, Cumulative Index to Nursing and Allied Health Literature; WHO-ICTRP, World Health Organization International Clinical Trials Registry Platform.

Participants

In total, 75 participants were enrolled. All studies included participants with PE whereas the study performed by Poncet et al. [16] was the only study to also include 5 participants with PC (Table 1). This study was not excluded because PE and PC data were reported separately. The percentage of male subjects with PE ranged from 80% to 100%, as reported by Bliss et al. [18] and Glinkowski et al. [14]. Individual sample sizes ranged from 4 to 39 participants. The mean age of participants with PE was reported by Bliss et al. [18], Glinkowski et al. [14] and Poncet et al. [16] and ranged from 13.8 to 16.5 years. The mean age of participants with PC was 11.6 (SD: 4.5) years [16].

Table 1: Study and patient characteristics.

Author	Country	Study design	Study period	Study size	Chest wall deformity studied	Age (years), mean (SD)	Male, n (%)
Bliss et al.	USA	Observational study	28 months	10	PE	16.5 (2.2)	8 (80.0)
Glinkowski et al.	Poland	Prospective observational study	November 2007 - December 2008	12	PE	16 (5)	12 (100.0)
Hebal et al.	USA	Prospective observational study	April 2015 - April 2017	39	PE	NR	NR
Poncet et al.	Canada	Prospective observational study	July 2005 - March 2006	5	PE	13.8 (1.5)	NR
Uccheddu et al.	Italy	Prospective observational study	NR	5 4	PC PE	11.6 (4.5) NR	NR NR

PE, pectus excavatum; PC, pectus carinatum; SD, standard deviation; n, number; NR, not reported.

Intervention

3D thoracic surface scan

See Tables 2, 3. All studies utilized 3D scanners of different manufacturers. Three studies used a static scanner type [14, 16, 18], while Hebal et al. [15] used a handheld scanner and Uccheddu et al. [17] mounted their scanner on a specially devised frame that allowed vertical translation. Despite these differences, all scanners used structured (white) light projectors to detect the 3D thoracic surface. Prior to acquisition, 4 studies [14-16, 18] positioned their participants in an upright standing position with the arms at the level of, or above the shoulders. The same 4 studies all acquired a 360° thoracic surface scan. In contrast, Uccheddu et al. [17] positioned their participants in a supine position on a semi rigid mattress and solely obtained a frontal acquisition. Among the reported studies, scans were all acquired at different phases of the respiratory cycle [14, 15, 17]. Acquisition of the 3D scans took several milliseconds to 180 seconds whereas reconstruction took up to 10 minutes [15, 18]. Scanner accuracy was reported to be 0.2–0.4 mm. for the study of Glinkowski et al. [14] and 0.006 mm. for Poncet et al. [16]. In four studies thoracic surface scan-based PE severity measurements were calculated by dividing the

widest external thoracic transverse diameter by the distance between the external vertebral body and external deepest point (Figure 3A) [14-16, 18]. Terminology of this measure differed among all four studies but will from this point on be referred to as the external Haller index (EHI). Bliss et al. [18] additionally derived two, self-developed PE measures: The Pectus Volume Ratio and Surface Area Ratio. The latter was obtained by calculating the ratio between the surface area of both the chest deformity (i.e., the area beneath the normal aspect of the anterior chest) and torso (i.e., sternal notch to xiphoid). The same applies to the Volume Ratio, for which volumes were used. In addition, Poncet et al. [16] also reported another self-developed PE measure that was modified from the EHI; the modified external Haller index (MEHI) (Figure 3A). This measure was calculated by dividing the widest external thoracic transverse diameter by the anteroposterior distance from the imaginary transverse diameter line to the external deepest point. Uccheddu et al. [17] only calculated the external Correction index (ECI) (Figure 3A), that is defined as: $(d-e)/d$, where d and e are the vertical distances of, respectively, the minimum and maximum sternal depression with respect to the reference plane (i.e., the semirigid mattress plane). To determine the severity of PC, Poncet et al. [16] utilized similar measures as for PE, however, for PC the point of maximal protrusion was used as reference point.

Comparison

See Table 3. To assess 3D surface scan performance, all studies acquired a comparative thoracic CT-scan [14-18]; the current gold standard for pectus severity quantification. All studies analyzed thoracic surface and CT-scan based measurements of the same participant. In comparison to the aforementioned 3D scan measures, CT-scan derived severity measurements were based on internal diameters. Four out of 5 studies calculated the conventional HI (Figure 3B) to determine PE severity [14-16, 18].

Table 2: Acquisition characteristics.

Author	3D-Scanner	Static, handheld, or mounted	3D-Scanning method	Accuracy, mm.	Patient position	Respiratory phase	Acquisition range, degrees	Duration of acquisition, seconds	Duration of reconstruction, minutes
Bliss et al.	3dMD torso photography system (3dMD LLC, Atlanta, Georgia, USA)	Static	Structured light	NR	Upright, standing position with arms in a T-pose position	NR	360	Several milliseconds	NR
Glinkowski et al.	Self-built scanner that consisted of MIT700 projectors (Toshiba, Minato, Tokio, Japan) and Flea B&W cameras (Point Grey Research Inc., Richmond, Canada)	Static	Structured light	0.2-0.4	Upright, standing position	Holding breath	360	0.7	NR
Hebal et al.	Rodin M4D (Rodin4d, Mérégnac, France)	Handheld	Structured white light	NR	Upright, standing position with shoulders abducted 45°	During expiration	360	180	5-10 ^a
Poncet et al.	InSpeck (InSpeck Inc., Montreal, Quebec, Canada)	Static	Structured white light	0.006	Upright, standing position with arms above shoulders.	NR	360	<24	NR
Uccheddu et al.	Microsoft Kinect v2 (Microsoft, Redmond, WA)	Mounted but translatable	Structured light	NR	Supine position on a semirigid mattress	Holding breath, following expiration	Frontal acquisition only	<1	NR

^a: Duration for the entire scanning process (acquisition & reconstruction), with often multiple acquisitions being needed. 3D, three-dimensional; NR, not reported.

Table 3: Measurement characteristics.

Author	Software used for 3D-scan measurements	Chest wall deformity studied	3D-scan measurement method (see Fig. 2)	Measured 3D value, mean (SD; range)	Method of reference	Reference measurement method (see Fig. 3)	Measured reference value, mean (SD; range)	Correlation, coefficient	P-value
Bliss et al.	3dMDvultus (3dMD LLC, Atlanta, Georgia, USA)	PE	EHI	NR	CT	Conventional HI	3.67 (0.92; 2.44-5.60)	r ² =0.76; r=0.87	0.001 ^a
		PE	Pectus Surface Area Ratio	NR	CT	Conventional HI	3.67 (0.92; 2.44-5.60)	r ² =0.46; r=0.68	0.03 ^a
		PE	Pectus Volume Ratio	NR	CT	Conventional HI	3.67 (0.92; 2.44-5.60)	r ² =0.30; r=0.58	0.1
Glinskowski et al.	Self-developed	PE	EHI	1.84 (0.11; 1.70-2.13)	CT	Conventional HI	3.82 (0.17; 3.58-4.22)	r ² =0.87; r=0.93	<0.001 ^a
		PE	EHI	1.84 (0.11; 1.70-2.13)	CT	EHI	1.93 (0.13; 1.77-2.24)	r ² =0.99; r=0.99	<0.001 ^a
Hebal et al.	NR	PE	EHI	NR	CT	Conventional HI	NR	r=0.87	<0.001 ^a
Poncet et al.	InSpeck (InSpeck Inc, Montreal, Quebec, Canada)	PE	EHI	2.06 (0.46; 1.72-2.82)	CT	Conventional HI	4.28 (1.40; 3.00-6.00)	r=0.92	0.03 ^a
		PE	MEHI	5.29 (3.45; 3.09-11.23)	CT	Modified Conventional HI	11.33 (8.07 (5.34-24.00)	r=0.97	0.006 ^a
Uccheddu et al.	Self-developed	PC	EHI	1.28 (0.15; 1.07-1.47)	CT	Conventional HI	1.66 (0.39; 1.19-2.20)	r=0.88	0.049 ^a
		PC	MEHI	1.81 (0.29; 1.33-2.07)	CT	Modified Conventional HI	2.55 (0.34; 2.27-3.10)	r=0.44	0.5
Uccheddu et al.	Self-developed	PE	EHI	17.50% (6.25%; 10-25%)	CT	Conventional Correction Index	17.00% (6.48%; 9-24%)	r=0.99	0.01 ^a

^a, Statistically significant (P<0.05).

3D, three-dimensional; PE, pectus excavatum; PC, pectus carinatum; SD, standard deviation; NR, not reported; CT, computed tomography; EHI, external Haller index; MEHI, modified external Haller index; ECI, external correction index; HI, Haller index.

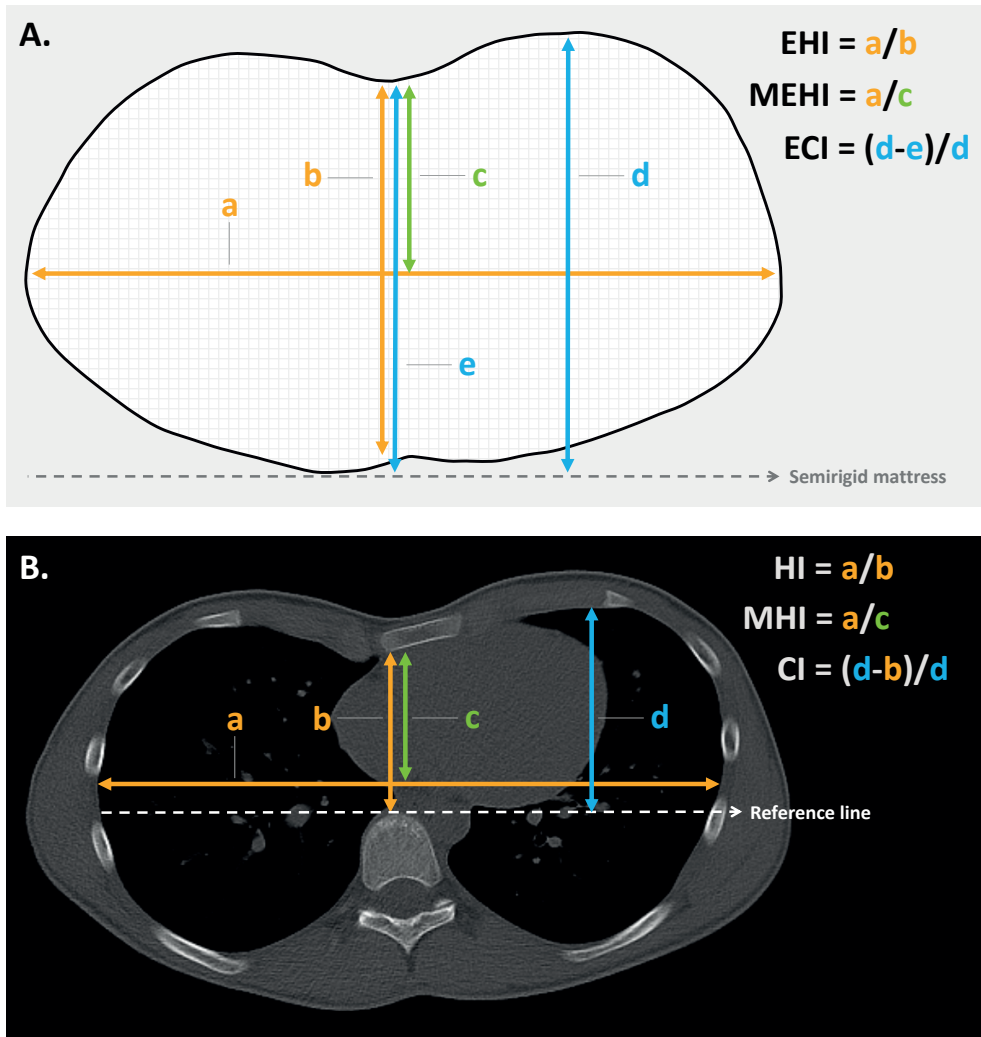


Figure 3: Pectus severity measurement methods. (A) Severity indices based on 3D surface scans; (B) severity indices based on CT-scans. *EHI*, external Haller index; *MEHI*, modified external Haller index; *ECI*, external correction index; *HI*, Haller index; *MHI*, modified Haller index; *CI*, correction index; *3D*, three-dimensional.

The HI was obtained by dividing the widest inner thoracic diameter by the anteroposterior distance from the posterior sternal surface to the anterior vertebral surface. Glinkowski et al. [14] additionally derived the CT-based EHI to assess 3D and CT-scan agreement. In line with the aforementioned thoracic surface scan indices, Poncet et al. [16] reported an additional, self-developed modified Haller index (MHI)

(Figure 3B), obtained by dividing the widest internal transverse diameter by the anteroposterior distance from the imaginary widest internal transverse diameter line to the posterior sternal surface. In comparison, Uccheddu et al. [17] used the Correction index to determine the CT-based PE severity. This index measures the percentage of PE to be corrected and is calculated by the following formula (Figure 3B): $(d-b)/d$, where d and b are the vertical distances of, respectively, the minimum and maximal sternal depression with respect to the anterior vertebral body reference line. To determine the CT-based PC severity, Poncet et al. [16] again utilized similar measures as for PE, however, for PC the point of maximal protrusion was used as point of reference.

Outcomes

One paper compared its thoracic surface and CT-scan derived pectus severity measurements using the Pearson's correlation coefficient (r) [15] while two studies reported the squared variant (r^2) [14, 18]. Uccheddu et al. [17] reported the raw outcome data only, whereas Poncet et al. [16] reported correlation data for their entire study population (i.e., PE and PC combined) including the raw data. The level of statistical significance was only denoted by Hebal et al. [15]. Missing correlation coefficients and P values were calculated post hoc.

Risk of bias within studies

See Figure 1 for the risk of bias assessment per study. The study of Glinkowski et al. [14], Hebal et al. [15] and Poncet et al. [16] were all judged to be of good methodological quality; i.e. outcome measures were not doubted. The study of Bliss et al. [18] and Uccheddu et al. [17] were considered to be of fair methodological quality.

Synthesis of results

Qualitative synthesis

See Table 3. For PE, correlation sizes (r) ranged from 0.87 to 0.93 among studies that assessed the correlation of 3D scan derived EHI and CT-scan derived HI [14-16, 18]. These correlations were all statistically significant. The size of correlation was not affected by the type of 3D scanner used, although the use of a handheld scanner was associated with a prolonged acquisition time. Bliss et al. [18] additionally determined their self-developed 3D scan based Pectus Surface Area Ratio and Pectus Volume Ratio and assessed its agreement to the conventional CT-based

HI. They found moderate positive correlations of 0.68 ($P=0.03$) and 0.58 ($P=0.1$), respectively. In a similar manner, Glinkowski et al. [14] assessed the correlation of the 3D- and CT-scan derived EHI and found a coefficient of 0.99 ($P<0.001$); suggesting near perfect agreement between both acquisitions. Poncet et al. [16] additionally assessed the correlation of their self-constructed MHI and MEHI that was respectively obtained from acquired CT- and 3D-scans of participants with PE. Correlation of these modified indices ($r=0.98$; $P<0.001$) was slightly superior to the correlation of the 3D-EHI and CT-scan derived HI ($r=0.96$; $P<0.001$). However, superiority of the 3D scan derived MEHI over the EHI remains unknown, while the MEHI was not compared to the gold standard (i.e., CT derived HI). Ucheddu et al. [17] quantified PE severity utilizing the 3D-derived ECI and CT-scan derived CI, and found a correlation coefficient of 0.99 ($P=0.01$).

As mentioned in the previous sections, Poncet et al. [16] also investigated the correlation of the 3D scan derived EHI and MEHI with the CT-based conventional HI and MHI to determine the severity of PC. They found a high and low correlation of 0.88 ($P=0.049$) and 0.44 ($P=0.5$), respectively.

Quantitative synthesis

The study of Bliss et al. [18], Glinkowski et al. [14], Hebal et al. [15] and Poncet et al. [16] were found to be sufficiently homogenous to be admitted for quantitative synthesis because they all included patients with PE and utilized identical severity metrics. From the study of Poncet et al. [16], only participants with PE were included for quantitative synthesis. Inspection of the individual correlation coefficients and forest plot (Figure 4) indicated the presence of an overall high positive correlation between the CT-based HI and 3D scan-based EHI. This was statistically confirmed by meta-analysis (Figure 4) that demonstrated a pooled Z-score of 1.40 (95% CI: 1.13 to 1.66; $P<0.001$) These Z-scores corresponded with a pooled correlation coefficient of 0.89 (95% CI: 0.81 to 0.93; $P<0.001$). No heterogeneity was detected ($I^2=0.00\%$; $P=0.834$). No subgroup analyses were performed.

Risk of bias across studies

A funnel plot of the studies that were included for quantitative synthesis was constructed. Graphical assessment demonstrated no evident asymmetry; indicating the absence of publication bias (Figure 5). This was statistically reproduced by Begg's and Mazumdar's rank correlation test ($P=0.497$) and by Egger's linear regression test ($P=0.407$).

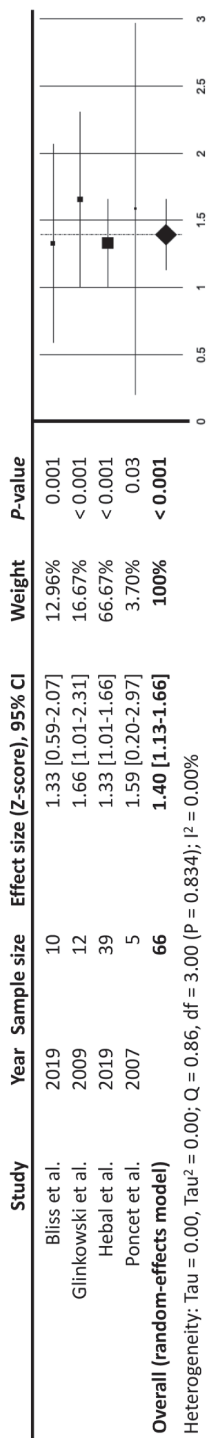


Figure 4: Meta-analysis demonstrating the correlation of 3D optical surface scan based EHI and CT-scan based HI among participants with pectus excavatum, using Fisher's Z-score as effect size.
CI, confidence interval; 3D, three-dimensional; CT, computed tomography; EHI, external Haller index; HI, Haller index

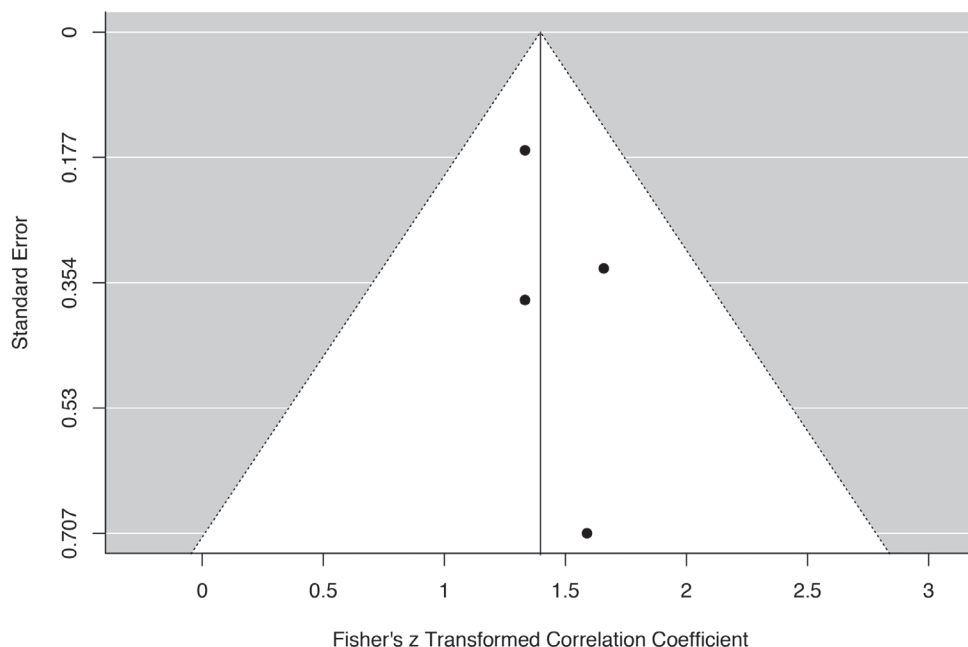


Figure 5: A standard error by Fisher's Z transformed correlation coefficient to detect the presence of publication bias among the studies that were included for quantitative synthesis.

Discussion

This systematic review and meta-analysis examined all studies that compared the use of 3D optical imaging and CT-scans or chest radiographies in the quantification of pectus severity. Based on the previously described eligibility criteria, 5 observational studies were included, enrolling a total of 75 participants. Of these, 70 were participants with PE. No studies were judged to be of poor methodological quality. No studies were included that assessed the use of two-view plain radiographies. All studies utilized CT-scan based severity metrics as comparison; the current gold standard for severity quantification. To assess 3D- and CT-scan agreement, all studies calculated correlation coefficients or correlation coefficients could be determined from the available raw data. Only one of these studies investigated the correlation among participants with PC [16]. This low number of studies describing the use of 3D scans to determine PC severity may be a direct consequence of the absence of a standardized PC severity measure. Among participants with PC ($n=5$), Poncet et al. [16] found a high correlation of 0.88 between the CT-based HI and 3D-based EHI with a 95% CI that ranged from

-0.01 to 0.92. We subsequently concluded that with the currently available limited data no evidence can be produced to either support nor discard the use of 3D scans to determine PC severity in comparison to CT-scans and chest radiographies. Nevertheless, 3D scans may be used to monitor treatments such as compressive orthotic bracing as described by Wong et al. [19].

Four out of five included studies acquired identical 3D scan and CT derived PE severity indices and were subjected to meta-analysis. Pooled analysis revealed a high positive, statistically significant correlation between the optical scan measured EHI and CT-scan derived conventional HI ($r=0.89$; $P<0.001$). Although pooled analysis demonstrated a high correlation, 3D thoracic surface scan derived External Haller indices are not yet a valid tool to aid in the multifactorial process of surgical decision making. Correlation coefficients express the direction and magnitude of a linear relationship between two measures, but they do not assess their exact agreement. This is best illustrated by Glinkowski et al. [14] and Poncet et al. [16] who found mean 3D scan-based EHI values of 1.84 and 1.67, with corresponding mean CT-based HI values of 3.82 and 2.97. Based on these means, fewer patients would have been operated on the basis of the 3D measurements, in comparison to CT if the same cut-off values would have been used. Consequently, for the 3D scan EHI to be used in the process of decision-making new threshold values should be determined. To date, no such studies exist.

The study of Uccheddu et al. [17] compared the 3D scan derived ECI and the CT-scan based correction index, and found similar mean index values 17.50% (SD: 6.25%; range: 10–25%) vs. 17.00% (SD: 6.48%; range: 9–24%) with a correlation coefficient of 0.99. One may subsequently assume that both imaging modalities can be used interchangeably to determine the (external) correction index. However, the power of evidence is low with only 4 included participants, therefore more data are needed to be able to draw a definite conclusion.

The novel 3D scan-based Pectus Surface Area Ratio and Volume Ratio that were introduced by Bliss et al. [18] demonstrated only moderate correlations with the conventional HI. This may be due to the fact that the HI is calculated from a single plane that exhibits the maximum depression. Yet, pectus morphologies are not restricted to a two-dimensional plane but are rather multiplanar. The HI is, moreover, dependent of the shape of the thorax. This means that a certain pectus depth results in different indices if the chest is for example flat or barrel shaped. In the past years, several alternative metrics have been proposed to better describe

the extent of PE deformities, however, their clinical use remains uncertain. Until now, the HI is still considered the reference standard for research purposes and reimbursement decisions. Nevertheless, considerations to determine surgical therapy are multifactorial and vary widely among institutions around the world. In our opinion indices should not be used as a hard criterion to determine surgical candidacy or its reimbursement but be part of the multifactorial decision wherein more attention is given to physiological symptoms such as cardiac and pulmonary impairment. To quantify cardiac function one may for example use the cardiac index, which was investigated by Maagaard et al. [4] and shown to increase following minimally invasive PE repair.

One of the main disadvantages of 3D scanning versus cross-sectional imaging is the missing intrathoracic anatomical information, such as sternal torsion and (cardio) pulmonary impression. However, as the majority of cases are not severe, they do not necessarily require cross-sectional imaging and a 3D optical image would suffice. Additional cross-sectional imaging could then be reserved for severe cases that are suspected for intrathoracic anomalies of the underlying heart and lungs. Cardiopulmonary impairment may also be assessed functionally by e.g., an electrocardiogram (ECG), echocardiography and spirometry, but their relation to cross-sectional imaging is yet to be investigated. Hypothetically, such diagnostics may even outperform conventional cross-sectional imaging as it provides dynamic information on (cardio) pulmonary functioning. For example, heart valve diseases and pulmonary function can neither be assessed by CT nor plain radiography nor with a 3D scan. It should subsequently be advised to offer functional tests such as ECG, echocardiography and spirometry or body plethysmography as adjunct methods to the standard preoperative panel, regardless of the imaging technique used to determine pectus severity. Another limitation is that 3D scans rely on body constitution. Measures in obese and female (because of the mammae) patients may subsequently differ from thin and male patients. Nevertheless, in contrast to cross-sectional images, 3D scans can be repeated endlessly without exposure to ionizing radiation. In most centers, 3D optical scanners are not available, whereas the vast majority features equipment to acquire CT-scans and plain radiographies. However, a reduction in exposure to radiation may easily justify the one-time costs of a 3D scanner.

During the respiratory cycle, chest dimensions are dynamic with the minimum anteroposterior diameter being achieved following full expiration. At this point,

the external and internal HI [i.e., (E)HI] are maximum, as also found by Birkemeier et al. [20] and Albertal et al. [21] who, moreover, reported PE severity indices to be significantly more severe at end-expiration. In this review, only Uccheddu et al. [17] acquired their 3D scans at end-expiration. In addition, no studies reported the respiratory phase in which the CT was acquired. Reported index values may subsequently be an underestimation.

None of the included studies compared their 3D scan severity measurements to those based on chest radiographies. Still, standard two-view chest radiographies are commonly acquired in the daily work- and follow-up of pectus patients and serve as a valid alternative to CT-scans [22]. Despite a reduction in dose compared to CT, chest radiographies still require exposure to radiation that is associated with long-term side effects ranging from growth derangements to malignancies [6, 7]. Following similar dogmas of minimization of radiation exposure and its potential harm, chest radiographies should ideally be replaced by a radiation free imaging method, such as 3D optical surface scanning. MRI could also serve as a radiation free alternative to radiographies and CT-scans. Its feasibility has already been demonstrated by Birkemeier et al. [23], while Lo Piccolo and colleagues [24] even found comparable severity values, comparing MRI and CT-scans. However, MRI is generally associated with increased costs, reduced availability, is more time-consuming, difficult to perform in claustrophobic patients, motion sensitive, and requires sedation in young patients, making it a less attractive alternative [23, 24].

Conclusion

In conclusion, 3D optical scanning is an attractive, feasible and promising imaging technique to determine the severity of PE without exposure to ionizing radiation. No evidence was found that supports nor discards the use of 3D scans to determine PC severity. Meta-analytical review of participants with PE demonstrated a pooled correlation of 0.89 between the CT derived HI and its 3D scan equivalent based on external measures. However, despite this high correlation, further research is imperative for 3D scans to be used in the clinical process of decision making and help determine surgical candidacy.

References

1. Chung CS, Myriantopoulos NC. Factors affecting risks of congenital malformations. I. Analysis of epidemiologic factors in congenital malformations. Report from the Collaborative Perinatal Project. *Birth Defects Orig Artic Ser* 1975;11:1-22.
2. Desmarais TJ, Keller MS. Pectus carinatum. *Curr Opin Pediatr* 2013;25:375-81.
3. Kelly RE, Jr., Cash TF, Shamberger RC, Mitchell KK, Mellins RB, Lawson ML et al. Surgical repair of pectus excavatum markedly improves body image and perceived ability for physical activity: multicenter study. *Pediatrics* 2008;122:1218-22.
4. Maagaard M, Tang M, Ringgaard S, Nielsen HHM, Frøkiær J, Haubuf M et al. Normalized Cardiopulmonary Exercise Function in Patients With Pectus Excavatum Three Years After Operation. *The Annals of Thoracic Surgery* 2013;96:272-8.
5. Haller JA, Jr., Kramer SS, Lietman SA. Use of CT scans in selection of patients for pectus excavatum surgery: a preliminary report. *J Pediatr Surg* 1987;22:904-6.
6. Brenner D, Elliston C, Hall E, Berdon W. Estimated risks of radiation-induced fatal cancer from pediatric CT. *AJR Am J Roentgenol* 2001;176:289-96.
7. Don S. Radiosensitivity of children: potential for overexposure in CR and DR and magnitude of doses in ordinary radiographic examinations. *Pediatr Radiol* 2004;34 Suppl 3:S167-72; discussion S234-41.
8. Sarwar ZU, DeFlorio R, O'Connor SC. Pectus excavatum: current imaging techniques and opportunities for dose reduction. *Semin Ultrasound CT MR* 2014;35:374-81.
9. Pazos V, Cheriet F, Song L, Labelle H, Dansereau J. Accuracy assessment of human trunk surface 3D reconstructions from an optical digitising system. *Medical and Biological Engineering and Computing* 2005;43:11-5.
10. Grant CA, Johnston M, Adam CJ, Little JP. Accuracy of 3D surface scanners for clinical torso and spinal deformity assessment. *Med Eng Phys* 2019;63:63-71.
11. Moher D, Liberati A, Tetzlaff J, Altman DG, Group P. Preferred reporting items for systematic reviews and meta-analyses: the PRISMA statement. *PLoS medicine* 2009;6:e1000097-e.
12. Mukaka MM. Statistics corner: A guide to appropriate use of correlation coefficient in medical research. *Malawi medical journal : the journal of Medical Association of Malawi* 2012;24:69-71.
13. National Heart L, and Blood Institute. Quality Assessment Tool for Observational Cohort and Cross-Sectional Studies. In. 2017.
14. Glinkowski W, Sitnik R, Witkowski M, Kocoń H, Bolewicki P, Górecki A. Method of pectus excavatum measurement based on structured light technique. *J Biomed Opt* 2009;14:044041.
15. Hebal F, Port E, Hunter CJ, Malas B, Green J, Reynolds M. A novel technique to measure severity of pediatric pectus excavatum using white light scanning. *J Pediatr Surg* 2019;54:656-62.
16. Poncet P, Kravarusic D, Richart T, Evison R, Ronsky JL, Alassiri A et al. Clinical impact of optical imaging with 3-D reconstruction of torso topography in common anterior chest wall anomalies. *J Pediatr Surg* 2007;42:898-903.

17. Uccheddu F, Ghionzoli M, Volpe Y, Servi M, Furferi R, Governi L et al. A Novel Objective Approach to the External Measurement of Pectus Excavatum Severity by Means of an Optical Device. *Ann Thorac Surg* 2018;106:221-7.
18. Bliss DP, Jr., Vaughan NA, Walk RM, Naiditch JA, Kane AA, Hallac RR. Non-Radiographic Severity Measurement of Pectus Excavatum. *J Surg Res* 2019;233:376-80.
19. Wong KE, Gorton GE, 3rd, Tashjian DB, Tirabassi MV, Moriarty KP. Evaluation of the treatment of pectus carinatum with compressive orthotic bracing using three dimensional body scans. *J Pediatr Surg* 2014;49:924-7.
20. Birkemeier KL, Podberesky DJ, Salisbury S, Serai S. Breathe in... breathe out... stop breathing: does phase of respiration affect the Haller index in patients with pectus excavatum? *AJR Am J Roentgenol* 2011;197:W934-9.
21. Albertal M, Vallejos J, Bellia G, Millan C, Rabinovich F, Buella E et al. Changes in chest compression indexes with breathing underestimate surgical candidacy in patients with pectus excavatum: a computed tomography pilot study. *J Pediatr Surg* 2013;48:2011-6.
22. Mueller C, Saint-Vil D, Bouchard S. Chest x-ray as a primary modality for preoperative imaging of pectus excavatum. *J Pediatr Surg* 2008;43:71-3.
23. Birkemeier KL, Podberesky DJ, Salisbury S, Serai S. Limited, fast magnetic resonance imaging as an alternative for preoperative evaluation of pectus excavatum: a feasibility study. *J Thorac Imaging* 2012;27:393-7.
24. Lo Piccolo R, Bongini U, Basile M, Savelli S, Morelli C, Cerra C et al. Chest fast MRI: an imaging alternative on pre-operative evaluation of Pectus Excavatum. *J Pediatr Surg* 2012;47:485-9.

Supplementary data

Supplementary Data S1: PubMed

Overview		
Interface	PubMed.com	
Date of search	April 30 th , 2019	
Number of results	721	
Syntax guide		
Mesh	Medical subject headings	
Mesh:NoExp	Medical subject headings without explosion	
tiab	Words in title or abstract	
*	Truncation	
Search	Query	Items found
#1	"funnel chest"[Mesh]	2,301
#2	funnel chest*[tiab] OR pectus excavatum*[tiab] OR funnel breast*[tiab] OR chonechondrosternon[tiab] OR funnel thorax[tiab] OR foveated chest*[tiab] OR foveated thorax[tiab] OR koilosternia[tiab]	25,89
#3	"pectus carinatum"[Mesh]	85
#4	pectus carinatum*[tiab] OR pouter pigeon breast*[tiab] OR pigeon chest*[tiab] OR pigeon breast*[tiab] OR pouter breast*[tiab] OR pigeon thorax[tiab]	584
#5	"sternum"[Mesh]	9,019
#6	sternum*[tiab]	6,663
#7	"thoracic wall"[Mesh]	4,034
#8	thorax wall*[tiab] OR thoracic wall*[tiab] OR chest wall*[tiab]	18,256
#9	#1 OR #2 OR #3 OR #4 OR #5 OR #6 OR #7 OR #8	33,053
#10	"imaging, three-dimensional"[Mesh:NoExp]	65,671
#11	3 D Imag*[tiab] OR three dimensional imag*[tiab] OR optic*[tiab] OR 3D imag*[tiab] OR threedimensional imag*[tiab] OR three dimensional reconstructi*[tiab] OR three-dimensional reconstructi*[tiab] OR 3 D scan*[tiab] OR three dimensional scan*[tiab] OR 3D scan*[tiab] OR threedimensional scan*[tiab] OR white light*[tiab] OR structured light*[tiab] OR laser*[tiab] OR body scan*[tiab] OR body imag*[tiab] OR torso scan*[tiab] OR torso imag*[tiab] OR modulated light*[tiab] OR torso topograp*[tiab]	608,365
#12	#10 OR #11	661,332
#13	#9 AND #12	721

Supplementary Data S2: EMBASE

Overview

Interface	EMBASE.com
Date of search	April 30 th , 2019
Number of results	1,061

Syntax guide

/exp	EMtree keyword with explosion
/de	EMtree keyword without explosion
:ab,ti	Words in title or abstract
*	Truncation

Search	Query	Items found
#1	'funnel chest'/exp	3,661
#2	'pigeon thorax'/exp	983
#3	'thorax wall'/exp	12,946
#4	'chest wall*':ab,ti OR 'thorax wall*':ab,ti OR 'thoracic wall*':ab,ti	25,818
#5	'chicken breast*':ab,ti OR 'pectus carinatum*':ab,ti OR 'pectus carinatus':ab,ti OR 'pigeon breast*':ab,ti OR 'pigeon thorax':ab,ti OR 'pigeon chest*':ab,ti OR 'pouter breast*':ab,ti OR sternum*':ab,ti	10,064
#6	'funnel breast*':ab,ti OR 'funnel chest*':ab,ti OR chonechondrosternon:ab,ti OR 'foveated chest*':ab,ti OR 'foveated thorax':ab,ti OR 'funnel thorax':ab,ti OR koilosternia:ab,ti OR 'pectus excavatum':ab,ti	3,120
#7	#1 OR #2 OR #3 OR #4 OR #5 OR #6	40,180
#8	'white light'/exp	3,635
#9	'three dimensional imaging'/de	85,213
#10	'three-dimensional imag*':ab,ti OR 'three dimensional imag*':ab,ti OR 'three dimensional reconstructi*':ab,ti OR 'three-dimensional reconstructi*':ab,ti OR '3 d imag*':ab,ti OR '3d scan*':ab,ti OR 'three dimensional scan*':ab,ti OR '3d scan*':ab,ti OR 'threedimensional scan*':ab,ti OR 'white light*':ab,ti OR 'structured light*':ab,ti OR laser*':ab,ti OR 'body scan*':ab,ti OR 'body imag*':ab,ti OR 'torso scan*':ab,ti OR 'torso imag*':ab,ti OR 'modulated light*':ab,ti OR 'torso topograp*':ab,ti	599,282
#11	#8 OR #9 OR #10	666,938
#12	#7 AND #11	1,061

Supplementary Data S3: Web of Science**Overview**

Interface Web of Science / Clarivate Analytics

Date of search April 30th, 2019

Number of results 2,290

Syntax guide

* Truncation

Search	Query	Items found
#1	<p>TOPIC: (funnel breast* OR funnel chest* OR chonechondrosternon OR foveated chest* OR foveated thorax OR funnel thorax OR koilosternia OR pectus excavatum OR chicken breast* OR pectus carinatum* OR pectus carinatus OR pigeon breast* OR pigeon thorax OR pigeon chest* OR pouter breast* OR sternum* OR chest wall* OR thorax wall* OR thoracic wall*)</p> <p><i>Indexes=SCI-EXPANDED, SSCI, A&HCI, ESCI Timespan=All years</i></p>	35,752
#2	<p>TOPIC: (three-dimensional imag* OR three dimensional imag* OR three dimensional reconstructi* OR three-dimensional reconstructi* OR 3 d imag* OR optic* OR 3d imag* OR threedimensional imag* OR 3 d scan* OR three dimensional scan* OR 3d scan* OR threedimensional scan* OR white light* OR structured light* OR laser* OR body scan* OR body imag* OR torso scan* OR torso imag* OR modulated light* OR torso topograp*)</p> <p><i>Indexes=SCI-EXPANDED, SSCI, A&HCI, ESCI Timespan=All years</i></p>	2,277,572
#3	<p>#1 AND #2</p> <p><i>Indexes=SCI-EXPANDED, SSCI, A&HCI, ESCI Timespan=All years</i></p>	2,290

Supplementary Data S4: Cochrane Library

Overview

Interface	Cochrane Library / Wiley
Date of search	April 30 th , 2019
Number of results	142 (Cochrane reviews: 2; Trials: 140)

Syntax guide

ti,ab,kw	Words in title, abstract or author keywords
*	Truncation

Search	Query	Items found
#1	(funnel breast* OR funnel chest* OR chonechondrosternon OR foveated chest* OR foveated thorax OR funnel thorax OR koilosternia OR pectus excavatum OR chicken breast* OR pectus carinatum* OR pectus carinatus OR pigeon breast* OR pigeon thorax OR pigeon chest* OR pouter breast* OR sternum* OR chest wall* OR thorax wall* OR thoracic wall*);ti,ab,kw	2,569
#2	(three-dimensional imag* OR three dimensional imag* OR three dimensional reconstructi* OR three-dimensional reconstructi* OR 3 d imag* OR optic* OR 3d imag* OR threedimensional imag* OR 3 d scan* OR three dimensional scan* OR 3d scan* OR threedimensional scan* OR white light* OR structured light* OR laser* OR body scan* OR body imag* OR torso scan* OR torso imag* OR modulated light* OR torso topograp*);ti,ab,kw	45,883
#3	#1 AND #2	142

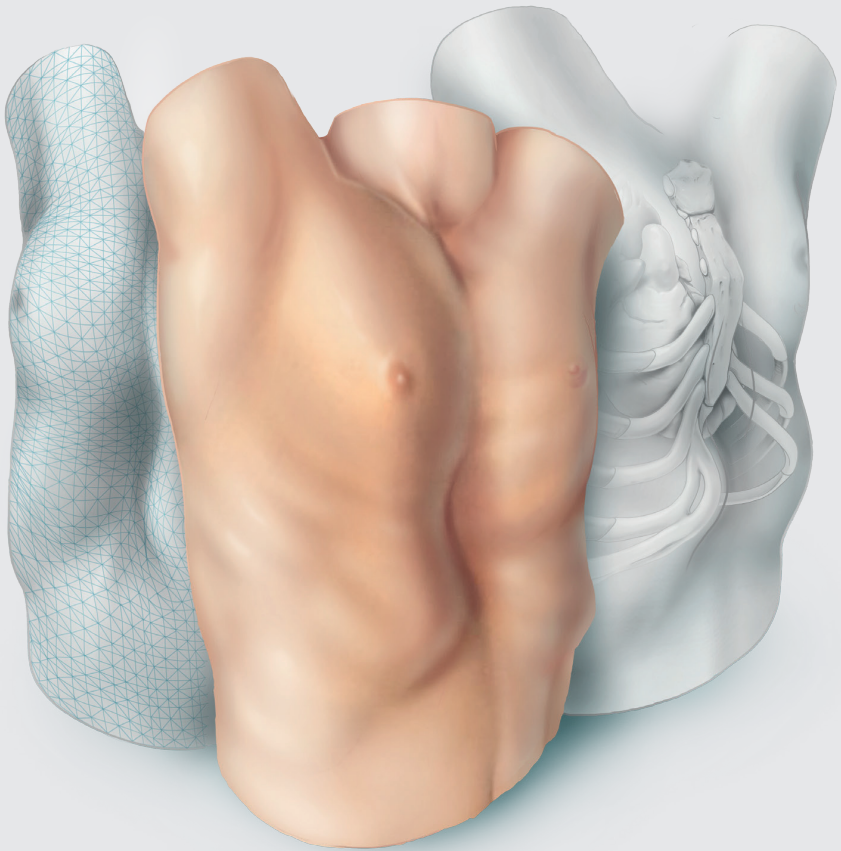
Supplementary Data S5: CINAHL**Overview**

Interface	CINAHL / EBSCOhost
Date of search	April 30 th , 2019
Number of results	98

Syntax guide

TI	Words in title
AB	Words in abstract
*	Truncation

Search ID#	Query	Items found
S1	TI (funnel breast* OR funnel chest* OR chonechondrosternon OR foveated chest* OR foveated thorax OR funnel thorax OR koilosternia OR pectus excavatum OR chicken breast* OR pectus carinatum* OR pectus carinatus OR pigeon breast* OR pigeon thorax OR pigeon chest* OR pouter breast* OR sternum* OR chest wall* OR thorax wall* OR thoracic wall*)	1,250
S2	AB (funnel breast* OR funnel chest* OR chonechondrosternon OR foveated chest* OR foveated thorax OR funnel thorax OR koilosternia OR pectus excavatum OR chicken breast* OR pectus carinatum* OR pectus carinatus OR pigeon breast* OR pigeon thorax OR pigeon chest* OR pouter breast* OR sternum* OR chest wall* OR thorax wall* OR thoracic wall*)	3,143
S3	S1 OR S2	3,797
S4	TI (three-dimensional imag* OR three dimensional imag* OR three dimensional reconstructi* OR three-dimensional reconstructi* OR 3 d imag* OR optic* OR 3d imag* OR threedimensional imag* OR 3 d scan* OR three dimensional scan* OR 3d scan* OR threedimensional scan* OR white light* OR structured light* OR laser* OR body scan* OR body imag* OR torso scan* OR torso imag* OR modulated light* OR torso topograp*)	22,666
S5	AB (three-dimensional imag* OR three dimensional imag* OR three dimensional reconstructi* OR three-dimensional reconstructi* OR 3 d imag* OR optic* OR 3d imag* OR threedimensional imag* OR 3 d scan* OR three dimensional scan* OR 3d scan* OR threedimensional scan* OR white light* OR structured light* OR laser* OR body scan* OR body imag* OR torso scan* OR torso imag* OR modulated light* OR torso topograp*)	39,431





Photographic documentation and severity quantification of pectus excavatum through three- dimensional optical surface imaging

Jean H.T. Daemen, Tom G.J. Loonen, Nadine A. Coorens, Jos G. Maessen,
Thomas J.J. Maal, Karel W.E. Hulsewé, Yvonne L.J. Vissers, Erik R. de Loos

Adapted from: J Vis Commun Med 2020;43:190-7.

Abstract

Conventional photography is commonly used to visually document pectus excavatum and objectively assess chest wall changes over time without repeated exposure to ionizing radiation, as in our centre since 2008. However, as conventional photography is labor-intensive and lacks three-dimensional (3D) information that is essential in 3D deformities like pectus excavatum, we developed a novel imaging and processing protocol based on 3D optical surface imaging. The objective of this study was to report our developed protocol to visually document pectus excavatum through 3D imaging. We also investigated the absolute agreement of the 3D image- and conventional photography-derived pectus excavatum depth to investigate whether both techniques could be used interchangeably to measure pectus excavatum depth and assess its evolution. The protocol consisted of three consecutive steps: patient positioning and instructions, data acquisition, and data processing. Three-dimensional imaging through the developed protocol was feasible for all 19 participants. The 3D image- and photography-derived pectus excavatum depth demonstrated good to excellent agreement (intraclass correlation coefficient: 0.97; 95%-confidence interval: 0.88 to 0.99; $P < 0.001$). In conclusion, 3D imaging through the developed protocol is a feasible and attractive alternative to document the surface geometry of pectus excavatum and can be used interchangeably with conventional photography to determine pectus severity.

Introduction

Pectus excavatum, also known as funnel chest, is the most common congenital anterior chest wall anomaly. It is characterized by a funnel-shaped thoracic deformity and often accompanied by winging (i.e. excessive outgrowth) of costae 8 to 10. In some cases, this may be accompanied by a disfiguring sternal rotation with unilateral costochondral prominence. Pectus excavatum is present in approximately 1 in 300-400 children and predominantly affects the male sex [1-3]. In 45% of cases there is a positive family history [4]. Patients with pectus excavatum often suffer from an impaired body image perception with subsequent lowered self-esteem, quality of life and increased psychological stress [5]. The inwardly deviated sternum may also cause cardiopulmonary impairment such as exercise intolerance, shortness of breath and fatigue [4]. Standard preoperative evaluation differs among institutions but conventionally includes computed tomography, pulmonary function tests and cardiac evaluation [4, 6] while numerous centres additionally perform photographic documentation of the deformity. Acquired photographs are used for preoperative planning purposes, to create insight into the patients' own disease and comparison with the postoperative result to assess (aesthetic) improvement. Nevertheless, the main application of photographic documentation is that it can be used to objectively assess chest wall changes over time without repeated exposure to ionizing radiation. This information is used in the multidimensional decision to determine eligibility for corrective surgery where progression of the deformity is one of the indications [4, 6]. The process of photographic documentation has previously been standardized and described by our former colleagues [7]. This documentation includes five routine photographs acquired from different angles and two special recordings. The latter encompass recordings used to determine the pectus excavatum depth and create a three-dimensional perspective image (i.e., rasterstereography). The resulting pectus excavatum depth is, as above-mentioned, used as an objective marker of pectus severity and used to objectively assess evolution of the deformity. In our high-volume tertiary referral centre, all patients with pectus excavatum underwent photographic documentation of their deformity, following its introduction in May 2008. Nevertheless, documentation through conventional photography is a labor-intensive process while the resulting photographs are two-dimensional, making it impossible to obtain a profound three-dimensional visuospatial understanding of the deformity. We subsequently developed a novel imaging and processing

protocol to visually document pectus excavatum through three-dimensional (3D) optical surface imaging. Three-dimensional optical images of the chest are acquired by a 3D scanner whose main parts encompass two ordinary photo cameras and a structured white light projector that projects a structured grid onto the torso surface. The grids' distortion is then captured by the camera and analyzed to build a 3D image utilizing triangulation. The objective of this study is to report our newly developed protocol and its rationale to visually document pectus excavatum through three-dimensional optical surface imaging. We also investigate the absolute agreement of the 3D image- and conventional photography-derived pectus excavatum depth to determine whether 3D images can be used to quantify pectus severity and follow its evolution over time.

Methods

Three-dimensional imaging protocol

In Zuyderland Medical Centre (Heerlen, the Netherlands) we developed a dedicated protocol to standardize visual documentation of pectus excavatum through 3D optical surface imaging. Consecutive steps include patient positioning and instructions, data acquisition, and data processing. Rationale was given for all choices made.

Patient positioning and instructions

Prior to acquisition, the patient is asked to stand in an upright position with their hands on the back of the head. Patients with long hair are requested to lift up their hair. These measures are necessary to guarantee adequate torso exposure for imaging and prevent artifacts introduced by hair. To enhance comparability with standard radiographical images (that are often acquired during breath hold) patients are asked to breath in and hold their breath for the images' duration (at maximum 20 seconds). Those who are unable to hold breath are requested to breathe as superficially as possible. The resulting motion artifacts may be corrected later on during processing.

Data acquisition

Three-dimensional images were acquired by the Artec Leo scanner (Artec3D, Luxembourg, Luxembourg). This handheld device weighs 2.6 kilograms and is

equipped with two color cameras and a white light projector to digitize real-world objects with the speed of 80 frames per second (Figure 1 & Table 1). It has a 3D point accuracy and resolution of up to 0.1 and 0.5 millimeters, respectively. The scanner operates by projecting a light pattern onto the patient's torso, capture its deformation from different angles and calculate the distance to specific torso points using triangulation. The resulting 3D point cloud is used to build a digital 3D torso reconstruction. We chose to use a handheld scanner instead of a static frame-mounted 3D stereophotogrammetry setup (such as 3dMD imaging systems) because of its transportability and possible use in unconventional places and settings such as operating theatres. The Artec Leo scanner was specifically chosen because it was the only commercially available handheld, battery-powered device with real-time visualization of the area captured, allowing easy fill in of any chest areas missed, making it intuitive and user-friendly. In addition, it was the only handheld device with a built-in 9-degrees of freedom inertial system, allowing the scanner to understand its position and environment. This means that the orientation of the scanned chest is known in the world-coordinate system. To acquire 360° chest images the scanner is circumferentially moved around the patient on an optimum working distance of 50 centimeters. Due to its large field of view (height 38.5°, width 23°) there is no need to vertically translate the scanner to capture the entire torso. The scan window is cranially and caudally bordered at the transversal level of the clavicle and umbilicus, respectively. The umbilicus was chosen to capture the entire disfiguring effect of winging that is present in part of the pectus excavatum patients.

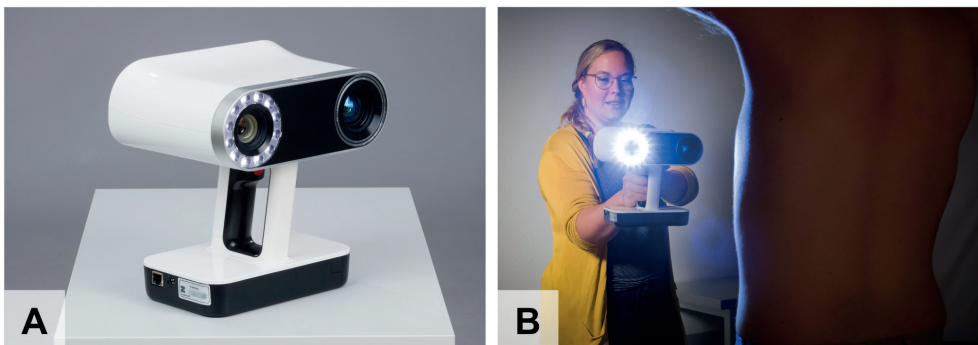


Figure 1: (A) The Artec Leo scanner that is used to (B) acquire three-dimensional optical surface images of the chest.

Table 1: Specifications of the Artec Leo three-dimensional imaging system.

Weight	2.6 kilograms
Framerate, up to	80 frames/second
Point accuracy, up to	0.1 millimeters
Resolution, up to	0.5 millimeters
Acquisition speed, up to	3 million points/second
Angular field of view	height 38.5°, width 23°
Working distance	0.35 to 1.2 meters

°, degrees

Data processing

Following acquisition, the raw image data (Figure 2A) is transferred to a mobile working station and processed using Artec Studio 14.0 (Artec3D, Luxembourg, Luxembourg). First of all, a global registration is performed of all single image frames. The algorithm first aligns all key frames on the basis of texture and geometry where-after missing information is filled using overlapping (non-key) frames that are selected within the given tolerance. Key frames are frames that describe the chest geometry and texture with as few frames as possible and are acquired upon scanner translation or if a new part of the target object comes into view. Next, single 3D image-frames are fused to create a watertight model (Figure 2B). Fusion is performed by the sharp fusion function and preferred over the smooth fusion function due to its superior calculation speed, as well as the level of detail and watertightness. However, in the presence of motion artifacts the smooth fusion function should be chosen since it is able to compensate for slight movement, such as shallow breathing. Isolated structures (see blue circle, Figure 2B) that are not attached to the chest (i.e. main object) often result from noise and can be easily removed using the small objects filter that leaves the biggest object. The resulting mesh may be simplified using the mesh simplification function to create a less data consuming mesh. This step of simplification can be based on different algorithms that optimize the model until the predetermined allowable deviation from the original model has been reached, remove triangles whose edge length is less than the predefined value, or an algorithm that optimizes the mesh until the specified number of triangles has been achieved. However, with this latter algorithm, the final deviation from the original model will remain unknown. Mesh simplification is not performed at an earlier stage as data points needed for reconstruction may be lost. In addition, it should also be kept in mind that refined meshes are always an approximation of the original model with a certain deviation

that potentially impairs model accuracy. Models that still contain unwanted mesh holes can be closed using the fix holes function, following smoothing of the holes' edges. Holes are fixed by triangulation of the shortest distance between edges. As a last step the textures from the individual frames are applied on the fused mesh to create a textured, life-like thoracic model (Figure 2C).

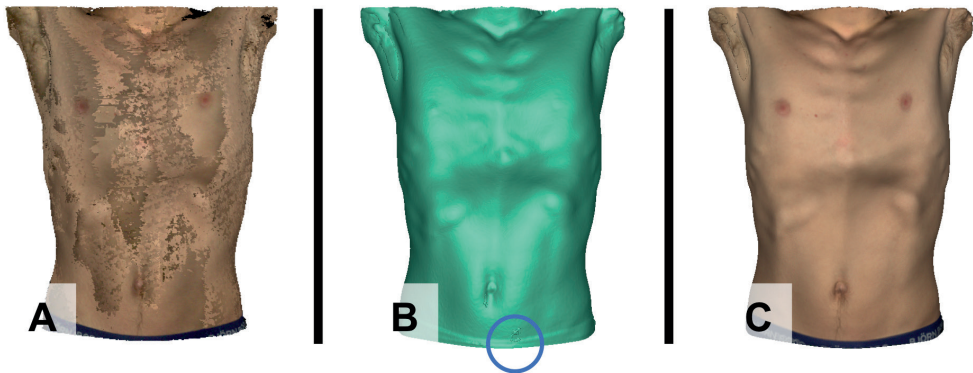


Figure 2: The processing process, shown from left to right. (A) Raw three-dimensional image data. (B) Fused three-dimensional image data. The blue circle demonstrates an isolated structure that is removed using the small objects filter. (C) Postprocessed three-dimensional image with applied texture map.

Agreement of pectus excavatum depth

Study design and setting

To investigate agreement, we conducted a single-centre retrospective case-control study wherein participants were their own control. The study was conducted in Zuyderland Medical Centre, Heerlen, the Netherlands. All images and participant characteristics were retrospectively collected from the available records. Prior to start, the study was approved by the local ethical committee for scientific research (METC Zuyderland, ID: METCZ20190151, 12 December 2019) and registered to the Clinicaltrials.gov trial registry (unique identification number: NCT04185870). The need for written informed consent was waived.

Participants

All patients with pectus excavatum that were referred to our outpatient clinic of thoracic surgery (Zuyderland Medical Centre, Heerlen, the Netherlands) from August to December 2019 were eligible for inclusion. Prior to consultation, standard

photographs (including the special recordings) and an additional 3D image were made to visually document their pectus excavatum. All patients that were imaged according to the full 3D image and conventional photography protocols during the transition phase were included.

Measurements

The agreement of the conventional photography and 3D image derived pectus excavatum depth was investigated to investigate whether 3D images could be used to quantify pectus depth and assess its evolution over time. To determine the 3D image-based pectus excavation depth, the 3D image was sliced in the transversal direction. The slice presenting the most severe excavation was selected for calculation. The tangent of the anterior chest wall was used as a reference line from which the depth was measured perpendicularly (see Figure 3A). The conventional photography derived pectus excavatum depth (part of the conventional photography protocol described elsewhere [7]) was calculated by placement of a rigid bar with digital ruler over the most excavated part of the thorax in the transversal direction (see Figure 3B) and captured from the right frontal oblique position at an angle of 45° downwards. Photographs were made with a single-reflex camera in a specially equipped photographic studio under identical and fixed conditions to guarantee uniformity and comparability of photographs. All photography-based pectus excavation depth measurements were alternately performed by two medical photographers, while the 3D image measurements were performed by a single researcher, fully blinded for the photography-based pectus excavatum depth results.

Statistical analyses

Statistical analyses were performed using SPSS statistics (IBM Corp. Released 2017. IBM SPSS Statistics for MacOS, Version 25.0, Armonk, NY, USA). Nominal variables were denoted as number of the total. Continuous variables were denoted as mean and standard deviation (SD) or median and interquartile range (IQR) in the presence of skewness. The presence of skewness was visually assessed by inspection of normal probability plots and histograms, and statistically by the Shapiro-Wilk test. P-values <0.05 were considered to be statistically significant. The difference between the mean pectus excavatum depths was assessed by the paired samples t-test since participants were their own control. In the presence of

skewness, the non-parametric Wilcoxon signed rank test was used. An arbitrarily chosen difference larger than 10% of the mean or median was considered clinically relevant. To assess absolute agreement of the 3D image- and photography measured pectus excavatum depths, the intraclass correlation coefficient (ICC) and its 95%-confidence interval (CI) was used. The ICC was based on a single-rater ($k=1$), absolute agreement, two-way mixed-effects model. The intraclass correlation coefficient was preferred over the Pearson's correlation coefficient as it reflects both the degree of correlation and agreement [8]. The resultant ICC and its 95%-CI were interpreted as follows: values less than 0.50 indicate poor reliability, whereas values from 0.50 to 0.75, 0.75 to 0.90, and values greater than 0.90 are indicative of moderate, good and excellent agreement, respectively [8].

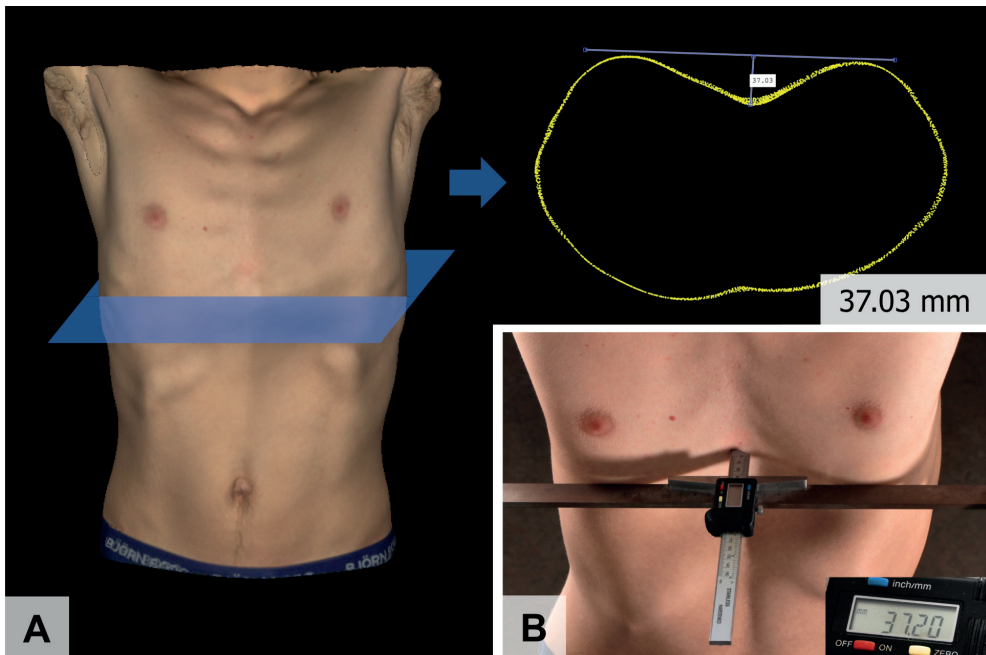


Figure 3: (A) Preoperative pectus excavatum depth based on a transversal three-dimensional chest image slice (37.03 mm.) and (B) its equivalent rule measured pectus excavatum depth recording (37.20 mm.).
mm, millimeters.

Results

Between August and December 2019, 23 patients underwent photographic documentation of their pectus excavatum through 3D imaging and conventional photography. Of these potentially eligible participants, 19 were imaged according to the specified protocols and subsequently included. Four female patients were excluded because their photography-based pectus excavatum depth was measured in the sagittal plane instead of the protocolized transversal plane. The sagittal measurement was chosen by the medical photographers because the breast size of these patients would have caused an overestimation of the true depth in the transversal plane. Of the included participants, 18 were male and 1 female with a median age of 15.8 years (IQR: 3.1) at the time of 3D image acquisition. The mean body mass index was 19.0 kg/m² (SD: 2.4). Acquisition of 3D images was feasible for all participants while no participants required more than one image attempt (see examples in Figure 4.) Three-dimensional image acquisition times ranged from 10 to 16 seconds while processing took 5 minutes on average. The mean 3D image-based pectus depth was 21.3 mm. (SD: 8.3), whereas the mean photography-based depth was 22.5 mm. (SD: 8.6). Paired samples t-test demonstrated a statistically significant mean difference (P=0.006) of 1.20 mm. (SD:1.70) between the 3D image- and photography-based pectus depth. However, this difference was not considered clinically relevant. Visual assessment of the conventional photography versus 3D image measurements scatter plot (see Figure 5) revealed the presence of a positive correlation. This was statistically confirmed by the ICC that was 0.97 (95%-CI: 0.88 to 0.99; P<0.001); indicating a good to excellent agreement between 3D image-based and photography-measured pectus excavatum depth.

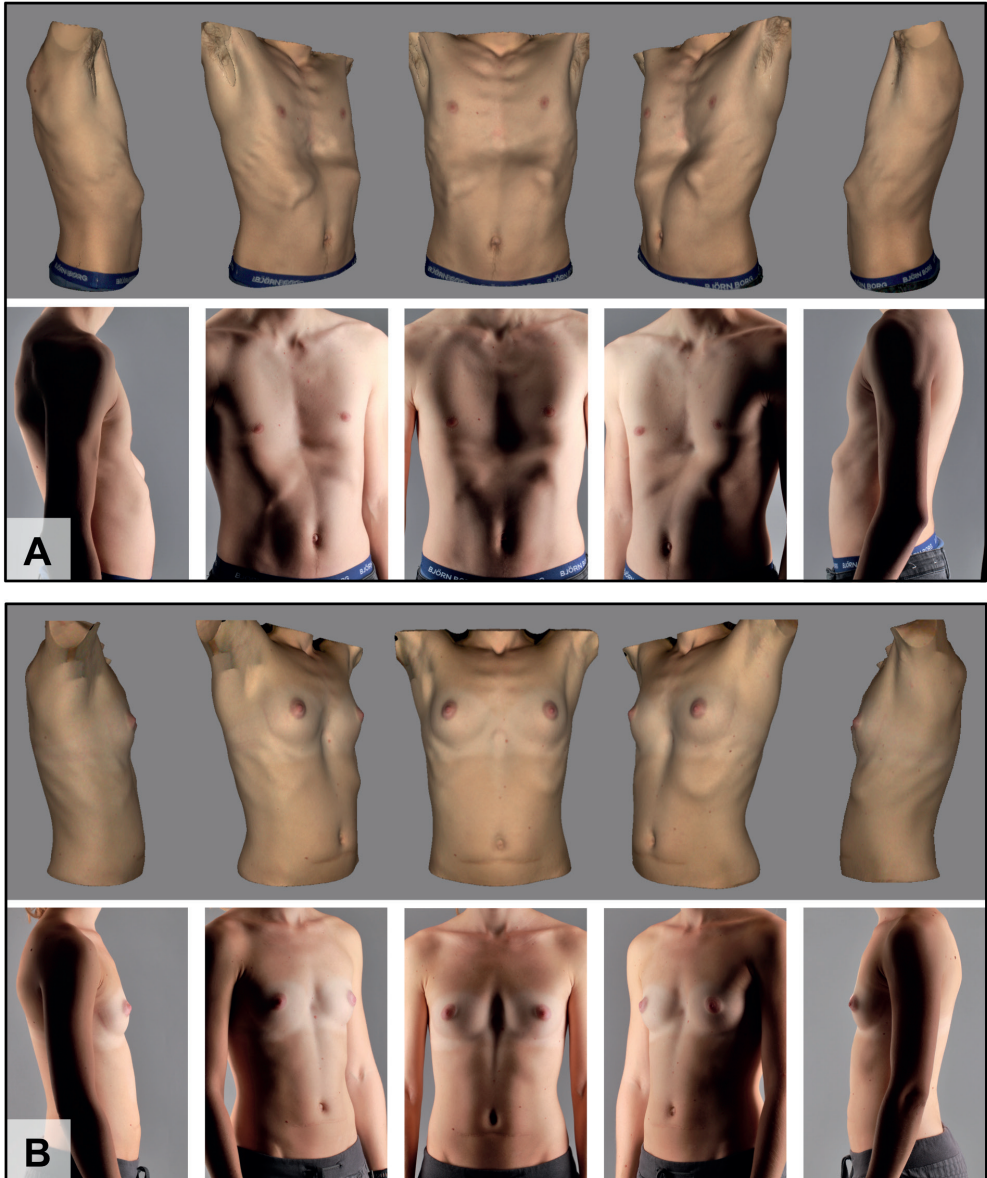


Figure 4: Three-dimensional images from a (A) 16 year old male and (B) 24 year old female participant, shown from different angles with corresponding conventional photographs.

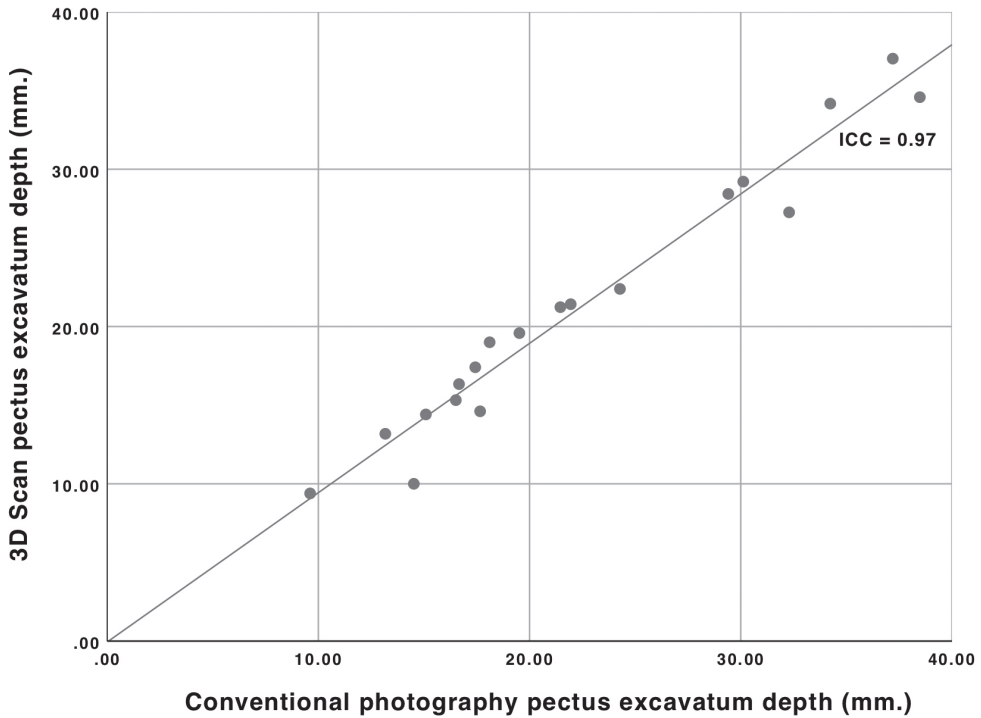


Figure 5: Scatterplot of the conventional photography versus three-dimensional image-based pectus excavatum depth measurements with linear regression line.

ICC, intraclass correlation coefficient.

Discussion

This study described the materials and methods used to document the surface geometry of pectus excavatum through three-dimensional optical surface imaging and investigated the absolute agreement between 3D image- and conventional photography-derived pectus excavatum depth that is used to quantify pectus severity and assess its changes over time. In total, 19 participants were included, and acquisition of 3D images was feasible for all participants. The pectus excavatum depth, an objective measure of severity, was used to determine the absolute agreement between both imaging modalities. The ICC demonstrated a good to excellent agreement. Paired samples t-test revealed a statistically significant but not clinically relevant mean difference of 1.20 mm. between the 3D image- and conventional photography-derived pectus excavatum depth. This overall higher

photography-based depth value may be caused by subcutaneous compression following application of the bar with ruler.

It was subsequently concluded that 3D images and conventional photographs can be used interchangeably for the quantification of pectus excavatum. Although 3D images and conventional photographs produce a visually identical representation of the chest, as seen in Figure 4, it is unknown whether they can be used fully interchangeably. This may for example be investigated by quantitative comparison of conventional photographs and 3D images acquired from a phantom or mannequin and should be subject of future research. In addition, reproducibility of 3D images was neither investigated and should also be subject of future research.

The incentive to start using three-dimensional optical images was primarily motivated by the fact that conventional photography was labor-intensive, given that repeated changes in camera and patient position alongside the use of additional tools was required [7], and the fact that the resulting images were two-dimensional, subsequently lacking depth information that is essential in the understanding of three-dimensional deformities like pectus excavatum. Acquisition of three-dimensional images took between 10 and 16 seconds whereas acquisition of conventional photographs took between 5 and 10 minutes. (Post)processing times of conventional photographs and 3D images were comparable (approximately 5 minutes), however, 3D image processing times may increase with increasing image size. The difference in acquisition time was likely to be caused by the simplicity of 3D image acquisitions in which there is no need to repeatedly change patient and camera positions or use additional tools; all seven conventional photographs can be replaced by a single 360° 3D image. Another advantage of three-dimensional images compared to two-dimensional conventional photographs is that they can promote visuospatial understanding of the deformity for surgeons. This effect has been previously investigated by Nicholson et al. (2006), who conducted a randomized controlled trial and found a positive effect of the use of 3D models of the ear on the knowledge of three-dimensional relationships [9].

As described by Van Dijk et al. (2011), conventional photography requires a specially equipped photographic studio with constant light output and color temperature. For 3D imaging there is no need for such regulated conditions because the scanner utilizes its own light source. As a consequence, images can be acquired in

unconventional places, such as the outpatient clinic or in the ward after surgery, allowing easy integration in the daily workflow. However, to be able to acquire the 3D images, a one-time investment is required. Scanner prices begin at around 500 euros and can go up to tens of thousands of euros with diminishing acquisition times and improving technical specifications. The Artec Leo scanner including software and mobile working station costed around 30,000 euros. Nevertheless, lower priced scanners may suffice because the chest is a geometrically simple object and the clinically relevant accuracy is unlikely to lie within one tenth of a millimeter.

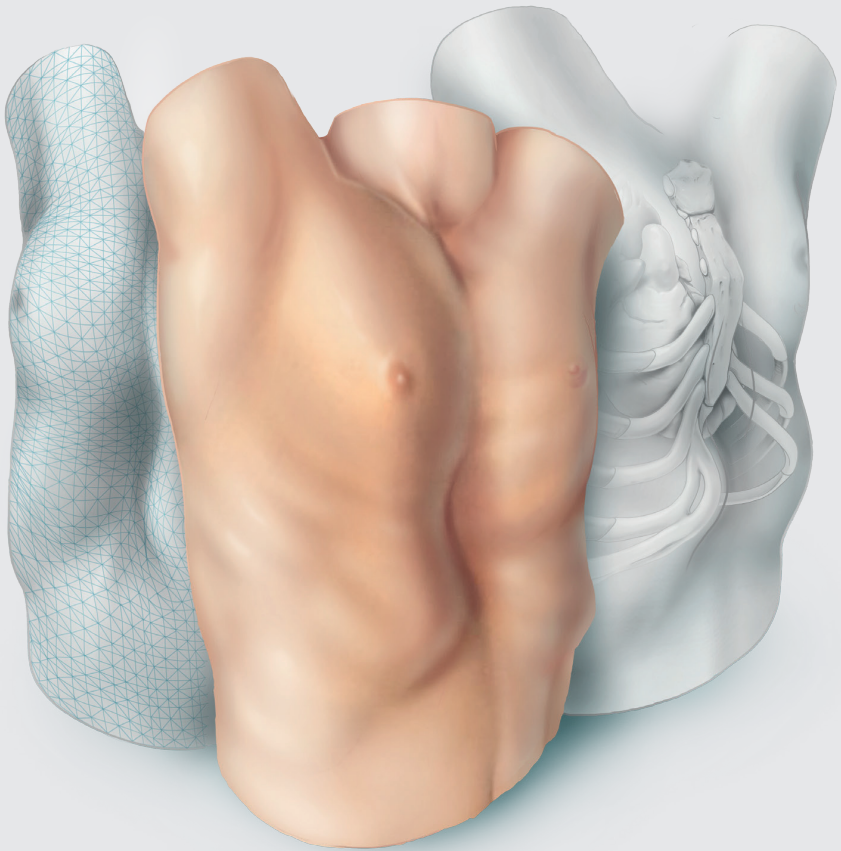
Until now, the rule-measured depth was the only photograph-derived measure to objectively assess thoracic wall changes after surgery. This measure is limited by the fact that it only provides information about one point while pectus morphologies are rather multiplanar. Utilizing pre- and postoperative 3D models one may create surface distance maps to objectively assess the effect of corrective surgery on the entire torso. In our opinion, 3D images are likely to take over the role of CT-images and two-view radiographies to determine pectus severity in standard patients within the coming years, since 3D images do not expose patients to ionizing radiation and its potential dangers. Several reports have already studied the use of three-dimensional imaging methods to quantify pectus severity, utilizing novel indices that are based on external measures [10-16]. These indices can also be derived from the 3D images that were acquired for the purpose of this study. However, the epidemiological value of these newly developed 3D image derived severity measures should be subject of future research before they can be used interchangeably with the current gold standard chest radiography or CT-derived Haller Index [17].

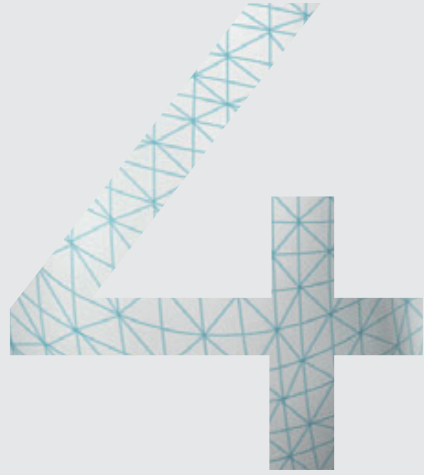
Conclusion

We developed and presented our dedicated protocol that can be used to document the surface geometry of pectus excavatum through three-dimensional optical surface imaging. Three-dimensional imaging in conjunction with this protocol is a feasible and attractive alternative to graphically document pectus excavatum and can be used interchangeably with conventional photography to determine the pectus excavatum depth.

References

1. Brochhausen C, Tural S, Müller FKP, Schmitt VH, Coerdts W, Wihlm J-M et al. Pectus excavatum: history, hypotheses and treatment options. *Interact Cardiovasc Thorac Surg* 2012;14:801-6.
2. Chung CS, Myrianthopoulos NC. Factors affecting risks of congenital malformations. I. Analysis of epidemiologic factors in congenital malformations. Report from the Collaborative Perinatal Project. *Birth Defects Orig Artic Ser* 1975;11:1-22.
3. Coskun ZK, Turgut HB, Demirsoy S, Cansu A. The Prevalence and Effects of Pectus Excavatum and Pectus Carinatum on the Respiratory Function in Children between 7-14 Years Old. *Indian J Pediatr* 2010;77:1017-9.
4. Goretsky MJ, Kelly RE, Jr., Croitoru D, Nuss D. Chest wall anomalies: pectus excavatum and pectus carinatum. *Adolesc Med Clin* 2004;15:455-71.
5. Lawson ML, Cash TF, Akers R, Vasser E, Burke B, Tabangin M et al. A pilot study of the impact of surgical repair on disease-specific quality of life among patients with pectus excavatum. *J Pediatr Surg* 2003;38:916-8.
6. Croitoru DP, Kelly RE, Goretsky MJ, Lawson ML, Swoveland B, Nuss D. Experience and modification update for the minimally invasive Nuss technique for pectus excavatum repair in 303 patients. *J Pediatr Surg* 2002;37:437-45.
7. van Dijk H, Hoppener PF, Siebenga J, Kragten HA. Medical photography: a reliable and objective method for documenting the results of reconstructive surgery of pectus excavatum. *J Vis Commun Med* 2011;34:14-21.
8. Koo TK, Li MY. A Guideline of Selecting and Reporting Intraclass Correlation Coefficients for Reliability Research. *Journal of chiropractic medicine* 2016;15:155-63.
9. Nicholson DT, Chalk C, Funnell WR, Daniel SJ. Can virtual reality improve anatomy education? A randomised controlled study of a computer-generated three-dimensional anatomical ear model. *Med Educ* 2006;40:1081-7.
10. Bliss DP, Jr., Vaughan NA, Walk RM, Naiditch JA, Kane AA, Hallac RR. Non-Radiographic Severity Measurement of Pectus Excavatum. *J Surg Res* 2019;233:376-80.
11. Glinkowski W, Sitnik R, Witkowski M, Kocoń H, Bolewicki P, Górecki A. Method of pectus excavatum measurement based on structured light technique. *J Biomed Opt* 2009;14:044041.
12. Hebal F, Port E, Hunter CJ, Malas B, Green J, Reynolds M. A novel technique to measure severity of pediatric pectus excavatum using white light scanning. *J Pediatr Surg* 2019;54:656-62.
13. Uccheddu F, Ghionzoli M, Volpe Y, Servi M, Furferi R, Governi L et al. A Novel Objective Approach to the External Measurement of Pectus Excavatum Severity by Means of an Optical Device. *Ann Thorac Surg* 2018;106:221-7.
14. Lain A, Garcia L, Gine C, Tiffet O, Lopez M. New Methods for Imaging Evaluation of Chest Wall Deformities. *Front Pediatr* 2017;5:257.
15. Poncet P, Kravarusic D, Richart T, Evison R, Ronsky JL, Alassiri A et al. Clinical impact of optical imaging with 3-D reconstruction of torso topography in common anterior chest wall anomalies. *J Pediatr Surg* 2007;42:898-903.
16. Daemen JHT, Loonen TGJ, Lozekoot PWJ, Maessen JG, Maal TJJ, Hulstewé KWE et al. Optical imaging versus CT and plain radiography to quantify pectus severity: a systematic review and meta-analysis. *J Thorac Dis* 2020;12:1475-87.
17. Haller JA, Jr., Kramer SS, Lietman SA. Use of CT scans in selection of patients for pectus excavatum surgery: a preliminary report. *J Pediatr Surg* 1987;22:904-6.





Three-dimensional imaging of the chest wall: a comparison between three different imaging systems

Jean H.T. Daemen, Tom G.J. Loonen, Arico C Verhulst, Thomas J.J. Maal, Jos G. Maessen, Karel W.E. Hulsewé, Yvonne L.J. Vissers, Erik R. de Loos

Adapted from: J Surg Res 2020;259:332-41.

Abstract

Background

Three-dimensional (3D) imaging is being used progressively to create models of patients with anterior chest wall deformities. Resulting models are used for clinical decision making, surgical planning and analysis. However, given the broad range of 3D imaging systems available and the fact that planning and analysis techniques are often only validated for a single system, it is important to analyze potential intra- and intersystem differences. The objective of this study was to investigate the accuracy and reproducibility of three commercially available 3D imaging systems that are used to obtain images of the anterior chest wall.

Methods

Among 15 healthy volunteers, 3D images of the anterior chest wall were acquired twice per imaging device. Reproducibility was determined by comparison of consecutive images acquired per device while the true accuracy was calculated by comparison of 3D image derived and calipered anthropometric measurements. A maximum difference of 1.00mm. was considered clinically acceptable.

Results

All devices demonstrated statistically comparable ($p=0.21$) reproducibility with a mean absolute difference of 0.59mm. (SD: 1.05), 0.54mm (SD: 2.08) and 0.48mm. (SD: 0.60) for the 3dMD, Einscan Pro 2X Plus and Artec Leo. The true accuracy was, respectively, 0.89mm. (SD: 0.66), 1.27mm. (SD: 0.94) and 0.81mm. (SD: 0.71) for the 3dMD, Einscan and Artec device, and did not statistically differ ($p=0.085$).

Conclusions

Three-dimensional imaging of the anterior chest wall utilizing the 3dMD and Artec Leo is feasible with comparable reproducibility and accuracy, while the Einscan Pro 2X Plus is reproducible but not clinically accurate.

Introduction

Three-dimensional (3D) surface imaging is being progressively used by various surgical specialisms. It is being deployed for analysis, follow-up, surgical planning and research purposes. Examples include the evaluation of facial changes following orthognathic surgery, planning and evaluation of orofacial cleft surgery, development of prosthesis, screening of genetic anomalies, and planning and follow-up of reconstructive breast surgery [1-5]. In recent years, 3D imaging applications have also found its way into thoracic surgery. Poncet and colleagues [6] were the first authors to describe the use of 3D imaging to create a 3D surface model with superimposed texture map of patients with anterior chest wall deformities. The resulting models were used as a non-radiological alternative to determine the severity of these pectus deformities. Following their initial series, several other studies also investigated the use of 3D imaging as a substitute for computed tomography (CT) scans to evaluate the severity of pectus deformities without exposure to ionizing radiation and found promising results [7-11]. However, among these studies there is a great diversity of 3D imaging systems being used, as also stressed by Daemen et al., [12]. Three-dimensional imaging devices range from static to mobile with varying prices, technical specifications and methods of data acquisition and processing. Despite the fact that all individual 3D imaging systems have been validated by their manufacturers it is unknown whether they are an accurate and reproducible tool to acquire anterior chest wall images. In addition, given that research outcomes, analysis methods and surgical planning techniques are commonly based on and have been validated for a single 3D imaging system, it is essential to analyze intersystem differences in order to determine if these validated techniques can be applied interchangeably when using different imaging systems. The subsequent aim of this study was to investigate the accuracy and reproducibility of three commercially available 3D imaging systems that are used to obtain images of the anterior chest wall.

Materials and methods

Study design and setting

We conducted a single-centre prospective case-control study, wherein participants were their own control. The study was conducted at the department of oral and maxillofacial surgery in Radboud University Medical Centre, Nijmegen, the

Netherlands. The study was approved by the local research ethics and clinical research committee (Research ethics committee of the Radboud University Nijmegen Medical Centre, Nijmegen, the Netherlands; ID: 2020-6130, approval date: February 13th, 2020). Following local approval, the study protocol was submitted to the clinicaltrials.gov registry (ID: NCT04279886, approval date: February 19th, 2020). This report was written in compliance with the STROBE guidelines for case-control studies [13].

Participants

A sample size of 15 individuals was chosen based on previously reported series that assessed the reproducibility and accuracy of 3D facial images [14, 15]. Healthy patients that volunteered to participate were recruited via an informative poster that was situated in the outpatient waiting area. All volunteers aged 18 years or above, physically fit on presentation and able to hold breath for at least 30 seconds were eligible for inclusion. Individuals with light-hypersensitivity or a diagnosis of photosensitive epilepsy were excluded due to the use of light flashes during image acquisition. Written informed consent was obtained from all participants prior to data acquisition.

Data acquisition

Three-dimensional images of the anterior chest wall were acquired by three different imaging systems. These included the 3dMD system (3dMD, Atlanta, GA, USA; Figure 1A), the Einscan Pro 2X Plus (Shining 3D, Hangzhou, China; Figure 1B) and the Artec Leo (Artec 3D, Luxembourg, Luxembourg; Figure 1C). The 3dMD system was selected and used as reference standard because it is the most covered imaging system in the available scientific literature [14, 16-18]. The 3dMD setup consisted of four pods with three cameras each (one of which is a texture camera to capture surface color information). The Einscan Pro 2X Plus and Artec Leo were selected because they are versatile, easy to transport and can be used in unconventional settings and places, such as the operating theater. Both devices consist of two cameras and require circumferential translation in order to scan the desired body part. An additional camera was mounted to the Einscan Pro 2X plus to capture the surface texture. The imaging protocol was adapted from Daemen et al., [19]. For image acquisition, participants were instructed to hold their hands on the back of their head such that adequate torso exposure was obtained. During acquisition, participants were instructed to inhale and hold breath in order to bypass motion artifacts due to

breathing. In addition, skin markers were placed at the jugular notch and sternum-xiphoid transition (identified through palpation) to delimitate the cranial and caudal border of the anterior chest wall area used for accuracy analysis. The lateral boundaries were formed by the lateral border of both areolae. Three-dimensional images of the anterior chest wall were acquired by an experienced user, and twice per imaging device. First, a 3dMD image was acquired, directly followed by an Einscan Pro 2X Plus image during the same breath hold. Next, a second 3dMD was captured and followed by an Artec Leo image. Again, during the same breath hold. The last two images (i.e. the second Einscan Pro 2X Plus and Artec Leo image) were acquired throughout different breath holds. The duration of acquisition was recorded for all devices but the 3dMD system, since the latter captures an image within 1.5 milliseconds. Following acquisition participants were asked to provide evaluation through a short two statement questionnaire. These statements addressed the satisfaction about the duration of acquisition and the inconvenience due to the light flashes that were used for image acquisition. The level of agreement to the statements was assessed through a five-point Likert scale.

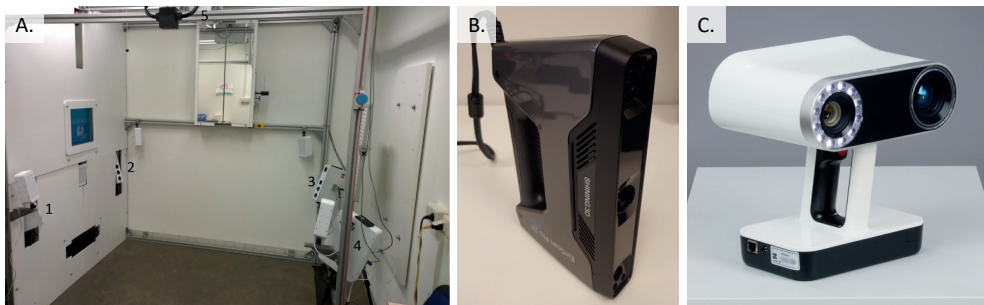


Figure 1: The three-dimensional imaging systems investigated. The (A) 3dMD, (B) Einscan Pro 2X Plus and (C) Artec Leo imaging system.

Data analysis

For data analysis, all 3D images were loaded into 3DMedX (3DMedX V1.2.0.4; 3D Lab Radboudumc, Nijmegen, the Netherlands). See Figure 2 for a schematic overview of all measurements performed. To assess the reproducibility of all imaging systems, the first image of every participant and imaging system was matched onto the second image of the same participant and imaging system (Figure 3). Matching of the field of interest (as defined in “Data acquisition”) was performed

through the surface-based iterative closest point (ICP) algorithm. After matching, the distance from each point on the first image towards the closest point on the second image was calculated. Resulting differences were visualized by a color-coded heat map (Figure 3). The accuracy was determined by matching the Einscan Pro 2X Plus and Artec Leo images onto the corresponding images obtained by the 3dMD system that was used as reference system. However, using the 3dMD system as reference standard supposes its accuracy as an ideal. The ‘true’ accuracy was subsequently determined by comparison of direct calipered and digitally calculated distances. The measure used was the distance between both skin markers. Direct measurements were like the 3D images obtained during breath hold and directly read from the caliper by a single observer. Digital measurements were performed by the same observer and obtained from the first image of every participant and imaging system utilizing the 3DMedX measurement tools.

The accuracy is henceforth defined as the mean absolute intersystem difference using the 3dMD as reference while the true accuracy is defined as the mean absolute intersystem difference using the calipered distance as reference.

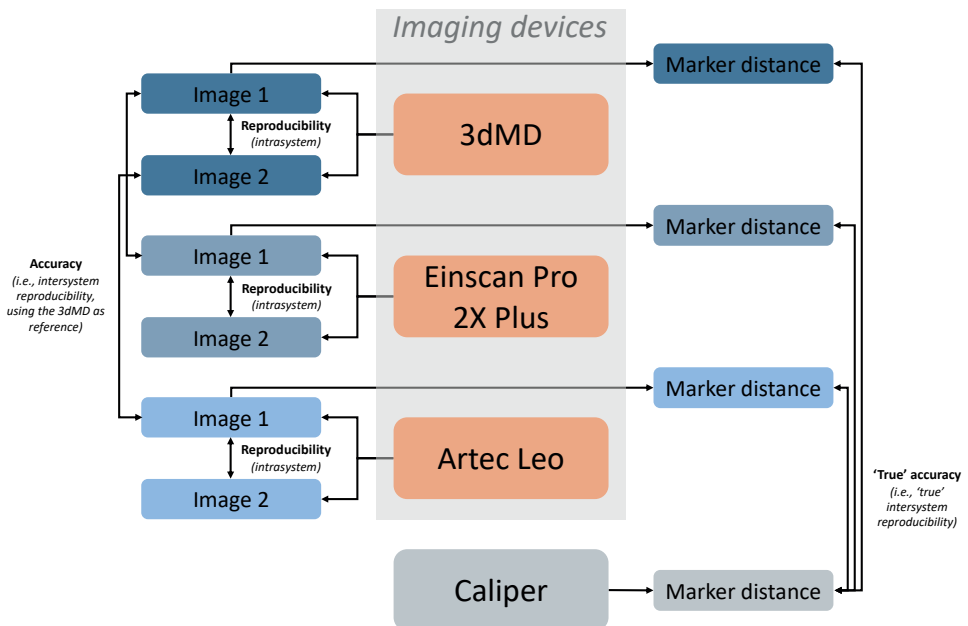


Figure 2: Schematic overview of the measurements performed to determine the reproducibility, accuracy and true accuracy of each imaging device.

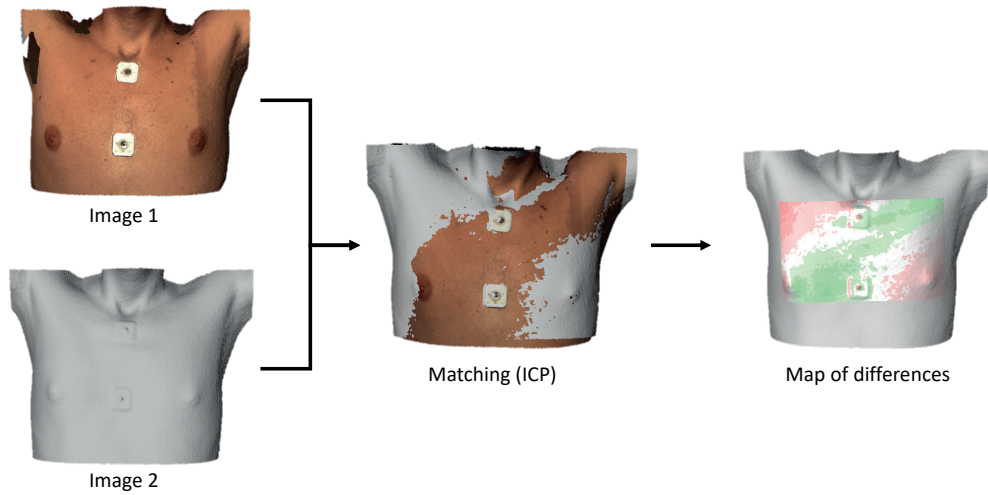


Figure 3: Overview of the process of data analysis to determine the reproducibility and accuracy. Two different images (left) are matched onto each other through an iterative closest point algorithm (ICP; middle) following which the differences between both images are calculated and visualized by a color-coded heat map (right).

Statistical analysis

All statistical analyses were performed using SPSS statistics (IBM Corp. Released 2017. IBM SPSS Statistics for MacOS, Version 25.0, Armonk, NY, USA). Continuous variables were denoted as mean and standard deviation (SD) or as median and interquartile range in the presence of skewness. Skewness was assessed by inspection of normal probability plots and histograms, and statistically by the Shapiro-Wilk test. Nominal variables were denoted as frequency and percentage. To analyze the reproducibility and accuracy between three-dimensional imaging, the absolute mean distance and standard deviation were calculated for each of the matched images. Repeated measures ANOVA with post hoc analyses was performed to assess differences regarding reproducibility. The non-parametric Friedman's test with post hoc analyses was used in the presence of skewness. One-sample t-tests were performed to determine whether the accuracy of the Einscan Pro 2X Plus and Artec Leo using the 3dMD system as reference was different from zero. The mean absolute difference and SD between the digital and caliper measured inter-marker distance were calculated to determine the true accuracy of all three imaging devices. Inter-marker distances were also submitted to repeated measures ANOVA or the non-parametric Friedman's test with post hoc analyses

to analyze differences between digital and caliper measurements. Acquisition times were submitted to the paired samples t-test or the non-parametric Wilcoxon signed-rank test. Questionnaire responses were summed and reported as such using bar charts. A p-value <0.05 was considered statistically significant. An arbitrarily chosen clinically acceptable limit of 1.00 millimeters or less was defined for the reproducibility, accuracy and true accuracy.

Results

Fifteen healthy male volunteers with a mean age of 27.8 years (SD: 4.4) and mean body mass index of 22.7 kg/m² (SD: 2.2) were included. No subjects have withdrawn during this study.

Reproducibility

Table 1 and the boxplot in Figure 4A demonstrate the mean absolute difference including measures of variability between two images that were acquired with the same imaging system during different phases of breath hold. These values demonstrate a reproducibility of 0.59 mm. (SD: 1.05) for the 3dMD imaging system, compared to 0.54 mm. (SD: 2.08) for the Einscan Pro 2X Plus and 0.48 mm. (SD: 0.60) for the Artec Leo imaging system. Despite this inequality, repeated measures ANOVA analysis with assumed sphericity found no statistically significant difference between the reproducibility of imaging systems ($F(2,28) = 1.641, p=0.212$). In addition, all imaging systems showed clinically acceptable levels of reproducibility.

Table 1: Reproducibility, accuracy and true accuracy of each imaging system.

	Mean absolute difference	Standard deviation
Reproducibility (vs itself)		
3dMD	0.59 mm.	1.05 mm.
Einscan Pro 2X Plus	0.54 mm.	2.08 mm.
Artec Leo	0.48 mm.	0.60 mm.
Accuracy (vs 3dMD)		
Einscan Pro 2X Plus	0.71 mm.	1.57 mm.
Artec Leo	0.57 mm.	0.87 mm.
True accuracy (vs caliper)		
3dMD	0.89 mm.	0.66 mm.
Einscan Pro 2X Plus	1.27 mm.	0.94 mm.
Artec Leo	0.81 mm.	0.72 mm.

mm, millimeters; NA, not applicable.

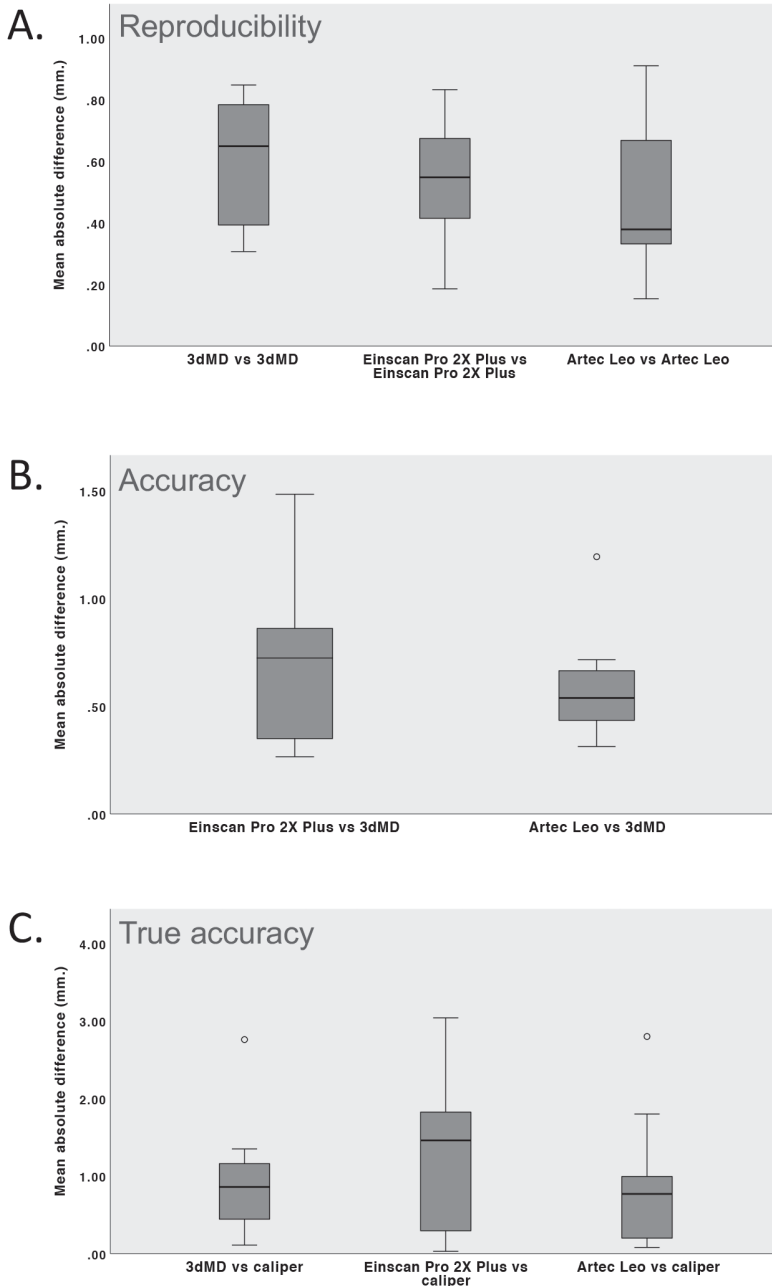


Figure 4: Boxplots of (A) the reproducibility of each imaging system, (B) the accuracy of the Einscan Pro 2X Plus and Artec Leo utilizing the 3dMD as reference, and (C) the true accuracy of each imaging device utilizing the caliper measured distance between the skin markers as reference.

Accuracy

The mean absolute difference between the Einscan Pro 2X Plus and 3dMD system and between the Artec Leo and 3dMD system are shown in Table 1 and in the boxplot in Figure 4B. The mean absolute difference between the Einscan Pro 2X Plus and reference 3dMD system was 0.71 mm. (SD: 1.57). The difference between the Artec Leo and reference 3dMD system was 0.57 mm. (SD: 0.87). One-sample t-tests demonstrated a statistically significant difference for both the Einscan Pro 2X Plus ($p < 0.001$) and Artec Leo ($p < 0.001$) compared to the 3dMD imaging system. Both differences were within the clinically acceptable limit and thus considered irrelevant.

True accuracy

Repeated measures ANOVA with assumed sphericity demonstrated no statistically significant difference among the digitally and caliper measured distances ($F(2,28) = 2.689$, $p = 0.085$). The true accuracy, defined as the mean absolute difference between the digitally and caliper measured distances, was 0.89 mm. (SD: 0.66) for the 3dMD, 1.27 mm. (SD: 0.94) for the Einscan Pro 2X Plus and 0.81 mm. (SD: 0.72) for the Artec Leo device (also see Table 1 and Figure 4C). All, but the true accuracy of the Einscan Pro 2X Plus device were considered clinically acceptable.

Acquisition time and questionnaire

The 3dMD has a fixed acquisition time of 1.5 milliseconds and was therefore, as mentioned in the “Materials and Methods” section, not measured. The mean acquisition time was 11.11 seconds (SD: 3.09) for the Einscan Pro 2X Plus and 5.46 seconds (SD: 1.00) for the Artec Leo device. Comparison through paired samples t-test demonstrated a statistically significant lower mean acquisition time (mean difference = 5.65 seconds (SD: 3.07), $p < 0.001$) in favor of the Artec Leo imaging system. Questionnaire responses are shown in Figure 5. From these bar charts it is observed that participants were most satisfied with the duration of image acquisition from the 3dMD, followed by the Artec Leo and Einscan Pro 2X Plus device (Figure 5A). In addition, participants experienced most inconvenience due to light flashes from the Einscan Pro 2X Plus, while the inconvenience was lowest for the 3dMD device (Figure 5B).

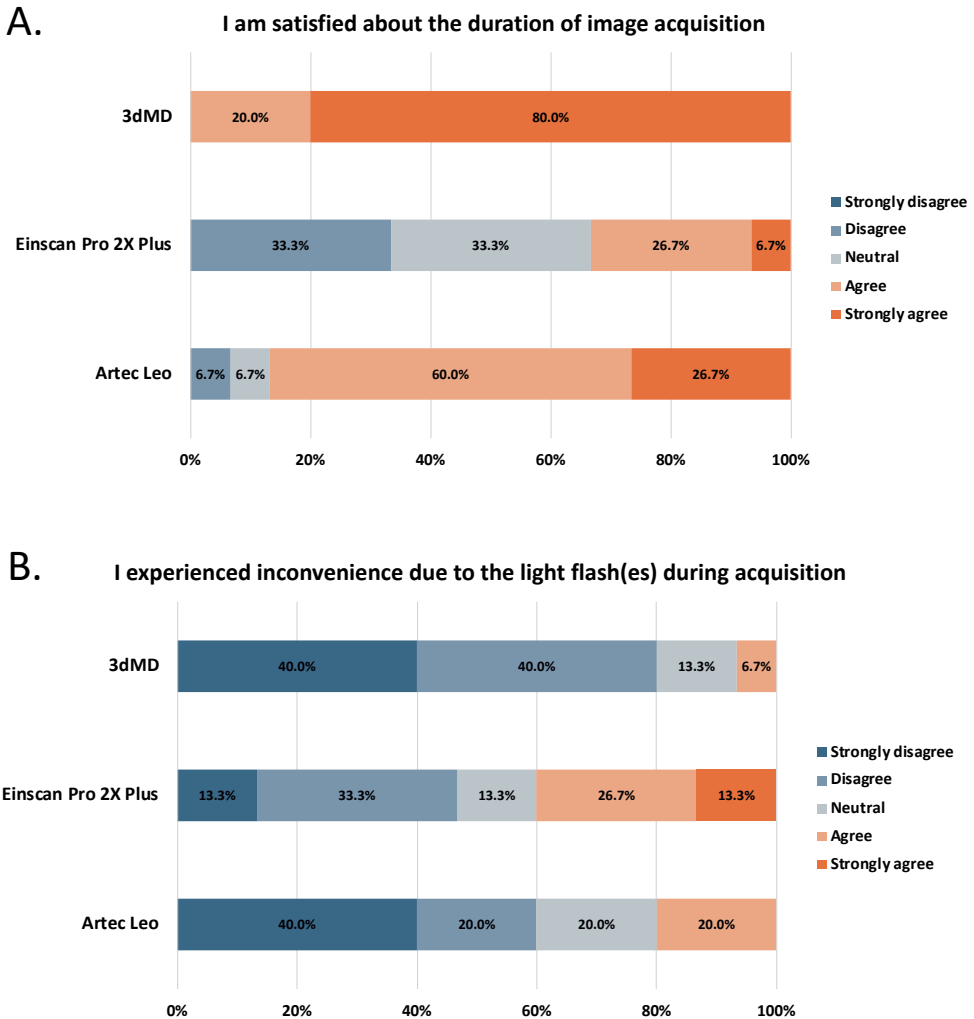


Figure 5: Questionnaire responses made on a 5-point Likert scale.

Discussion

Three-dimensional imaging is an upcoming and promising modality to analyze anterior chest wall deformities without exposure to ionizing radiation. Given the great diversity of commercially available 3D imaging systems, knowledge on intra- and intersystem differences is essential to select the optimal imaging system and determine whether validated analysis methods and surgical planning techniques can be applied interchangeably when using different imaging systems. In this

study we prospectively investigated the reproducibility and accuracy of two leading innovative imaging systems (i.e., the Artec Leo and Einscan Pro 2X Plus) and the gold standard 3dMD imaging system. This is the first ever study that compared these three systems for anterior chest wall imaging. Fifteen healthy volunteers were included and received two images per device. Reproducibility was investigated by analysis of the absolute difference between two matched images of the same participants that were acquired by a single device. All imaging devices demonstrated not statistically different ($p=0.212$) and clinically acceptable values of reproducibility.

Accuracy was investigated through the difference between matched images captured by the Einscan Pro 2X Plus or Artec Leo, and 3dMD. We chose to use the 3dMD as reference standard because it was and is still considered the gold standard surface imaging system, primarily due to its extensive coverage in literature and the fact that most analysis and planning techniques are validated based on 3dMD images [14, 16-18]. The Einscan Pro 2X Plus and Artec Leo both produced significantly different images (both $p<0.001$) compared to those formed by the 3dMD. However, both accuracies (0.71 and 0.57mm. for the Einscan Pro 2X Plus and Artec Leo, respectively) were well within the 1.00-millimeter limit and considered clinically acceptable. The true accuracy investigated through comparison of the digital and caliper measured inter-marker distance was, despite no statistical differences, best for the Artec Leo (0.81 mm.) followed by the 3dMD (0.89 mm.) and Einscan Pro 2X Plus (1.27 mm.). The Artec Leo and 3dMD were the only systems that demonstrated sub-millimeter differences and were subsequently deemed able to produce an accurate image of the anterior chest wall within the provided clinical limits and may, moreover, be used interchangeably.

Although the 3dMD system is considered the gold standard and was used as reference standard, it demonstrated inferior reproducibility and true accuracy compared to the Artec Leo. This could be due to the fact that the 3dMD system utilized was one of the first introduced with potentially outdated specifications. However, it may also be a result of the Artec Leo's comprehensive data processing in which motion artifacts and potential errors are corrected. The 3dMD system also demonstrated lower reproducibility compared to the Einscan Pro 2X Plus that may similarly result from the 3dMD software specifications being older. However, 3D images captured with the Einscan Pro 2X Plus also demonstrated substantial data loss and noise among participants with chest hair, as seen from Figure 6 and

demonstrated by the relatively high standard deviation (see Table 1). Hair consists of fine and partially translucent filaments that scatter light introducing image errors and noise. This means that the potentially most erroneous areas were not included for analysis due to data loss by which the reproducibility of the Einscan may be overestimated. In contrast, the 3dMD and Artec Leo are superior to the Einscan Pro 2X Plus at coping with chest hair (see Figure 6). The loss of data related to the Einscan Pro 2X Plus could also explain its lower true accuracy while skin markers were partially missing in a number of cases, as a result of which accurate anthropometric measurements could not always be performed.

The gold standard method to quantify the extent of deformity and aid in the multifactorial process of clinical decision making of pectus excavatum is by determining the Haller index based on CT imaging [20]. In the past years, three-dimensional optical imaging and its Haller index equivalent based on external distances have been introduced and are being progressively used as substitute imaging modality without exposure to ionizing radiation [6-12]. Three-dimensional images can in addition to simple visual inspection also be used to visually and quantitatively assess over-time evolution of the deformity. The interactive images can, moreover, be viewed by the operating surgeon for preoperative planning purposes and to obtain profound visuospatial understanding of the deformity, while they could even facilitate objective discussion of cases in a multidisciplinary setting. The concept of improved visuospatial understanding was previously investigated by Nicholson et al., through a randomized controlled trial who found improved knowledge and visuospatial understanding of 3D relationships when using interactive 3D models of the ear [21]. Given that there is a broad diversity of 3D imaging systems used in conjunction with the fact that all image analysis techniques have been validated based on a single imaging system [6-12] and that 3D imaging systems have not been validated in the clinical setting, it was essential to determine their accuracy, reproducibility and ability to be used interchangeably.

Magnetic resonance imaging (MRI) has, next to 3D imaging, been proposed as alternative to CT without exposure to ionizing radiation. Albeit, MRI is associated with increased costs and reduced availability, is more difficult to perform in claustrophobic patients, motion-sensitive, requires sedation in young patients and is more time-consuming [22, 23], therefore posing a less attractive alternative than 3D imaging.

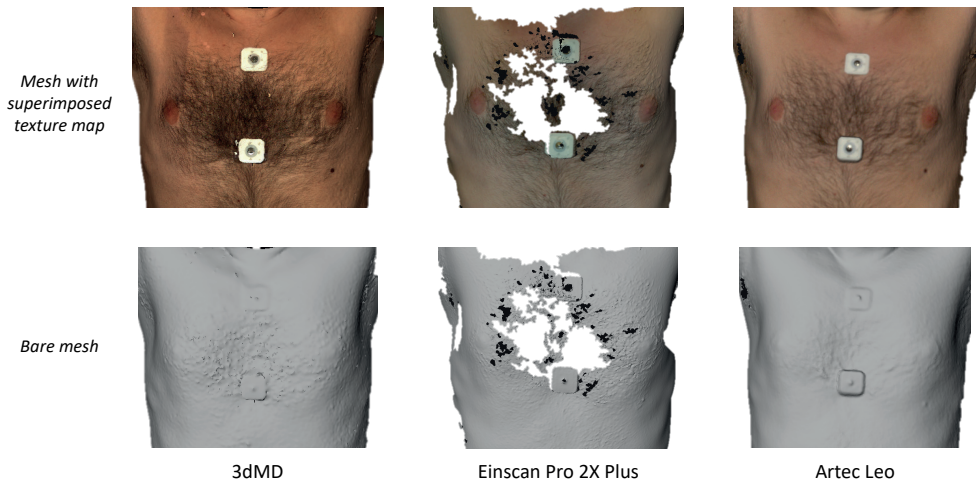


Figure 6: Examples of anterior chest wall images acquired by each of the three devices. The middle figures show substantial data loss caused by the scattering effect of chest hair.

We were unable to directly compare our results to other series since this is, to the best of our knowledge, the first ever series that investigated the accuracy and reproducibility of the 3dMD, Einscan Pro 2X Plus and Artec Leo for anterior chest wall imaging. Moreover, the Einscan Pro 2X Plus and Artec Leo were such novel devices that there was only one recent scientific paper available that described the accuracy of the Einscan Pro 2X Plus for facial imaging [24]. The 3dMD system is, as aforementioned, widely used with one of its main applications in facial imaging. The true accuracy of facial images is reported between 0.21 and 0.26mm. [18, 25]. This is substantially lower than our reported values for anterior chest wall images and may be explained by the inability to reproduce the exact same pose due to breath hold differences. Minor changes in patient pose may also occur during actual imaging itself and lead to a less accurate 3D image. These changes are more likely to occur when using active imaging systems that require continuous scanning to construct a 3D image, such as the Einscan Pro 2X Plus and Artec Leo. Imaging through these two devices took respectively 11.11 and 5.46 seconds, whereas the 3dMD captured an image within 1.5 milliseconds. The total imaging time of the Einscan Pro 2X Plus was higher than reported while multiple attempts were often required due to lost surface tracking. In contrast, the 3dMD and Artec Leo device only required one attempt to obtain a high-quality image. Acquisition times may not only impair the accuracy of 3D images but also be a burden for patients that are requested to hold breath and stand still during imaging. This was supported by the results from

the questionnaire which found increasing satisfaction with decreasing acquisition time.

Another aspect addressed by the questionnaire was the inconvenience due to light flashes. The inconvenience was least for the single flash 3dMD, followed by the Artec Leo and Einscan Pro 2X Plus that flash 80 and 30 times per second, respectively. This can be explained by the concept of flicker fusion. The higher the flash frequency, the closer it is to the flicker fusion threshold, making the individual flashes less distinguishable by the human eye. One may argue that this discomfort can easily be circumvented by closing the eyes, however, this could affect stability and cause motion artifacts.

A major advantage of the Einscan Pro 2X Plus and Artec Leo is that both are mobile scanners with the ability to capture 3D images in any place desired, such as the consultation room, the ward or operating theatre. Using these novel mobile scanners that are intuitive and provide active feedback, training and experience are in comparison to their aged variants no longer obligatory to obtain high-quality images, even at the first try. In addition, mobile scanners often have a larger field of view compared to static scanners. However, manual data processing is often still required in contrast with static systems such as the 3dMD. Another disadvantage associated with mobile scanners is, as shown in this series, the increased acquisition time. This makes static scanners easier to implement into standard clinical workflows. Nevertheless, static scanners are generally more expensive and require frequent use to be cost-efficient. The main limitations of this study included the use of a single anthropometric measurement to investigate the true accuracy and that only males had volunteered to participate. However, for anterior chest wall images this may not be a major limitation as for other conditions while anomalies of the chest wall are 2 to 9 times more common among males [26].

The fact that healthy volunteers were included instead of patients with anterior chest wall deformities may be regarded as limitation. Yet, it was deliberately chosen to enroll healthy volunteers because from a technical stand of view there is no difference in accuracy and reproducibility between healthy volunteers and those with chest wall anomalies. The primary determinants for the level of accuracy are the specifications of the imaging device and its processing software used to create 3D models of the chest. The reproducibility is a derivative of the ability to reproduce the patients' pose, as well as the reproducibility of the imaging system and processing software. The only way in which accuracy and reproducibility can theoretically be affected is if the targeted surface cannot be captured (i.e., if the cameras cannot 'see' the surface). In order to

capture depth of an excavated area, at least two cameras have to capture the bottom surface of the excavation to allow depth computation using triangulation. Theoretically, problems are thus expected in extremely narrow and deep (small-diameter tube-like) excavations causing a situation wherein both cameras cannot see the distal end of the excavation from their respective angles. Since chest wall anomalies like pectus excavatum are characterized by a central excavation fanning out to the sides, we can from a technical point of view state that there will be no acquisition problems and thus justify the use of healthy volunteers to determine accuracy and reproducibility of different imaging systems. This is confirmed by the fact that no acquisition errors were observed at the site of the umbilicus that can be regarded as a narrow excavation, considerably narrower than any pectus excavatum is ever expected to be. For other chest wall anomalies, like pectus carinatum, no problems are anticipated since it is characterized by an anterior protrusion of the chest wall that is easily captured by both cameras of the imaging systems. In addition, by choosing to scan healthy volunteers we aimed to enlarge the external validity of our comparison that cannot only be applied to patients with for example pectus excavatum, but for all applications in which a surface image of the chest is desired.

Another limitation is that not all images were acquired during the same breath hold, however, this is also not the case in actual clinical practice. The last limitation of this study is that only three different imaging systems were evaluated while dozens of different imaging systems are available. Future research should therefore focus to evaluate other available imaging systems that can be used to acquire 3D images of the chest. This will allow centers aiming to start a 3D imaging program to select a valid and optimal platform based on scientific evidence. In this series we evaluated three promising imaging systems and stressed the need to determine validity (i.e., accuracy and reproducibility) before such systems can be employed in the clinical setting, whereas the Einscan Pro 2X Plus demonstrated a clinically unacceptable level of accuracy.

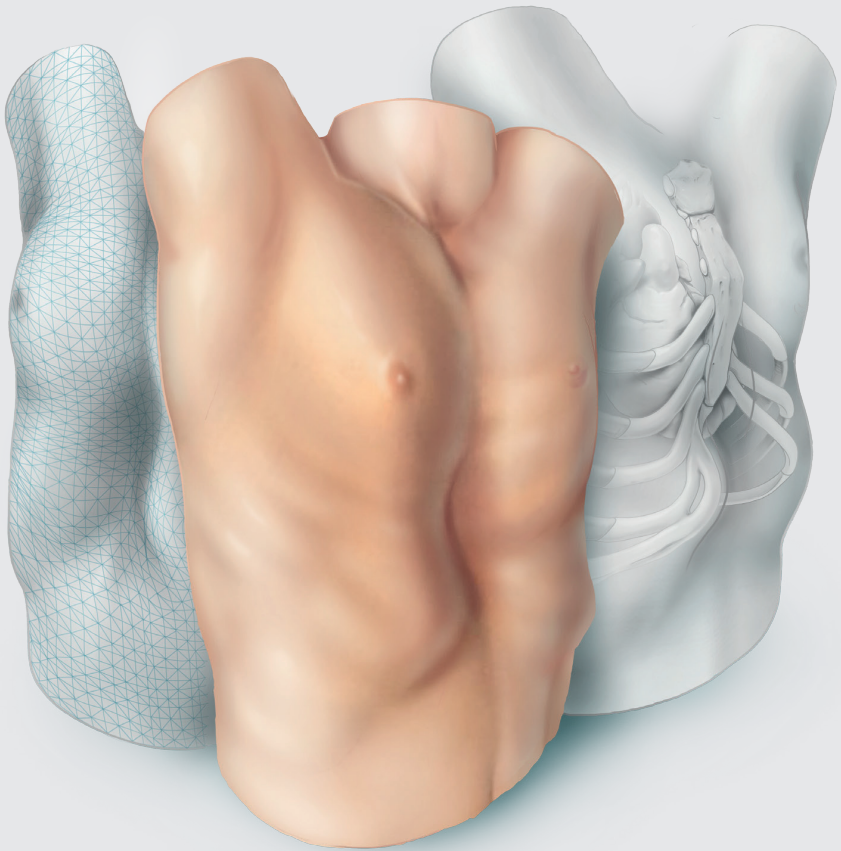
Conclusion

Three-dimensional imaging of the anterior chest wall is an upcoming and promising modality. Evaluating three different imaging systems, the 3dMD and Artec Leo system showed comparable and clinically acceptable reproducibility and accuracy while 3D images acquired by the Einscan Pro 2X Plus were reproducible but not accurate. Future research should focus to evaluate other available imaging systems and perpetuate the position of 3D imaging of chest wall deformities.

References

1. Hajeer MY, Ayoub AF, Millett DT, Bock M, Siebert JP. Three-dimensional imaging in orthognathic surgery: the clinical application of a new method. *Int J Adult Orthodon Orthognath Surg* 2002;17:318-30.
2. Liacouras P, Garnes J, Roman N, Petrich A, Grant GT. Designing and manufacturing an auricular prosthesis using computed tomography, 3-dimensional photographic imaging, and additive manufacturing: A clinical report. *J Prosthet Dent* 2011;105:78-82.
3. van Loon B, Maal TJ, Plooij JM, Ingels KJ, Borstlap WA, Kuijpers-Jagtman AM et al. 3D Stereophotogrammetric assessment of pre- and postoperative volumetric changes in the cleft lip and palate nose. *Int J Oral Maxillofac Surg* 2010;39:534-40.
4. Hameeteman M, Verhulst AC, Maal TJ, Ulrich DJ. An analysis of pose in 3D stereophotogrammetry of the breast. *J Plast Reconstr Aesthet Surg* 2016;69:1609-13.
5. Hammond P. The use of 3D face shape modelling in dysmorphology. *Archives of disease in childhood* 2007;92:1120-6.
6. Poncet P, Kravarusic D, Richart T, Evison R, Ronsky JL, Alassiri A et al. Clinical impact of optical imaging with 3-D reconstruction of torso topography in common anterior chest wall anomalies. *J Pediatr Surg* 2007;42:898-903.
7. Bliss DP, Jr., Vaughan NA, Walk RM, Naiditch JA, Kane AA, Hallac RR. Non-Radiographic Severity Measurement of Pectus Excavatum. *J Surg Res* 2019;233:376-80.
8. Glinkowski W, Sitnik R, Witkowski M, Kocoń H, Bolewicki P, Górecki A. Method of pectus excavatum measurement based on structured light technique. *J Biomed Opt* 2009;14:044041.
9. Hebal F, Port E, Hunter CJ, Malas B, Green J, Reynolds M. A novel technique to measure severity of pediatric pectus excavatum using white light scanning. *J Pediatr Surg* 2019;54:656-62.
10. Lain A, Garcia L, Gine C, Tiffet O, Lopez M. New Methods for Imaging Evaluation of Chest Wall Deformities. *Front Pediatr* 2017;5:257.
11. Uccheddu F, Ghionzoli M, Volpe Y, Servi M, Furferi R, Governi L et al. A Novel Objective Approach to the External Measurement of Pectus Excavatum Severity by Means of an Optical Device. *Ann Thorac Surg* 2018;106:221-7.
12. Daemen JHT, Loonen TGJ, Lozekoot PWJ, Maal TJJ, Hulsewé KWE, Vissers YLJ et al. Optical imaging versus CT and plain radiography to quantify pectus severity: a systematic review and meta-analysis. *J Thorac Dis* 2020;12:1475-87.
13. von Elm E, Altman DG, Egger M, Pocock SJ, Gøtzsche PC, Vandenbroucke JP. The Strengthening the Reporting of Observational Studies in Epidemiology (STROBE) statement: guidelines for reporting observational studies. *J Clin Epidemiol* 2008;61:344-9.
14. Aldridge K, Boyadjiev SA, Capone GT, DeLeon VB, Richtsmeier JT. Precision and error of three-dimensional phenotypic measures acquired from 3dMD photogrammetric images. *Am J Med Genet A* 2005;138A:247-53.
15. Verhulst A, Hol M, Vreeken R, Becking A, Ulrich D, Maal T. Three-Dimensional Imaging of the Face: A Comparison Between Three Different Imaging Modalities. *Aesthetic Plast Surg* 2018;38:579-85.
16. Lübbers H-T, Medinger L, Kruse A, Grätz KW, Matthews F. Precision and Accuracy of the 3dMD Photogrammetric System in Craniomaxillofacial Application. *J Craniofac Surg* 2010;21:763-7.

17. Losken A, Seify H, Denson DD, Paredes AAJ, Carlson GW. Validating Three-Dimensional Imaging of the Breast. *Ann Plast Surg* 2005;54:471-6.
18. Weinberg SM, Naidoo S, Govier DP, Martin RA, Kane AA, Marazita ML. Anthropometric Precision and Accuracy of Digital Three-Dimensional Photogrammetry: Comparing the Genex and 3dMD Imaging Systems with One Another and with Direct Anthropometry. *J Craniofac Surg* 2006;17:477-83.
19. Daemen JHT, Loonen TGJ, Coorens NA, Maessen JG, Maal TJJ, Hulsewé KWE et al. Photographic documentation and severity quantification of pectus excavatum through three-dimensional optical surface imaging. *J Vis Commun Med* 2020;43:190-7.
20. Haller JA, Jr., Kramer SS, Lietman SA. Use of CT scans in selection of patients for pectus excavatum surgery: a preliminary report. *J Pediatr Surg* 1987;22:904-6.
21. Nicholson DT, Chalk C, Funnell WR, Daniel SJ. Can virtual reality improve anatomy education? A randomised controlled study of a computer-generated three-dimensional anatomical ear model. *Med Educ* 2006;40:1081-7.
22. Birkemeier KL, Podberesky DJ, Salisbury S, Serai S. Limited, fast magnetic resonance imaging as an alternative for preoperative evaluation of pectus excavatum: a feasibility study. *J Thorac Imaging* 2012;27:393-7.
23. Lo Piccolo R, Bongini U, Basile M, Savelli S, Morelli C, Cerra C et al. Chest fast MRI: an imaging alternative on pre-operative evaluation of Pectus Excavatum. *J Pediatr Surg* 2012;47:485-9.
24. Amornvit P, Sanohkan S. The Accuracy of Digital Face Scans Obtained from 3D Scanners: An In Vitro Study. *Int J Environ Res Public Health* 2019;16.
25. Dindaroğlu F, Kutlu P, Duran GS, Görgülü S, Aslan E. Accuracy and reliability of 3D stereophotogrammetry: A comparison to direct anthropometry and 2D photogrammetry. *The Angle Orthod* 2016;86:487-94.
26. Cobben JM, Oostra R-J, van Dijk FS. Pectus excavatum and carinatum. *Eur J Med Genet* 2014;57:414-7.





Three-dimensional surface imaging for clinical decision making in pectus excavatum

Jean H.T. Daemen, Nadine A. Coorens, Karel W.E. Hulswé,
Thomas J.J. Maal, Jos G. Maessen, Yvonne L.J. Vissers, Erik R. de Loos

Adapted from: Semin Thorac Cardiovasc Surg 2022;34:1364-73.

Abstract

Background

To evaluate pectus excavatum, three-dimensional surface imaging is a promising radiation-free alternative to computed tomography and plain radiographs. Given that three-dimensional images concern the external surface, the conventional Haller index and correction index are not applicable as these are based on internal diameters. Therefore, external equivalents have been introduced for three-dimensional images. However, cut-off values to help determine surgical candidacy using external indices are lacking.

Methods

A prospective cohort study was conducted. Consecutive patients referred for suspected pectus excavatum received a computed tomography (≥ 18 years) or plain radiographs (< 18 years). The external Haller index and external correction index were calculated from additionally acquired three-dimensional images. Cut-off values for the three-dimensional image derived indices were obtained by receiver-operating characteristic curve analyses, using the conventional Haller index ≥ 3.25 and computed tomography derived correction index $\geq 28.0\%$ as indicative for surgery.

Results

Sixty-one and 63 patients were included in the computed tomography and radiograph group, respectively. To determine potential surgical candidacy, receiver-operating characteristic analyses found an optimum cut-off of ≥ 1.83 for the external Haller index in both the computed tomography and radiograph groups with a positive predictive value between 0.90-0.97 and negative predictive value between 0.72-0.81. The optimal cut-off for the external correction index was $\geq 15.2\%$ with a positive predictive value of 0.86 and negative predictive value of 0.93.

Conclusions

The three-dimensional image derived external Haller index and external correction index are accurate radiation-free alternatives to facilitate surgical decision-making among patients suspected of pectus excavatum with values of ≥ 1.83 and $\geq 15.2\%$ indicative for surgery.

Introduction

Pectus excavatum is the most common congenital anterior chest wall deformity [1]. It is characterized by an inwardly deviated sternum and adjacent costal cartilage, affecting up to 1 in 400 live births [2]. Patients may suffer from (cardio) respiratory impairment and associated complaints such as exercise intolerance, but also express psychosocial complaints due to body image disturbances [3-6]. Evaluating eligibility for surgical treatment of pectus excavatum is a multifactorial process without a uniform world-wide consensus on indications. However, the gold standard Haller index with a value larger than or equal to 3.25 [7] is widely used to determine eligibility for surgical treatment as demonstrated by its routine use by 80% of experts [8]. A correction index larger than or equal to 28.0% is often used as an auxiliary severity measure because of its superior ability to distinguish between patients with and without pectus excavatum [9]. Although both indices have initially been developed for computed tomography (CT), two-view plain radiographs are conducted in up to half of centers [8] to assess pectus severity with limited radiation exposure. Yet, exposure to potentially harmful ionizing radiation remains of concern particularly in pediatric patients [10, 11] because of the approximately 0.2% increased life-time attributable risk of malignancy (based on a hypothetical model) for a single CT acquisition among pediatric patients [12].

In an effort to replace diagnostic studies with radiation exposure, three-dimensional (3D) optical surface imaging has gained increasing interest [13-17]. Because 3D images solely reflect the external chest surface, alternative severity indices derived from these images are based on external measures. Although CT and 3D image derived indices demonstrate a high positive correlation [18], cut-off values are necessary before 3D images and the resulting external indices can be applied as a diagnostic tool to help determine surgical candidacy.

The aim of this study was to determine a diagnostic cut-off value for the 3D image based external Haller index and external correction index to facilitate surgical decision making in patients suspected of pectus excavatum. The conventional CT and radiograph-derived indices (i.e., Haller index and correction index) were used as reference test. It was hypothesized that 3D images and their corresponding external indices yield adequate diagnostic value and can be interchangeably used with CT and radiograph-derived severity measures.

Materials and Methods

Study design

A single-center prospective diagnostic cohort study was conducted. Participants acted as their own control. Prior to start, the study protocol was approved by the local ethics and clinical research committee (Medical Ethics Review Committee Zuyderland, ID: METCZ20190048, approval date: April 9th, 2019) and registered to the Clinicaltrials.gov registry (ID: NCT03926078, approval date: April 18th, 2019). Written informed consent was obtained prior to inclusion. Additional consent was obtained from the patient's parent(s) or legal guardian if younger than 16 years of age. This report was written in compliance with the Standards for Reporting of Diagnostic Accuracy Studies (STARD) guidelines [19].

Participants

Eligible patients were enrolled between August 2019 and November 2020 and identified at the outpatient clinic of our tertiary referral center for chest wall disorders (Department of Surgery, division of General Thoracic Surgery, Zuyderland Medical Center, Heerlen, the Netherlands). All consecutive patients referred for suspected pectus excavatum were considered. Patients that underwent previous chest wall surgery were excluded. In addition, those diagnosed with photosensitive epilepsy, or any other form of light hypersensitivity were excluded since the flickering light emitted during 3D imaging may provoke seizures.

Patients were divided in a CT- and radiograph group. According to our institutional preoperative protocol, patients aged 18 years and above underwent a CT to evaluate the severity of their deformity. Patients younger than 18 years of age received two-view plain radiographs and, if indicated, an additional CT or Magnetic Resonance Imaging (MRI) scan to assess the presence of cardiac compression. Patients exposed to both CT and plain radiographs were enrolled in both groups.

Measurements and variables

Baseline patient characteristics including gender, age, body mass index (BMI) and preoperative symptoms were obtained.

Index test

All patients received a 3D image of their chest from which the external Haller index and external correction index were derived. Three-dimensional images (see example

in Figure 1) were acquired by the Artec Leo (Artec3D, Luxembourg, Luxembourg) imaging system and processed by Artec Studio 14 (Artec3D, Luxembourg, Luxembourg) according to the acquisition and processing protocol described in an earlier study [20]. The external Haller index was defined as the widest external thoracic transverse diameter divided by the sagittal distance between the external point of maximum depression and back surface (Figure 2A). In addition, the external correction index was defined as the difference between the smallest (i.e., between the external deepest point and back surface) and largest (i.e., between the anterior and posterior chest wall surface) anteroposterior distance divided by the latter and expressed as percentage (Figure 2A). The external indices were computed by an automated MATLAB R2020a (MathWorks, Massachusetts, USA) algorithm that normalizes the 3D image orientation, transversally slices the 3D image, and selects the slice that exhibits the most severe excavation to calculate the indices on.

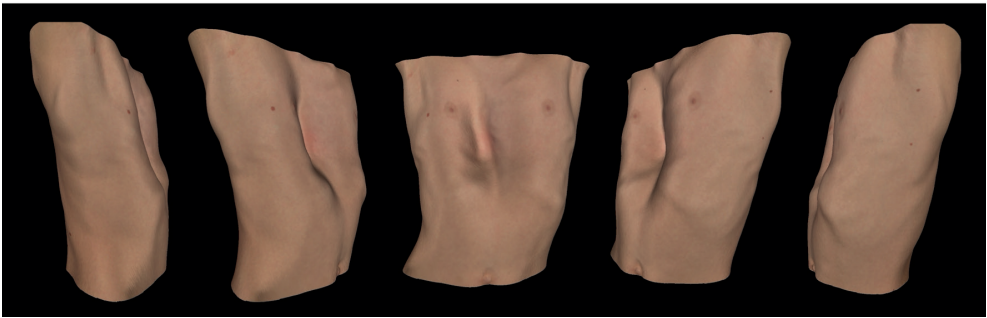


Figure 1: An example of a three-dimensional chest image acquired by the Artec Leo (Artec3D, Luxembourg, Luxembourg), viewed from different angles.

Reference test

Since the CT derived Haller index ≥ 3.25 [7] and correction index $\geq 28.0\%$ [9] are considered indicative for surgical correction, both indices were used as separate reference standards among patients in the CT group. For patients in the radiograph group, only the Haller index ≥ 3.25 [21] was used because the correction index cannot be accurately obtained from plain radiographs. The (internal) Haller index was computed by dividing the widest intrathoracic diameter by the anteroposterior distance between the posterior sternal surface and anterior vertebral surface at the transverse level of most severe depression (Figure 2B & C). The correction index was defined as the percentage of chest depth represented by the deformity (i.e., the difference between – the minimum distance between the posterior sternal surface and anterior vertebral surface – and the

maximum distance between the anterior vertebral surface and the most anterior chest surface – divided by the latter and expressed as percentage; Figure 2B). The Haller index and correction index values were determined using the Sectra Patient Archiving and Communication System application (Sectra AB, Linköping, Sweden). Measurements were performed by a single assessor who was blinded for the index test results.

Computed tomography scans, plain radiographs and 3D images were all obtained during breath hold following inspiration. In addition, CT scans were acquired in supine position in contrast to plain radiographs and 3D images that were obtained standing.

Statistical analysis

Statistical analyses were performed by SPSS statistics (IBM Corp. IBM SPSS Statistics for MacOS, Version 27.0, Armonk, NY, USA). Continuous variables were denoted as mean and standard deviation (SD) or as median, interquartile range (IQR) and range in the presence of skewness. Categorical variables were depicted as frequencies and percentages. The relationship between conventional and external indices was evaluated by Pearson's or Spearman's rank correlation coefficient. Receiver-operating characteristic (ROC) curves were constructed for the 3D image based external Haller index and external correction index. The cut-off points used in clinical practice (CT and radiograph derived Haller index ≥ 3.25 [7, 21] and CT derived correction index $\geq 28.0\%$ [9]) were used as the reference standards. Youden's J index was utilized to select cut-off values for the external indices with an optimal trade-off between sensitivity and specificity. Diagnostic accuracy (i.e., discriminative ability for pectus severity corresponding to the adopted dichotomous eligibility cut-off point for surgery) was obtained by determining the area under the curve (AUROC) with corresponding 95% confidence interval (CI). Post-hoc analyses were not prespecified and performed upon indication. A p-value < 0.05 was considered statistically significant.

Sample size estimation

Sample size estimation was performed by MedCalc (MedCalc Software v19.2.0, Ostend, Belgium). Based on the first 12 consecutive patients in the CT group, an AUROC of 0.81 (95% CI: 0.53 to 1.00) was found for the external Haller index. A minimum total sample size of 60 participants with an arbitrarily chosen allocation ratio (i.e., ratio between eligibility and no eligibility for surgery) ranging from 0.5 to 2.0 was required per group to have a 95% chance of detecting a significant difference at the 5% level between the pre-specified AUROC of 0.81 and null hypothesis (AUROC of 0.50), including a 10% correction for potential drop-out.

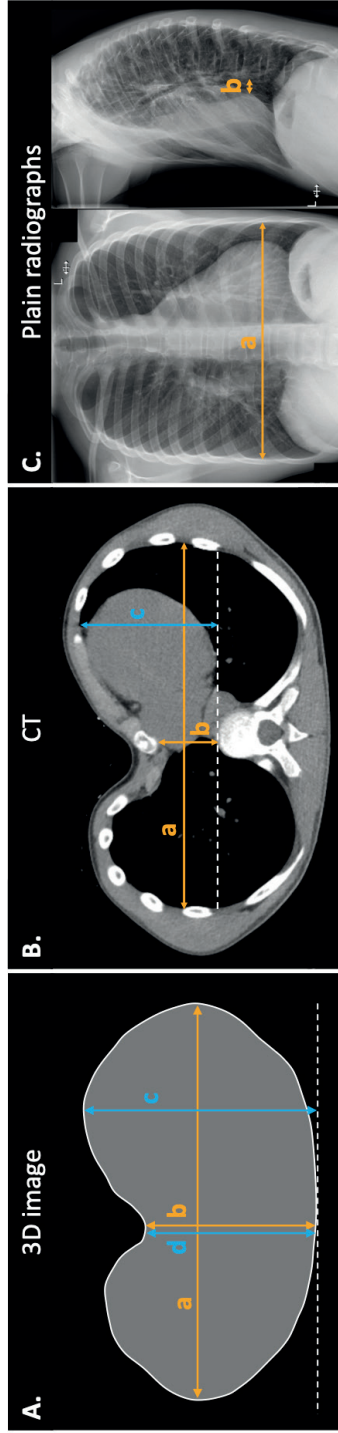


Figure 2: The measurement methods. (A) A transversal three-dimensional image slice that exhibits the most severe excavation and from which the external Haller index (a/b) and external correction index ((c-d)/c) are calculated. (B) A transversal CT image slice that like the three-dimensional image exhibits the most severe excavation and from which the conventional Haller index (a/b) and correction index ((c-b)/c) are calculated. (C) Two-view plain radiographs used to determine the conventional Haller index (a/b).
 3D, three-dimensional; CT, computed tomography.

Results

The process of patient selection into both groups is depicted in Figure 3.

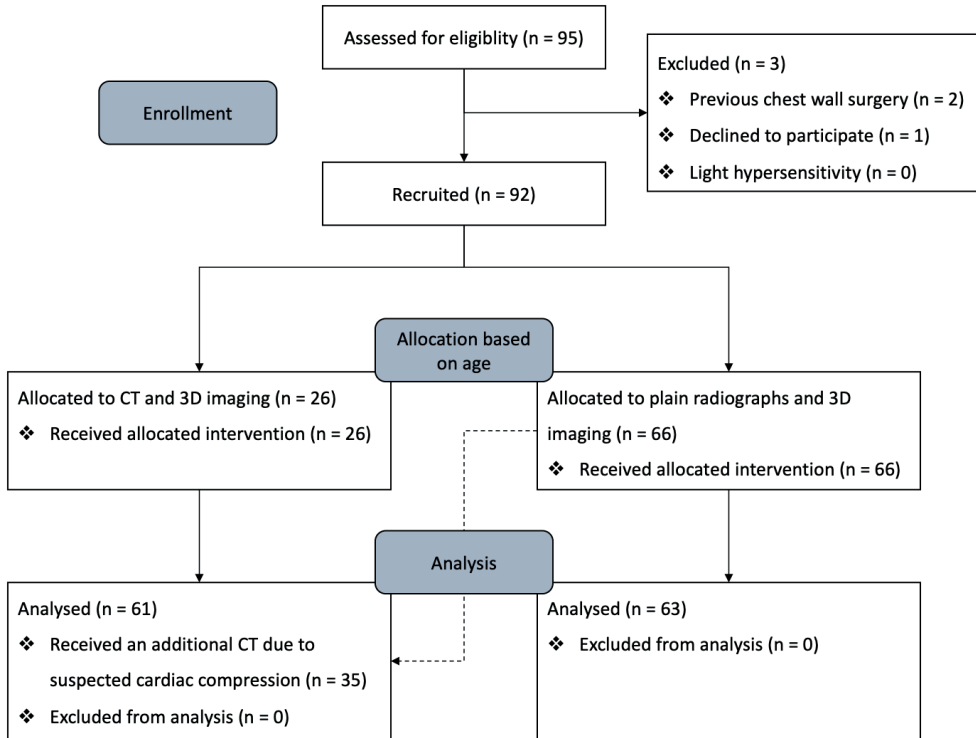


Figure 3: A STARD diagram depicting the process of patient selection. CT, computed tomography, 3D, three-dimensional image.

Computed tomography arm

See the STARD diagram in Figure 4 for an overview of the flow of patients within the CT arm. Sixty-one patients were included of whom 35 were also included in the radiograph arm. The majority of patients were male (85%) with a median age of 17 years (IQR: 15-23) and median BMI of 20kg/m² (IQR: 19-21). The most frequently observed symptom was exercise intolerance in 61% of patients.

The median time between 3D image and CT acquisition was 0 days (IQR: 0-19). Despite absolute differences between the CT derived and 3D derived indices (see Table 1), a correlation coefficient of 0.80 ($p < 0.001$) and 0.89 ($p < 0.001$) was found between the Haller index and external Haller index and between the correction index and external correction index respectively.

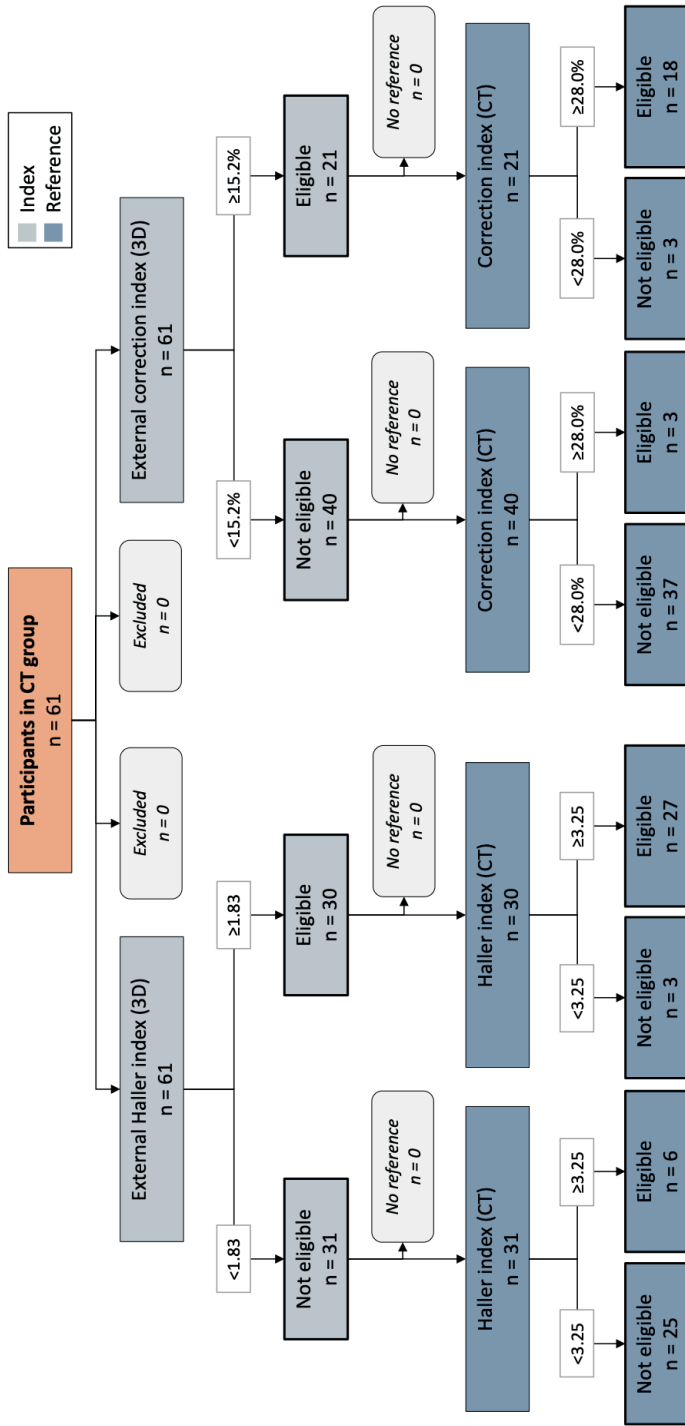


Figure 4: A STARD diagram demonstrating the flow of participants in the CT group (n=61) based on their index (i.e., the 3D image derived external Haller index and external correction index) and reference test (i.e., the CT derived conventional Haller index and correction index) outcomes used to evaluate surgical eligibility.

CT, computed tomography; 3D, three-dimensional image.

Using a CT derived Haller index larger than or equal to 3.25, 33 of 61 patients (54%) were potentially eligible for corrective surgery. In order to discriminate between indication and no indication for surgery, solely based on the external Haller index, ROC analysis in found an optimum cut-off point of ≥ 1.83 with an AUROC of 0.93 (95% CI 0.86-0.99; $p < 0.001$; Figure 5), sensitivity of 0.82 (95% CI 0.65-0.93) and specificity of 0.89 (95% CI 0.72-0.98). The associated positive (PPV) and negative predictive value (NPV) were 0.90 (95% CI 0.75-0.96) and 0.81 (95% CI 0.67-0.90; Table 2).

Among the same patients, 21 of 61 (34%) were potentially eligible for surgery based on a correction index $\geq 28.0\%$. Using the correction index as reference, an optimum cut-off value of $\geq 15.2\%$ was found with an AUROC of 0.94 (95% CI 0.88-1.00; $p < 0.001$; Figure 5) when only the external correction index was considered as an indication for surgery. The sensitivity, specificity, PPV and NPV were 0.93 (95% CI 0.80-0.98), 0.86 (95% CI 0.64-0.97), 0.93 (95% CI 0.81-0.97) and 0.86 (95% CI 0.67-0.95; Table 2).

Table 1: Baseline patient characteristics and index values derived from conventional modalities and three-dimensional images.

	CT group (n=61)	Radiograph group (n=63)
Male, n (%)	52 (85)	58 (92)
Age, years, median (IQR; range)	17.1 (15.1-23.3; 12.7-69.3)	14.8 (13.8-15.8; 9.1-17.7)
BMI, kg/m², median (IQR; range)	19.9 (18.9-21.0; 14.9-26.8)	18.7 (17.2-19.9; 13.8-23.0)
Symptoms, n (%)		
Palpitations	14 (23)	10 (16)
Thoracic pain/tightness	19 (31)	15 (24)
Dyspnea	18 (30)	13 (21)
Exercise intolerance	37 (61)	32 (51)
Cosmetic	28 (46)	35 (56)
Conventional indices, median (IQR; range)		
Haller index	3.33 (2.82-4.08; 2.12-10.21)	3.52 (3.03-4.19; 2.38-19.75)
Correction index	23.8% (13.8-33.4; 4.0-72.9)	ND
Three-dimensional image indices, median (IQR; range)		
External Haller index	1.82 (1.72-1.95; 1.38-2.53)	1.83 (1.74-1.98; 1.51-2.53)
External correction index	12.3% (7.8-18.5; 2.7-32.6)	ND

CT, computed tomography; n, number; IQR, interquartile range; ND, not determined.

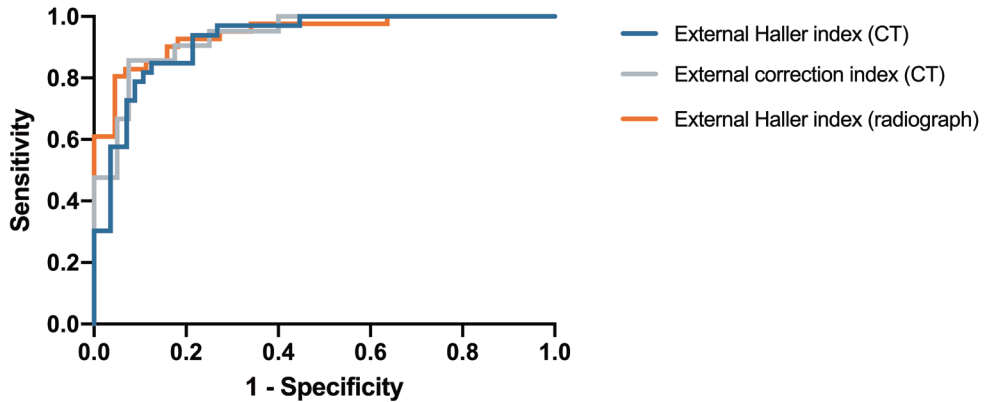


Figure 5: Receiver-operating characteristic curves of the three-dimensional image derived external indices, using the conventional CT and radiograph derived indices as reference. CT, computed tomography.

Table 2: Threshold values of the three-dimensional image derived external Haller index and external correction index indicative for corrective surgery and their associated diagnostic value among patients in the CT and radiograph group.

	External Haller index (CT)	External correction index (CT)	External Haller index (radiograph)
Threshold indicative for surgery	≥1.83	≥15.2%	≥1.83
AUROC (95% CI)	0.93 (0.86-0.99)	0.94 (0.88-1.00)	0.94 (0.89-1.00)
Sensitivity (95% CI)	0.82 (0.65-0.93)	0.86 (0.64-0.97)	0.81 (0.65-0.91)
Specificity (95% CI)	0.89 (0.72-0.98)	0.93 (0.80-0.98)	0.96 (0.77-1.00)
PPV (95% CI)	0.90 (0.75-0.96)	0.86 (0.67-0.95)	0.97 (0.83-1.00)
NPV (95% CI)	0.81 (0.67-0.90)	0.93 (0.81-0.97)	0.72 (0.58-0.83)
LR+ (95% CI)	7.64 (2.59-22.52)	11.43 (3.80-34.41)	17.71 (2.59-120.88)
LR- (95% CI)	0.20 (0.10-0.42)	0.15 (0.05-0.44)	0.20 (0.11-0.38)

CT, computed tomography; AUROC, area under the receiver-operating characteristic curve; CI, confidence interval; PPV, positive predictive value; NPV, negative predictive value; LR+, positive likelihood ratio; LR-, negative likelihood ratio.

Radiograph arm

See Figure 6 for the STARD flow diagram of patients within the radiograph arm. Sixty-three unique patients were enrolled, of whom the majority were male (92%) with a median age of 15 years (IQR: 14-16). The median BMI was 19kg/m² (IQR: 17-20). Patients most often suffered from cosmetic complaints (56%).

Plain radiographs and 3D image were both acquired on the same day for all patients. The 3D image derived external Haller index values were, as in the CT group, lower than the conventional Haller index (see Table 1). Both indices showed a correlation of 0.82 ($p < 0.001$).

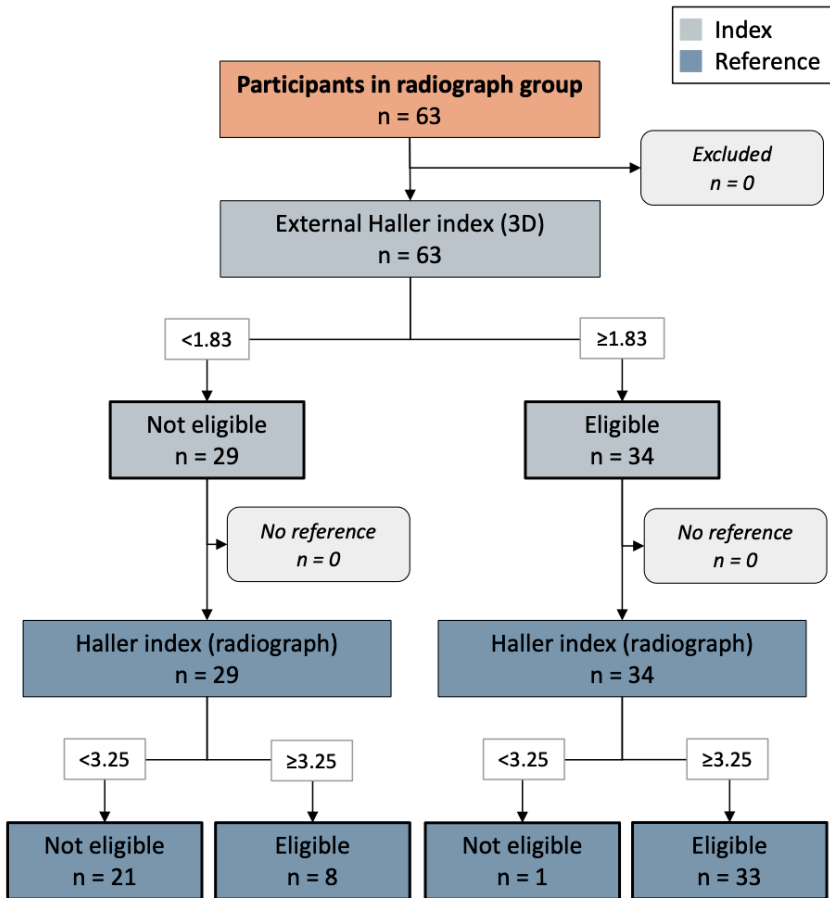


Figure 6: A STARD diagram demonstrating the flow of participants in the radiograph group ($n=63$) based on their index (i.e., the 3D image derived external Haller index) and reference test (i.e., the radiograph derived conventional Haller index) outcomes used to evaluate surgical eligibility. *3D, three-dimensional.*

Based on the conventional Haller index (≥ 3.25), 41 of 63 patients (65%) were potentially eligible for surgical repair. Using the conventional index as reference, an optimum cut-off point of ≥ 1.83 was found indicative for surgery based on the

external Haller index with an AUROC of 0.94 (95% CI 0.89-1.00; $p < 0.001$; Figure 5), sensitivity of 0.81 (95% CI 0.65-0.91), specificity of 0.96 (95% CI 0.77-1.00), PPV of 0.97 (95% CI 0.83-1.00) and NPV of 0.72 (95% CI 0.58-0.83; Table 2)

Post-hoc analysis

Post-hoc analysis was based on the 35 patients (see Figure 3) who received a chest CT, plain radiographs and a 3D image. This analysis intended to evaluate the performance of the radiograph derived Haller index (≥ 3.25) versus the 3D image derived external Haller index (≥ 1.83) to determine surgical candidacy, using a CT derived Haller index ≥ 3.25 as reference for surgical eligibility. Radiographs demonstrated an AUROC of 0.89 (95% CI 0.76-1.00; $p < 0.001$), sensitivity of 0.96 (95% CI: 0.78-1.00), specificity of 0.83 (95% CI: 0.52-0.98), PPV of 0.92 (95% CI: 0.76-0.98) and NPV of 0.91 (95% CI: 0.59-0.99). The external Haller index calculated from 3D images demonstrated comparable performance predicting surgical candidacy with an AUROC of 0.89 (95% CI: 0.77-1.00; $p < 0.001$), sensitivity of 0.87 (95% CI: 0.66-0.97), specificity of 0.92 (95% CI: 0.62-1.00), PPV of 0.95 (95% CI: 0.75-0.99) and NPV of 0.79 (95% CI: 0.56-0.91).

Discussion

In the past two decades, several studies have evaluated the use of 3D image based severity measures as alternatives to the currently established Haller and correctional indices derived from plain radiographs and CT [13-17]. However, none of these studies evaluated the discriminatory capacity of the novel 3D image based measures to aid in the process to determine surgical candidacy, but predominantly focused on the correlation with conventional indices [18]. The presented study is the first to determine cut-off values for the 3D image based external Haller index and external correction index.

Applying a cut-off value of ≥ 1.83 and $\geq 15.2\%$ for the external Haller index and the external correction index respectively, an excellent discriminatory capacity was observed compared to the gold standard indices currently used to determine potential eligibility for surgical intervention. This confirmed our hypothesis previously formulated. Nevertheless, evaluation of patients to determine the need for surgical intervention is a multifactorial process to which indices contribute but are not decisive on themselves.

Application of the new cut-off values for the external Haller index resulted in a PPV of 0.90 and above, while the predictive value of a negative result was lower (0.72-0.81). Therefore, if the value of the external Haller index is larger than or equal to the cut-off point it can replace the conventional index in the selection for corrective surgery. However, if values are below the cut-off, additional diagnostic testing may be advisable when high clinical suspicion of severe pectus excavatum exists. Though, it must be noted that these predictive values are dependent on the a priori probability of severe pectus excavatum. In the current series the a priori probability ranged from 51% to 65% based on a Haller index ≥ 3.25 . In comparison, surgical repair was indicated among 51% of initially evaluated patients in a large series by Kelly and colleagues. Yet, they did not only consider the Haller index, but also used the presence of (cardio)pulmonary compression, mitral valve prolapse, arrhythmia, restrictive lung disease, failed previous repair and significant body image disturbance as determinants for surgery, of which at least two had to be apparent [22]. Applying the criteria of Kelly et al. to our CT group yielded a comparable prevalence of patients with an indication for surgery (55%). However, it should be noted that patients with previous repair were excluded in the current study.

Based on the broad range of conventional indices, the diversity of pectus excavatum was considered to be covered. The CT and radiograph derived Haller index respectively ranged from 2.12 to 10.21 and 2.38 to 19.75, while the CT derived correction index ranged from 4.0% to 72.9%. Although both age and male-to-female ratio corresponded with previously reported studies on surgical repair of pectus excavatum [22-24], the investigated patient sample may not be representative for other countries where patients with suspected pectus are not referred by their general practitioner or specialist but are offered primary consultation by a (cardio) thoracic or pediatric surgeon following self-referral. This probably would lower the above-mentioned prior probability and therefore affect predictive values.

Taylor and associates recently developed a model to predict the Haller index based on the optical index, equivalent to the external Haller index, and patient biometric data (i.e., height and weight) [25]. This model, when applied to their training and test set, showed a median error of 8% (IQR: 4-18) in predicting the radiograph derived Haller index with a PPV of 0.94 using a Haller index larger than or equal to 3.25 as reference. However, the study of Taylor et al., was limited by sample size (n=28) [25]. In contrast, our study included 63 patients in the radiograph arm and reached an adequate statistical power of 95%. In addition, our cut-off point of 1.83

does not require conversion and is therefore simpler to use clinically. Our cut-off, moreover, revealed a similar PPV (0.97 [95% CI: 0.83-1.00]) but superior NPV (0.72 [95% CI 0.58-0.83]) to evaluate surgical eligibility based on the external Haller index compared to the PPV (0.97 [95% CI: 0.81-0.99]) and NPV (0.62 [95% CI: 0.52-0.72]) found after application of Taylor's model to our radiograph group data.

As previously mentioned, up to 52% of international chest wall experts acquire radiographs during preoperative work-up instead of gold standard CT, applying a similar cut-off value for surgical candidacy (i.e., ≥ 3.25) [8]. However, it is often unknown that the radiograph derived Haller index has a sensitivity of 0.95 and specificity of 0.67 to 0.75 using CT as reference [21].

In post-hoc analysis, the radiograph derived Haller index (≥ 3.25) and 3D image derived external Haller index (≥ 1.83) yielded comparable performance predicting surgical candidacy. Both modalities can thus be used interchangeably to predict surgical candidacy. The choice for either is subsequently dependent on availability as well as their additional (dis)advantages and surgeon's preference. Despite the minimal radiation exposure associated with radiographs, 3D images are, as repeatedly mentioned, entirely free of ionizing radiation. In addition, since 3D images capture the outer chest surface, they can be used for visual documentation of the deformity which also addresses pectus aspects such as asymmetry. Therefore, they can also be used to comprehensively evaluate postoperative improvement and keep track of the remodeling process after Nuss bar implantation and removal. Moreover, repeated follow-up during conservative treatment is allowed without negative effects on health. On the contrary, 3D imaging systems are less widely available than imaging systems to acquire radiographs which belong to the standard equipment.

Since the primary goal has been to replace current diagnostic studies with radiation exposure, one can also argue for the routine use of MRI. The feasibility of MRI for preoperative assessment of pectus excavatum has previously been demonstrated [26, 27]. However, its routine use as radiation-free alternative is disadvantaged by increased costs, difficulty to perform in claustrophobic patients, sensitivity to motion and may even require sedation in young patients [26, 27]. Moreover, MRI is also associated with increased time-consumption (approximately 8 minutes using a limited, fast imaging protocol [26]) compared to 3D imaging which takes 5 to 16 seconds per image [20, 28]. The latter can thus easily be obtained during routine

clinic visits without a separate appointment which is often required for MRI. In addition, the handheld device used provides the opportunity to obtain images in unconventional places such as the ward and operating room.

The Artec Leo imaging system, employed in the present study, is commercially available at approximately 30,000 US dollars. However, given the relatively simple geometry of the chest, even in perceived complex deformities, less costly devices may also suffice. For example, Guillot and colleagues used the structure sensor (Occipital Inc., San Francisco, CA, USA) to acquire 3D images of patients with pectus excavatum and carinatum [29]. This device is priced below 1,000 US dollars.

In our experience little to no expertise was needed to acquire the 3D images.

Limitations

Due to the prospective nature of this study in conjunction with the fact that no patients opted out, no bias due to missing data was present. Given that only one patient denied participation during the enrollment period, the probability of selection bias was low. Nevertheless, our results solely apply to patients that are imaged according to the identical imaging protocols employed in the current series where alterations in, for example, respiration phase may affect index values. The latter was previously investigated by Birkemeier et al., who described significantly lower Haller index values at inspiration than expiration [30]. Theoretically, index values could also differ while employing different 3D imaging systems. However, the Artec Leo imaging system, used in our series, was previously validated and showed sub-millimeter, clinically acceptable, accuracy and reproducibility when acquiring 3D images of the chest [28]. As the accuracy is primarily affected by the used imaging system rather than the morphology of the chest surface, no problems are expected with complex deformities.

The present study is, moreover, limited by use of the conventional Haller index as reference. Despite it providing an objective marker for surgical candidacy, it poses considerable limitations, as summarized by Martinez-Ferro [8]. For example, index values show an 48% overlap between patients with pectus excavatum and healthy controls [31]. Though, its routine use as gold standard is presumably motivated by its ease of measurement and that surgeons and radiologists are used to calculate and interpret its values [8]. In part of the USA, the Haller index even determines reimbursement rates.

Moreover, by choice of the reference standard in the present study, the external Haller index can only be inferior in terms of performance. This was also previously observed for the seemingly superior conventional correction index which was able to perfectly separate individuals with pectus excavatum and controls [31], but showed inferior performance in selecting patients for surgery using the Haller index as reference standard [9]. To improve future evaluation of new methods, better reference methods should be sought for.

Albeit it should not be forgotten that determining candidacy for surgical correction of pectus excavatum is not as contrasting; it is a multifactorial process, not solely dependent on indices such as the Haller index. Though, these indices provide us with objective markers that are applied in the multifactorial process.

The main disadvantage of 3D imaging derived indices is that they are based on outer chest surface dimensions, where conventional indices are determined using intrathoracic landmarks. Consequently, external indices are potentially affected by patient factors including BMI, gender, age and breast size. For example, the external correction index may be overestimated among adult female patients due to breasts. In addition, the deformity may be partially concealed by subcutaneous tissue in adult female patients or pectoralis hypertrophy in males but also in patients who received implants, resulting in an underestimation of the external Haller index. In contrast, these problems are not foreseen in the majority of pectus patients as they are slender with limited amounts of subcutaneous fat. Moreover, in Western countries, pectus excavatum is occasional in (young) females, as observed in the present as well as in other series, such as the experience of Pilegaard et al., [23]. Nevertheless, group specific cut-off values could potentially improve diagnostic value of the external indices and should be subject of future research.

Another disadvantage of 3D imaging with respect to the gold standard CT is the lack of intrathoracic information (e.g., the presence of cardiac compression). Nonetheless, 3D images may serve as primary screening tool to quantify severity. Severity based on the external Haller index or correction index could be used as derivative to indicate potential presence of cardiac compression since the conventional Haller index and correction index yield significantly higher values among patients with cardiac compression, as reported by Deviggiano et al., [32]. The conventional indices, moreover, demonstrate increasing values with increasing severity of compression [32]. Computed tomography may subsequently be

reserved as a second step to evaluate severe cases or those with clinical symptoms suspected of cardiac impairment. Alternatively, cardiac MRI may yield superior diagnostic value. Whether it will be possible to predict the presence of cardiac compression based on the extent and morphology of the deformity derived from 3D images is subject of future research.

In addition to cardiac compression, the presence of other thoracic anomalies cannot be evaluated by 3D images. Significant incidentalomas (i.e., the ones that affect surgical decisions) are only found in 1% of pectus excavatum patients evaluated for surgical repair [33]. This is in accordance with the current series in which one significant anomaly was found which concerned an anterior mediastinal lymphangioma causing a delay of surgical correction without other therapeutic consequences.

We acknowledge that intra-thoracic information, as seen on axial imaging, may be essential for part of pectus surgeons. However, given that up to 52% routinely acquire two-view plain radiographs during preoperative work-up [8] this is predominantly based on surgeon's preference.

Conclusion

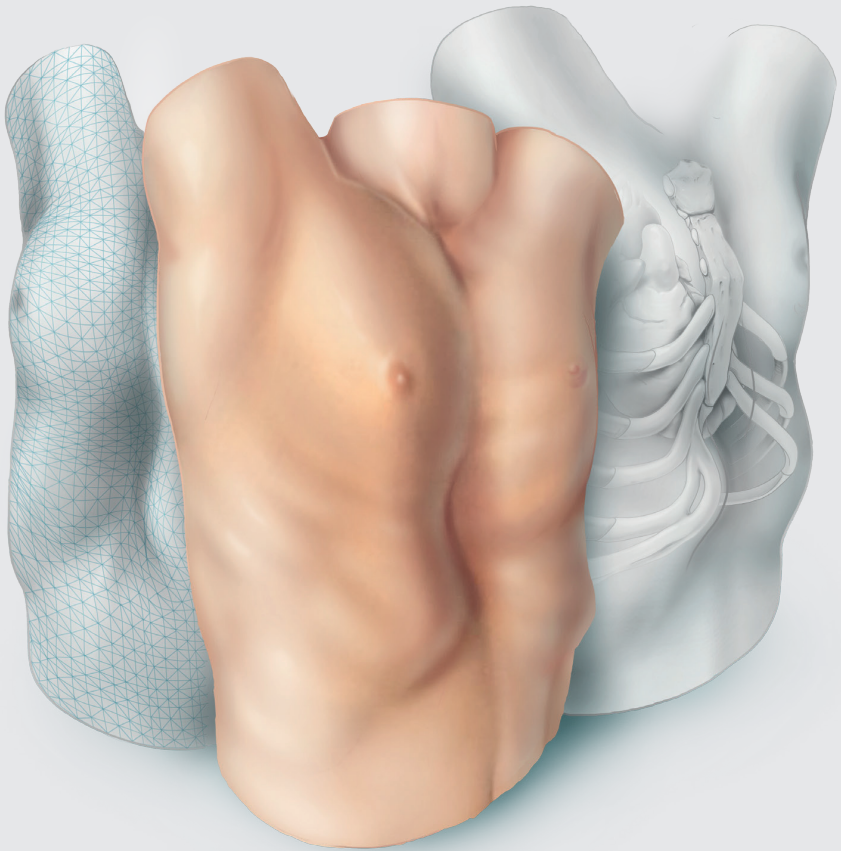
The 3D image derived external Haller index and external correction index are an attractive and accurate alternative for the conventional radiographic studies with a high positive predictive value to facilitate surgical decision-making among patients suspected of pectus excavatum., respectively applying a cut-off point of ≥ 1.83 and ≥ 15.2 for surgical candidacy. However, given the relatively lower negative predictive values of the external Haller index, additional diagnostic tests may be advisable in case of high clinical suspicion of severe pectus excavatum in conjunction with a below-cut-off external severity measure value.

References

1. Fokin AA, Steuerwald NM, Ahrens WA, Allen KE. Anatomical, histologic, and genetic characteristics of congenital chest wall deformities. *Semin Thorac Cardiovasc Surg* 2009;21:44-57.
2. Chung CS, Myriantopoulos NC. Factors affecting risks of congenital malformations. I. Analysis of epidemiologic factors in congenital malformations. Report from the Collaborative Perinatal Project. *Birth Defects Orig Artic Ser* 1975;11:1-22.
3. Ewert F, Syed J, Kern S, Besendörfer M, Carbon RT, Schulz-Drost S. Symptoms in Pectus Deformities: A Scoring System for Subjective Physical Complaints. *Thorac Cardiovasc Surg* 2017;65:43-9.
4. Fonkalsrud EW, Dunn JC, Atkinson JB. Repair of pectus excavatum deformities: 30 years of experience with 375 patients. *Ann Surg* 2000;231:443-8.
5. Kelly RE, Jr., Shamberger RC, Mellins RB, Mitchell KK, Lawson ML, Oldham K et al. Prospective multicenter study of surgical correction of pectus excavatum: design, perioperative complications, pain, and baseline pulmonary function facilitated by internet-based data collection. *J Am Coll Surg* 2007;205:205-16.
6. Miller KA, Woods RK, Sharp RJ, Gittes GK, Wade K, Ashcraft KW et al. Minimally invasive repair of pectus excavatum: A single institution's experience. *Surgery* 2001;130:652-9.
7. Haller JA, Jr., Kramer SS, Lietman SA. Use of CT scans in selection of patients for pectus excavatum surgery: a preliminary report. *J Pediatr Surg* 1987;22:904-6.
8. Martinez-Ferro M. Indexes for Pectus Deformities. In Kolvekar S, Pilegaard H (eds): *Chest Wall Deformities and Corrective Procedures*. Cham: Springer International Publishing 2016; 35-60.
9. Poston PM, Patel SS, Rajput M, Rossi NO, Ghanamah MS, Davis JE et al. The correction index: setting the standard for recommending operative repair of pectus excavatum. *Ann Thorac Surg* 2014;97:1176-9; discussion 9-80.
10. Brenner D, Elliston C, Hall E, Berdon W. Estimated risks of radiation-induced fatal cancer from pediatric CT. *AJR Am J Roentgenol* 2001;176:289-96.
11. Don S. Radiosensitivity of children: potential for overexposure in CR and DR and magnitude of doses in ordinary radiographic examinations. *Pediatr Radiol* 2004;34 Suppl 3:S167-72; discussion S234-41.
12. Miglioretti DL, Johnson E, Williams A, Greenlee RT, Weinmann S, Solberg LI et al. The use of computed tomography in pediatrics and the associated radiation exposure and estimated cancer risk. *JAMA Pediatr* 2013;167:700-7.
13. Bliss DP, Jr., Vaughan NA, Walk RM, Naiditch JA, Kane AA, Hallac RR. Non-Radiographic Severity Measurement of Pectus Excavatum. *J Surg Res* 2019;233:376-80.
14. Glinkowski W, Sitnik R, Witkowski M, Kocoń H, Bolewicki P, Górecki A. Method of pectus excavatum measurement based on structured light technique. *J Biomed Opt* 2009;14:044041.
15. Hebal F, Port E, Hunter CJ, Malas B, Green J, Reynolds M. A novel technique to measure severity of pediatric pectus excavatum using white light scanning. *J Pediatr Surg* 2019;54:656-62.

16. Poncet P, Kravarusic D, Richart T, Evison R, Ronsky JL, Alassiri A et al. Clinical impact of optical imaging with 3-D reconstruction of torso topography in common anterior chest wall anomalies. *J Pediatr Surg* 2007;42:898-903.
17. Uccheddu F, Ghionzoli M, Volpe Y, Servi M, Furferi R, Governi L et al. A Novel Objective Approach to the External Measurement of Pectus Excavatum Severity by Means of an Optical Device. *Ann Thorac Surg* 2018;106:221-7.
18. Daemen JHT, Loonen TGJ, Lozekoot PWJ, Maessen JG, Maal TJJ, Hulsewé KWE et al. Optical imaging versus CT and plain radiography to quantify pectus severity: a systematic review and meta-analysis. *J Thorac Dis* 2020;12:1475-87.
19. Cohen JF, Korevaar DA, Altman DG, Bruns DE, Gatsonis CA, Hooft L et al. STARD 2015 guidelines for reporting diagnostic accuracy studies: explanation and elaboration. *BMJ Open* 2016;6:e012799.
20. Daemen JHT, Loonen TGJ, Coorens NA, Maessen JG, Maal TJJ, Hulsewé KWE et al. Photographic documentation and severity quantification of pectus excavatum through three-dimensional optical surface imaging. *J Vis Commun Med* 2020;43:190-7.
21. Khanna G, Jaju A, Don S, Keys T, Hildebolt CF. Comparison of Haller index values calculated with chest radiographs versus CT for pectus excavatum evaluation. *Pediatr Radiol* 2010;40:1763-7.
22. Kelly RE, Goretsky MJ, Obermeyer R, Kuhn MA, Redlinger R, Haney TS et al. Twenty-one years of experience with minimally invasive repair of pectus excavatum by the Nuss procedure in 1215 patients. *Ann Surg* 2010;252:1072-81.
23. Pilegaard HK, Licht PB. Early results following the Nuss operation for pectus excavatum – a single-institution experience of 383 patients. *Interact Cardiovasc Thorac Surg* 2008;7:54-7.
24. Zhang DK, Tang JM, Ben XS, Xie L, Zhou HY, Ye X et al. Surgical correction of 639 pectus excavatum cases via the Nuss procedure. *J Thorac Dis* 2015;7:1595-605.
25. Taylor JS, Madhavan S, Szafer D, Pei A, Koppolu R, Barnaby K et al. Three-Dimensional Optical Imaging for Pectus Excavatum Assessment. *Ann Thorac Surg* 2019;108:1065-71.
26. Birkemeier KL, Podberesky DJ, Salisbury S, Serai S. Limited, fast magnetic resonance imaging as an alternative for preoperative evaluation of pectus excavatum: a feasibility study. *J Thorac Imaging* 2012;27:393-7.
27. Lo Piccolo R, Bongini U, Basile M, Savelli S, Morelli C, Cerra C et al. Chest fast MRI: an imaging alternative on pre-operative evaluation of Pectus Excavatum. *J Pediatr Surg* 2012;47:485-9.
28. Daemen JHT, Loonen TGJ, Verhulst AC, Maal TJJ, Maessen JG, Vissers YLJ et al. Three-Dimensional Imaging of the Chest Wall: A Comparison Between Three Different Imaging Systems. *J Surg Res* 2020;259:332-41.
29. Guillot MS, Rouchaud A, Mounayer C, Tricard J, Belgacem A, Auditeau E et al. X-ray-free protocol for pectus deformities based on magnetic resonance imaging and a low-cost portable three-dimensional scanning device: a preliminary study. *Interact Cardiovasc Thorac Surg* 2021.
30. Birkemeier KL, Podberesky DJ, Salisbury S, Serai S. Breathe in... breathe out... stop breathing: does phase of respiration affect the Haller index in patients with pectus excavatum? *Am J Roentgenol* 2011;197:W934-9.
31. St Peter SD, Juang D, Garey CL, Laituri CA, Ostlie DJ, Sharp RJ et al. A novel measure for pectus excavatum: the correction index. *J Pediatr Surg* 2011;46:2270-3.

32. Deviggiano A, Carrascosa P, Vallejos J, Bellia-Munzon G, Vina N, Rodríguez-Granillo GA et al. Relationship between cardiac MR compression classification and CT chest wall indexes in patients with pectus excavatum. *J Pediatr Surg* 2018;53:2294-8.
33. Rattan AS, Laor T, Ryckman FC, Brody AS. Pectus excavatum imaging: enough but not too much. *Pediatr Radiol* 2010;40:168-72.





Development of a prediction model for cardiac compression in pectus excavatum based on three-dimensional surface images

Jean H.T. Daemen, Samuel Heuts, Ashkan Rezazadah Ardabili, Jos G. Maessen, Karel W.E. Hulsewé, Yvonne L.J. Vissers, Erik R. de Loos

Adapted from: Semin Thorac Cardiovasc Surg 2023;35:202-12.

Abstract

Background

In pectus excavatum, three-dimensional (3D) surface imaging provides an accurate and radiation-free alternative to computed tomography (CT) to determine severity. Yet, it does not allow for cardiac evaluation since 3D imaging solely captures the chest wall surface. The objective was to develop a 3D image-based prediction model for cardiac compression in patients evaluated for pectus excavatum.

Methods

A prospective cohort study was conducted including consecutive patients referred for pectus excavatum who received a thoracic CT. Additionally, 3D images were acquired. The external pectus depth, its length, craniocaudal position, cranial slope, asymmetry, anteroposterior distance, and chest width were calculated from 3D images. Together with baseline patient characteristics they were submitted to forward multivariable logistic regression to identify predictors for cardiac compression. Cardiac compression on CT was used as reference. The model's performance was depicted by the area under the receiver operating characteristic (AUROC) curve. Internal validation was performed using bootstrapping.

Results

Sixty-one patients were included of whom 41 had cardiac compression on CT. A combination of the 3D image derived external pectus depth and external anteroposterior distance was identified as predictive for cardiac compression, yielding an AUROC of 0.935 (95%-confidence interval [CI]: 0.878-0.992) with an optimism of 0.006. In a second model for males alone, solely the external pectus depth was identified as predictor, yielding an AUROC of 0.947 (95%-CI: 0.892-1.000) with an optimism of 0.0002.

Conclusions

We have developed two 3D image-based prediction models for cardiac compression in patients evaluated for pectus excavatum which provide an outstanding discriminatory performance between the presence and absence of cardiac compression with negligible optimism.

Introduction

Pectus excavatum is the most common congenital chest wall deformity, characterized by a posterior displacement of the sternum and adjacent costal cartilage. The inwardly curved deformity causes cardiac compression in up to 90% of cases [1, 2], most often affecting the right heart side [3, 4]. Although cardiac function of patient with pectus excavatum at rest is similar to that of healthy controls [5], pectus excavatum is associated with reduced exercise capacity due to impaired cardiac performance [5, 6]. Following surgical repair, cardiac function has shown to significantly improve [7].

Currently, computed tomography (CT) is the most established imaging technique in the diagnostic work-up of pectus excavatum, as indicated by its routine use by 59% of chest wall experts [8]. The primary goal of CT is to determine the severity of deformity through the gold standard Haller index [8, 9] and to evaluate the presence of cardiac and/or pulmonary compression. Both are used as objective criteria in the multifactorial process to determine candidacy for surgical treatment [10].

A major drawback of routine use of CT is the carcinogenic property of the ionizing radiation. Especially among pediatric patients this is of concern [11, 12], provided that a single chest CT is associated with a life-time attributable risk of 0.2% on solid cancer and leukemia [12].

In an effort to eliminate this potentially harmful exposure, three-dimensional (3D) surface imaging has gained increasing interest in recent years [13, 14]. It has been shown to provide an accurate and radiation-free alternative to determine the severity of pectus excavatum [15], but 3D imaging is limited by the fact that it solely captures the chest wall surface. Consequently, it is considered unsuitable for evaluation of cardiac status, requiring additional diagnostic studies such as echocardiography and cardiac magnetic resonance imaging.

However, since most patients operated for pectus excavatum are slender, with limited amounts of subcutaneous fat, it is conceivable that the presence of cardiac compression could be predicted based on 3D image derived measures and baseline patient characteristics. Examples of measures include the external pectus excavatum depth, length of deformity and its cranial slope, and the anteroposterior distance of the thorax [16].

Objective of the present study is to develop a prediction model for cardiac compression in patients evaluated for pectus excavatum based on 3D image derived measures and baseline patient characteristics.

Materials and Methods

Study design

A single-center prospective cohort study was conducted between August 2019 and November 2020. The study was approved by the local ethics and clinical research committee (Medical Ethics Review Committee Zuyderland, ID: METCZ20190048, approval date: April 9th, 2019). Written informed consent was obtained from all patients. This report was written in compliance with the Transparent Reporting of a multivariable prediction model for Individual Prognosis or Diagnosis statement [17].

Study population

Consecutive patients referred for pectus excavatum to the outpatient clinic of our tertiary referral center for chest wall disorders (Department of Surgery, Division of General Thoracic Surgery, Zuyderland Medical Center, Heerlen, the Netherlands) who received a thoracic CT were eligible. Patients aged 18 years and above routinely received a CT as part of their work-up. In patients younger than 18 years this was only indicated in case of suspicion on cardiac compression. For this study, all participants received an additional 3D image of the chest. Because flickering light is emitted during 3D imaging, patients with any form of light hypersensitivity (e.g., photosensitive epilepsy) were excluded. Patients with prior chest wall surgery were also excluded. Patients were stratified into two groups based on the presence or absence of cardiac compression on CT.

Variables and data acquisition

Baseline patient characteristics including sex, age, body mass index (BMI) and subjective preoperative symptoms were obtained.

Computed tomography

Scans were performed on a single-source CT (Somatom Definition AS, Siemens Healthineers, Forchheim, Germany), using a non-contrast-enhanced and non-electrocardiography-triggered protocol. Cardiac compression was judged by a

dedicated thoracic radiologist and experienced thoracic surgeon (EdL), producing a single expert team conclusion. Assessors were blinded to potential predictor variables. Gradation of compression was applied for characterization of the enrolled cohort, using the classification proposed by Deviggiano et al., [18]. Type 0 reflected the absence of cardiac compression, while type 1 indicated right ventricle compression without atrioventricular groove involvement. Type 2 presented right ventricle compression with involvement of the atrioventricular groove [18]. The severity of compression was moreover quantified through the cardiac compression index that was calculated by dividing the transverse diameter of the heart by the narrowest anteroposterior diameter at the xiphoid process. The cardiac asymmetry index was calculated by the widest paramedian anteroposterior diameter by the narrowest anteroposterior diameter at the xiphoid process [19]. In addition, routinely used CT derived pectus severity measures [8], including the Haller index and correction index, were obtained.

Three-dimensional images

Three-dimensional images (see Figure 1 for examples) were obtained by the Artec Leo (Artec3D, Luxembourg, Luxembourg). Images were acquired at end inspiration, applying the imaging protocol previously described [21]. Pectus measures evaluated as potential predictors for cardiac compression were based on the pectus excavatum characteristics described by Cartoski et al., [16] and included the depth, width, and length of the depression, its craniocaudal position, cranial slope, as well as asymmetry. The external pectus excavatum depth was calculated in the sagittal direction with respect to a craniocaudal tangent of the anterior chest wall (Figure 2A). The sagittal direction was chosen over the transverse due to the potential overestimation among females because of breast tissue, and among patients with pectoralis hypertrophy. For the same reasons it was not possible to accurately determine the pectus width, which was therefore not considered. Pectus length was defined as the Euclidean distance between the cranial and caudal edges of the deformity (Figure 2A). The craniocaudal position of the most excavated point was expressed as percentage where 0% depicts the suprasternal notch and 100% the umbilicus (Figure 2B). The slope was defined as the angle between the point of maximum depression and cranial edge of the deformity (Figure 2C), while asymmetry was based on relative volumetric differences between the left and right hemithorax. Asymmetry was expressed as percentage where a negative value indicates asymmetry at the expense of the left hemithorax.



Figure 1: Examples of three-dimensional images with increasing cardiac compression index from left to right.

Although there is no established relationship between cardiac compression and the abovementioned phenotypical measures, the gold standard Haller index and the correction index have previously been reported to elicit higher values among patients with compression of the heart [18]. Its external equivalents derived from 3D images (i.e., the external Haller index and external correction index [22]) could therefore be potential predictors. Since both are composite measures, their input values were used to prevent interaction of predictors. Subsequently, the external anteroposterior distance at the most depressed point (Figure 2D.1) and the widest external transverse width (Figure 2D.2) were also evaluated. The paramedian maximal anteroposterior distance, part of the external correction index, was not considered given that its external measurement may also be overestimated among females and patients with pectoralis hypertrophy.

All the above-mentioned measures were calculated from the 3D images by a self-developed automatic MATLAB R2020A (MathWorks, Massachusetts, United States of America) algorithm which was previously verified for accuracy and reproducibility by Coorens and colleagues [23].

Statistical analysis

Continuous variables were denoted as mean and standard deviation (SD) or as median and interquartile range (IQR) in the absence of normality. Categorical variables were depicted as frequencies and percentages. Differences between patients with and without cardiac compression on CT were assessed by Fisher's exact test for binary variables and the unpaired samples t-test or Mann-Whitney U test for continuous data.

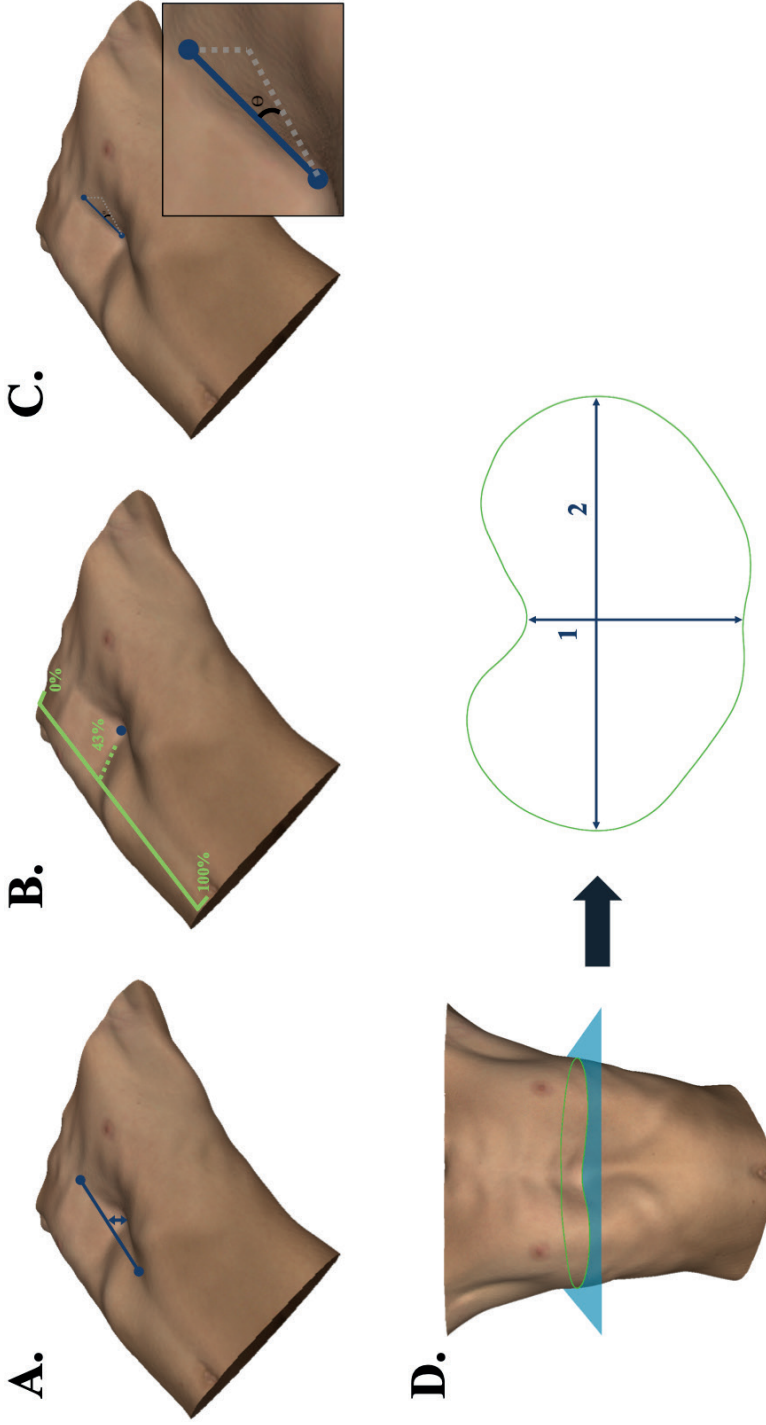


Figure 2: Three-dimensional image measurement methods. (A) The external pectus excavatum depth was calculated with respect to a craniocaudal tangent of the anterior chest wall while the pectus length was defined as the distance between the cranial and caudal edge of the deformity. (B) The craniocaudal position of the most depressed point expressed as percentage. (C) The slope was defined as the angle between the point of maximum depression and cranial edge of the deformity. (D) The external anteroposterior distance (D.1) and transverse width (D.2) were calculated from the transverse slice exhibiting the most depressed point. θ , angle.

Multivariable logistic regression was used to identify predictors for cardiac compression and develop a prediction model. All 3D image derived pectus measurements and baseline patient characteristics (including subjective symptoms) were explored in the model building-process. The forward stepwise selection method was used with entry ($P \leq 0.05$) and removal ($P > 0.10$) based on likelihood ratio testing. Model assumptions on linearity, multicollinearity and independence of errors were checked. Linearity was evaluated by the Box-Tidwell test. Multicollinearity was indicated by a variance inflation factor (VIF) > 5 and tolerance < 0.2 . In addition, the impact of influential cases was evaluated by Cook's distance. A distance larger than 1 indicated the presence of an influential case. Predicted probabilities of the multivariable regression model were calculated and submitted to receiver operating characteristic (ROC) curve analysis to determine its discriminative ability between the presence and absence of cardiac compression, depicted by the area under the ROC curve (AUROC).

Internal validation was performed by the bootstrap procedure to account for overfitting. One thousand bootstrap samples were drawn with replacement from the original sample. The optimism corrected estimate of the AUROC was obtained. In addition, the shrinkage factor was obtained to calculate the bias-corrected regression coefficients.

Youden's J index was utilized to select the cut-off probability for cardiac compression with an optimal trade-off between sensitivity and specificity.

Statistical analyses were performed by SPSS statistics (IBM Corp. IBM SPSS Statistics for MacOS, Version 27.0, Armonk, New York, United States of America) and R (version 4.0.3; R Foundation for Statistical Computing, Vienna, Austria). A P value ≤ 0.05 was considered statistically significant. Post-hoc analyses were not prespecified.

Results

Study population

Sixty-one patients referred for pectus excavatum were enrolled of whom 41 presented with cardiac compression on CT. Patients predominantly encompassed males (85%) and most often experienced exercise intolerance (61%). Patients without cardiac compression were significantly older (median: 19 years [IQR: 16-

26]) and had a higher median BMI (20.4kg/m² [IQR: 19.6-21.7]) compared to those with cardiac compression (median: 16 years [IQR: 14-22]; P=0.025 and median: 19.6kg/m² [IQR: 18.7-20.9]; P=0.029; Table 1). In addition, patients with compression demonstrated more severe pectus excavatum, as depicted by the gold standard CT derived Haller index (3.71 [IQR: 3.16-4.67] versus 2.75 [IQR: 2.52-2.98]; P<0.001). Among patients with compromise of their heart, type 1 cardiac compression was most frequent (61%). This indicates right ventricle compression without atrioventricular groove involvement. As expected, both the cardiac compression index and cardiac asymmetry index were significantly higher in patients with cardiac compression (both P<0.001; Table 2). Comparable differences were observed among males with and without cardiac compression.

Table 1: Clinical patient characteristics.

	Males and females (n=61)			Males only (n=52)		
	Cardiac compression (n=41)	No cardiac compression (n=20)	P value ^a	Cardiac compression (n=32)	No cardiac compression (n=20)	P value ^a
Male, n (%)	32 (78)	20 (100)	0.024 ^b	32 (100)	20 (100)	-
Age, years, median (IQR)	16 (14-22)	19 (16-26)	0.025 ^b	15 (14-18)	19 (16-26)	0.001 ^b
BMI, kg/m², median (IQR)	19.6 (18.7-20.9)	20.4 (19.6-21.7)	0.029 ^b	19.5 (18.2-20.9)	20.4 (19.6-21.7)	0.026 ^b
Preoperative symptoms, n (%)						
<i>Palpitations</i>	9 (22)	5 (25)	1.00	5 (16)	5 (25)	0.48
<i>Thoracic pain/tightness</i>	10 (24)	9 (45)	0.14	6 (19)	9 (45)	0.061
<i>Exercise intolerance</i>	28 (68)	9 (45)	0.099	23 (72)	9 (45)	0.079
<i>Dyspnea</i>	13 (42)	5 (25)	0.77	9 (28)	5 (25)	1.00
<i>Body image disturbance</i>	17 (41)	11 (55)	0.41	15 (47)	11 (55)	0.78

^aUsing the Mann-Whitney U test for continuous data and Fisher's exact test for binary data.

^bStatistically significant at P≤0.05.

n, number; IQR, interquartile range; BMI, body mass index.

Pectus excavatum measures

Of the evaluated 3D image derived measures, the external pectus depth, cranial slope, anteroposterior distance, and transverse width demonstrated statistically significant differences between both groups (Table 3). The largest differences

were observed for the pectus depth (21mm [IQR: 17-31] versus 11mm [IQR: 5-15]) and anteroposterior distance (168mm [SD: 23] versus 200mm [SD: 20]). In addition, the cranial slope was steeper while the chest was less wide in patients with cardiac compression. Similar differences were observed among males with and without cardiac compression, apart from the transverse width which did not significantly differ (see Table 3).

Table 2: Computed tomography based measures of pectus excavatum severity and cardiac compression.

	Males and females (n=61)			Males only (n=52)		
	Cardiac compression (n=41)	No cardiac compression (n=20)	P value ^a	Cardiac compression (n=32)	No cardiac compression (n=20)	P value ^a
Haller index, median (IQR)	3.71 (3.16-4.67)	2.75 (2.52-2.98)	<0.001 ^b	3.66 (3.19-4.70)	2.75 (2.52-2.98)	<0.001 ^b
Correction index, median (IQR)	28.9% (23.8-37.3)	12.0% (9.2-15.2)	<0.001 ^b	28.2% (24.0-36.6)	12.0% (9.2-15.2)	<0.001 ^b
Cardiac compression type, n (%)						
Type 0	-	20 (100)	-	-	20 (100)	-
Type 1	25 (61)	-	-	21 (66)	-	-
Type 2	16 (39)	-	-	11 (34)	-	-
Cardiac compression index, median (IQR)	2.68 (2.24-3.04)	1.56 (1.45-1.71)	<0.001 ^b	2.64 (2.23-3.01)	1.56 (1.45-1.71)	<0.001 ^b
Cardiac asymmetry index, median (IQR)	1.57 (1.26-1.90)	1.08 (1.03-1.11)	<0.001 ^b	1.51 (1.23-1.86)	1.08 (1.03-1.11)	<0.001 ^b

^aUsing the Mann-Whitney U test for continuous data. ^bStatistically significant at $P \leq 0.05$.
n, number; IQR, interquartile range.

Cardiac compression model

Model 1: males and females

Using forward multivariable logistic regression, a combination of the external pectus excavatum depth and external anteroposterior distance was found to be predictive for cardiac compression, yielding an AUROC of 0.935 (95% confidence interval [CI]: 0.878-0.992). The assumptions on linearity, multicollinearity (VIF: 1.72,

tolerance: 0.58) and independence of errors were met. No influential cases were identified. Internal validation by the bootstrap procedure demonstrated a bias corrected AUROC of 0.929 (optimism: 0.006) and shrinkage factor of 0.913. The adjusted coefficients and the model's formula are shown in Table 4.

Table 3: Three-dimensional image derived measures.

	Males and females (n=61)			Males only (n=52)		
	Cardiac compression (n=41)	No cardiac compression (n=20)	P value ^a	Cardiac compression (n=32)	No cardiac compression (n=20)	P value ^a
Pectus depth, mm, median (IQR)	21 (17-31)	11 (5-15)	<0.001 ^b	22 (17-31)	11 (5-15)	<0.001 ^b
Pectus length, mm, mean (SD)	183 (29)	173 (58)	0.45	181 (29)	173 (58)	0.48
Craniocaudal position, %, mean (SD)	44 (3)	45 (7)	0.67	44 (2)	45 (7)	0.68
Cranial slope, degrees, median (IQR)	4 (-1-11)	2 (-10-7)	0.034 ^b	6 (3-13)	2 (-10-7)	0.012 ^b
Asymmetry, %, median (IQR)	-2 (-3-2)	0 (-2-2)	0.36	-1 (-3-2)	0 (-2-2)	0.53
Anteroposterior distance, mm, mean (SD)	168 (23)	200 (20)	<0.001 ^b	168 (25)	200 (20)	<0.001 ^b
Transverse width, mm, median (IQR)	314 (300-328)	331 (313-352)	0.010 ^b	322 (307-331)	331 (313-352)	0.061

^aUsing the unpaired samples t-test or Mann-Whitney U test for continuous data. ^bStatistically significant at P≤0.05.

n, number; *mm*, millimeter; *IQR*, interquartile range; *SD*, standard deviation.

The model's sensitivity and specificity were respectively 0.76 (95% CI: 0.60-0.88) and 1.00 (95% CI: 0.83-1.00), applying a cut-off probability of 85% for cardiac compression.

It should be noted that sex was omitted from logistic regression analysis since all participating female patients suffered from cardiac compression.

Model 2: males only

Since all female patients presented with cardiac compression, a second multivariable logistic regression model was developed. For males alone (32 with and 20 without

cardiac compression), the external pectus excavatum depth was found as sole predictor for cardiac compression, yielding an AUROC of 0.947 (95% CI: 0.892-1.000). The applicable assumptions were met. No influential cases were identified. Bootstrapping demonstrated a bias corrected AUROC of 0.947 (optimism: 0.0002) and shrinkage factor of 0.942 (Table 4). The model's sensitivity and specificity were respectively 0.91 (95% CI: 0.75-0.98) and 0.85 (95% CI: 0.62-0.97), applying an optimal cut-off probability of 61% for cardiac compression among males.

See Supplementary Table 1 for all variables which were explored in the model-building process and their results.

Table 4: Results from the multivariate logistic regression model of three-dimensional image derived measures and clinical characteristics.

Predictors & intercept	Multivariate logistic regression model 1 ^a Males and females					Multivariate logistic regression model 2 ^c Males only				
	B	B [†]	P value	OR	95% CI	B	B ^{††}	P value	OR	95% CI
Pectus depth (mm)	0.273	0.249	0.003 ^b	1.31	1.10-1.57	0.489	0.461	0.002 ^b	1.63	1.19-2.23
Anteroposterior distance (mm)	-0.050	-0.046	0.027 ^b	0.95	0.91-0.99	-	-	0.39	-	-
Intercept	5.728	5.231	-	-	-	-7.362	-6.938	-	-	-
	AUROC (95% CI): 0.935 (0.878-0.992) ^b					AUROC (95% CI): 0.947 (0.892-1.000) ^b				
	Bootstrap optimism corrected AUROC: 0.929					Bootstrap optimism corrected AUROC: 0.947				

^aNote on the multivariate logistic regression model: R²=0.678 (Nagelkerke), 0.487 (Cox-Snell); model: $\chi^2=40.69$, P<0.001. ^bStatistically significant at P≤0.05. ^cNote on the multivariate logistic regression model: R²=0.730 (Nagelkerke), 0.537 (Cox-Snell); model: $\chi^2=40.06$, P<0.001. [†]Regression coefficients multiplied by a shrinkage factor of 0.913. ^{††}Regression coefficients multiplied by a shrinkage factor of 0.942. Model 1 formula: $P(\text{cardiac compression}) = 1/(1+\exp(-(5.231+(0.249*\text{pectus depth})-(0.046*\text{anteroposterior distance})))$. Model 2 formula: $P(\text{cardiac compression}) = 1/(1+\exp(-(-6.398+(0.461*\text{pectus depth})))$.

OR, odds ratio; CI, confidence interval; mm, millimeter; AUROC, area under the receiver operating characteristic.

Discussion

Physiologic impairment associated with pectus excavatum is predominantly due to cardiac compression by the inwardly deviated sternum and adjacent costal cartilage [6]. Identification of patients suffering from compression is an important part of the diagnostic work-up of pectus excavatum since it is applied as objective criterium in the multifactorial process to establish surgical candidacy [10].

In the present series, we have developed two 3D image-based prediction models for cardiac compression and shown that a combination of the external pectus depth and external anteroposterior distance is predictive for cardiac compression among patients of both sexes referred for pectus excavatum. For males, the external pectus depth was identified as sole predictor. Notwithstanding, both models provide an outstanding [27] discriminative ability between the presence and absence of cardiac compression, depicted by an optimism corrected AUROC of 0.929 and 0.947 respectively. The optimism of just 0.006 and 0.0002, moreover, indicates that the model may hold for future patients.

Identification of the external pectus depth and external anteroposterior distance as predictors for cardiac compression by model 1 (including males and females) was expected since a deep deformity combined with a small anteroposterior distance (at the point of maximum depression) contributes to reduced cardiac space, increasing the probability for compression. In addition, contribution of the external anteroposterior distance is also explained by the Haller index and correction index which elicit higher values among patients with cardiac compression [18]. Both measures consider the internal anteroposterior distance (sternum-spine) and are correlated with their 3D derived external equivalents [22]. Intuitively it may be assumed that the model's predictor variables are related. Yet, no multicollinearity was observed. In other words, a small anteroposterior chest diameter does not necessarily imply the presence of a deep pectus excavatum.

The second model, specifically created for males, solely incorporated the external depth of pectus excavatum as predictor for cardiac compression, compared to the model including both males and females which also considered the external anteroposterior distance as predictor. Post hoc analyses revealed a considerably higher correlation between the external pectus depth and anteroposterior distance among males in comparison to females. This difference could be explained by the heterogeneity of females included. Especially older females with a deep deformity

have a considerable amount of presternal subcutaneous tissue (see Figure 3 for examples) compared to relatively young females without or minimal breast development and males. As a result, the pectus depth is underestimated in the former females, preventing an accurate prediction based on the depth alone. The anteroposterior distance may subsequently have been selected by forward logistic regression due to the fact that it is naturally smaller among females compared to males [28] in conjunction with the fact that males with a deep deformity and thus higher probability for compression also had a relatively small anteroposterior distance. Notwithstanding, the bottom line is that separate future models may be required for males and females and should be subject of future research.

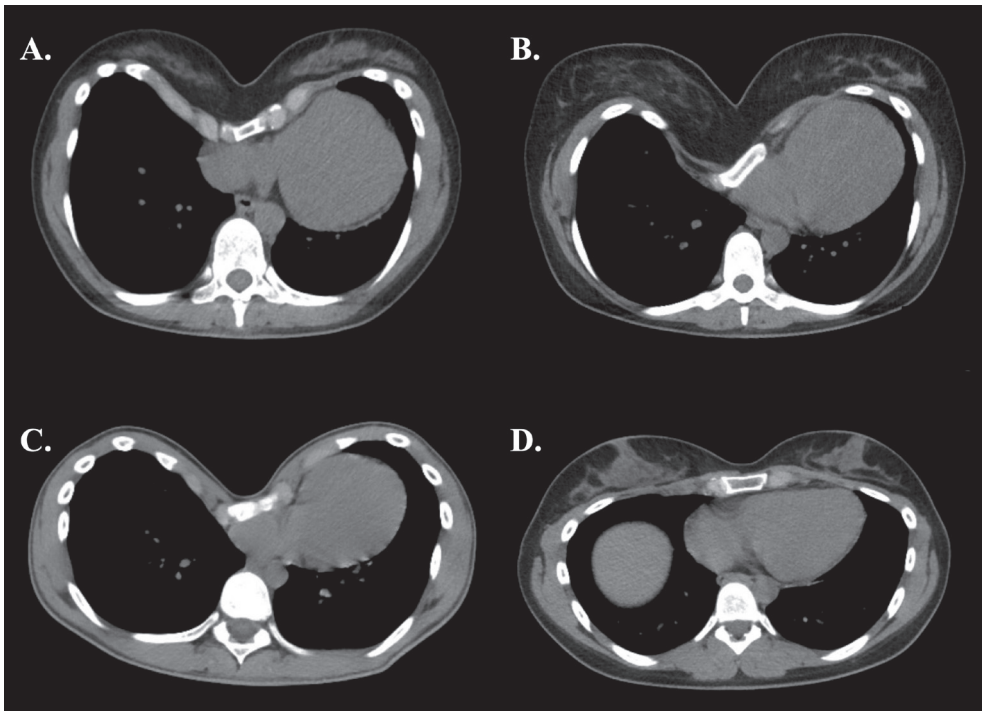


Figure 3: Transverse computed tomography slices of (A, B) two female patients with a relatively deep pectus excavatum, (C) a male patient with a deep deformity, and (D) a female patient with a shallow deformity.

Even though 3D image derived measures were based on external dimensions, BMI did not significantly ($P > 0.10$) contribute to the model's fit based on likelihood ratio testing. Not as predictor, nor as interaction term with the external pectus

excavatum depth and external anteroposterior distance. Yet, the median BMI of the entire cohort was only 19.9kg/m² (IQR: 18.9-21.0; range: 14.9-26.8) and only 2 patients were identified as having overweight (BMI \geq 25.0). A potential effect of BMI could therefore not be ruled out reliably. Careful interpretation of the prediction model among patients with a BMI below 14.9 and above 26.8 is thus advocated.

In addition, the fact that none of the subjective symptoms were identified as predictive for cardiac compression is supported by Ewert et al., who showed that symptoms of patients with pectus excavatum are independent of severity [29]. Moreover, post-hoc analyses revealed no statistically significant differences regarding the cardiac compression and cardiac asymmetry index between patients with or without subjective physiologic symptoms.

Although 3D imaging does not (yet) allow for evaluation of pulmonary compression, it may not elicit problems for clinical decision making since respiratory limitations are generally considered of less importance [6, 30]. Another argument in favor of standard CT evaluation regards detection of incidentalomas. If present, these could affect surgical candidacy. Rattan and colleagues reviewed thoracic CT scans of 209 children and young adults evaluated for surgical treatment of pectus excavatum and identified only three (1.4%) clinically relevant unanticipated findings [31]. This is in concordance with the current study wherein one (1.6%) asymptomatic anterior mediastinal lymphangioma was found. Consequently, standard CT use yields a number needed to expose of 63 to 71 patients, to detect a single relevant incidentaloma, which seems to be unjustified for this patient category.

Development of the prediction model was initiated to overcome the inability of cardiac evaluation by 3D imaging. Yet, this could also be covered by routine deployment of additional diagnostic studies, such as echocardiography and cardiac magnetic resonance imaging. Nonetheless, by applying the prediction model as first-line diagnostic, one is provided the ability to stratify patients based on their probability for cardiac compression and prevent unnecessary diagnostics. Applying the optimal cut-off probabilities, model 1 demonstrated a positive predictive value of 1.00 detecting the presence of cardiac compression compared to 0.91 for model 2 by which further diagnostic studies become redundant. In the present study this would have prevented 51% (n=31/61) diagnostic studies among males and females combined and 62% (n=32/52) studies among males alone. On the contrary, additional investigations are advised upon a negative result in combination with

a clinical suspicion of physiologic impairment, given the relatively lower negative predictive value of respectively 0.67 and 0.85. Especially for the former model; model 1. Nevertheless, applying secondary cut-off probabilities could also prevent additional diagnostics in patients with a negative result by maximizing sensitivity. For example, a secondary cut-off of 25% increases the sensitivity to 0.98 for model 1. Depending on the desired test certainty, additional diagnostic studies could then be reserved for patients yielding a probability between the primary and secondary cut-off probability for cardiac compression.

Clinically, the models' outcomes should be applied in the same way that the presence or absence of cardiac compression on CT is currently interpreted and used in the multifactorial process for surgical decision-making. For example, a patient with questionable physiologic symptoms, but a high probability of cardiac compression may be offered additional exercise testing while the same patient with a low probability of cardiac compression may be counseled for follow-up.

The median age [32, 33] and male-female ratio [33, 34] of the entire cohort (respectively 17 years [IQR: 15-23] and a ratio of 6:1) were in concordance with other series and subsequently deemed representative. However, the preoperative Haller index (entire cohort: 3.33 [IQR: 2.82-4.08]) was considerably lower compared to other series [1, 32, 33]. The same was observed for cardiac compression yielding a frequency up to 90% in previous studies [1, 2], compared to 67% in the current study. This is explained by the fact that we enrolled patients preoperatively evaluated for pectus excavatum, while other series solely reported on surgical treatment results. In addition, it should be noted that this study was conducted in a tertiary referral center for chest wall disorders situated in the Netherlands, which requires referral by a general practitioner or medical specialist. This may provide a different patient sample compared to other centers and countries. Overall, these aspects may pose a threat to the extrapolability of the study's results.

Despite that CT is an established part of the current diagnostic trajectory [8], it only provides a static representation of the cardiac status. Cardiac compression on CT may thus not necessarily imply functional cardiac impairment. Evaluation by means of cardiac magnetic resonance imaging or echocardiography could potentially provide more clinically useful information due to functional assessment and may be subject of future research to improve the presented model. Future studies could, moreover, aim to develop a prediction model concerning the type

of cardiac compression (i.e., type 1/2). Yet, the clinical significance of the difference between these types for surgical decision-making needs to be determined first. In addition, associated disorders such as thoracic scoliosis may also be explored for their contribution to cardiac compression by future models.

Given the primary rationale for the use of 3D images being the exposure to ionizing associated with current diagnostic studies, one could also argue for the routine use of magnetic resonance imaging which can moreover, as repeatedly mentioned, provide information on functional cardiac status. Yet, the routine use of magnetic resonance imaging is handicapped by relatively high costs, time consumption (up to 8 minutes using a fast-imaging protocol), reduced availability due to capacity issues, unviability for claustrophobic patients as well as motion-sensitivity which may even require sedation in young subjects [35, 36].

The main advantage of 3D imaging with respect to current diagnostic procedures is prevention of unnecessary exposure to ionizing radiation. In addition, despite the upfront costs of the 3D imaging system, both the fixed and variable costs are lower than CT. A complete 3D image of the thorax is moreover acquired in about 10 seconds and can be obtained in unconventional places (e.g., the ward).

Limitations

Given the prospective nature of the present study, no bias due to missing data was present. In addition, since only one patient denied participation during the study period, the probability of selection bias was negligible. Despite the fact that no sample size estimation was performed, we adhered to the one predictor per 10 events rule of thumb [37]. Moreover, with at most only two predictor variables incorporated in a single model, the general strive for parsimony was achieved. Nevertheless, a major limitation remains the relatively small sample size with state imbalance (i.e., 67% of patients have cardiac compression), which inevitably implies a high risk of overfitting. Yet, both models demonstrated negligible optimism. Another limitation of the present study is that cardiac compression was solely evaluated on a dichotomous scale. Future studies should aim to develop a model incorporating the severity and type of cardiac compression as this could provide clinically useful information.

Internal validation of the model was performed by the bootstrap procedure which revealed only little optimism. However, external validation is necessary to ascertain

whether the developed model is appropriate for prediction in other settings and evaluate its diagnostic value in terms of sensitivity and specificity. This should be topic of future research.

CT scans were acquired using a non-contrast-enhanced and non-electrocardiography-triggered protocol. Consequently, patients were imaged at different timepoints of the cardiac cycle which may have affected uniform evaluation of cardiac status. Moreover, the numerator of the cardiac compression index is also affected by the cardiac cycle. In addition, as stressed earlier, the fact that cardiac compression may not necessarily imply functional cardiac impairment should be regarded as limitation.

In theory, 3D image measurements are subjective to the imaging system's and automated algorithm's reproducibility and accuracy, but also to alterations of respiration phase at which 3D images are acquired. Although the system and algorithm employed in the present study were previously validated and verified for thoracic 3D images yielding adequate reproducibility and accuracy [23, 38], the developed prediction model solely applies to patients imaged during end inspiration, given that chest dimensions significantly change during the respiratory cycle [39]. Since the anteroposterior distance typically decreases upon expiration, increasing the potential for cardiac compression, future studies should evaluate the effect of imaging at different phases of the respiratory cycle.

Another limitation of 3D images is the limited availability and upfront costs of the imaging systems as well as the required software to obtain measurements. The imaging system employed in the present study is commercially available for about US\$30,000, but given the minimal resolution required to obtain 3D images of the chest, devices under US\$1,000, such as the tablet-mountable structure sensor (Occipital Inc., San Francisco, California, USA) have also proven to be effective for imaging of pectus excavatum [40]. Nevertheless, since the current models are built upon 3D images obtained by the Artec Leo imaging system, other systems should first be verified. On the other hand, one could also determine the external pectus depth and external anteroposterior distance using respectively a ruler and thoracic caliper. However, such measurements should be interpreted with care since they are subject to variability due to the degree of compression applied.

Although 3D imaging has previously been shown to provide an accurate and radiation-free alternative to determine the severity of pectus excavatum by an

external equivalent of the Haller index [15], it has necessitated additional diagnostic studies for cardiac evaluation. This limitation has been overcome by development of a 3D image-based prediction model for cardiac compression in the present study. Based on the model's performance we suggest that 3D imaging could be employed as primary diagnostic in the work-up of pectus excavatum, with the advantage that it is free from exposure to potentially harmful ionizing radiation associated with current diagnostic procedures.

Conclusion

We have developed two three-dimensional image-based prediction models for cardiac compression in patients evaluated for pectus excavatum. The models consist of the external pectus excavatum depth and external posterior distance as predictors and provide outstanding discriminatory performance between the presence and absence of cardiac compression with negligible optimism. Future studies should focus on external validation of the developed models to ascertain appropriateness for prediction.

References

1. Croitoru DP, Kelly RE, Jr., Goretsky MJ, Lawson ML, Swoveland B, Nuss D. Experience and modification update for the minimally invasive Nuss technique for pectus excavatum repair in 303 patients. *J Pediatr Surg* 2002;37:437-45.
2. Rodriguez-Granillo GA, Raggio IM, Deviggiano A, Bellia-Munzon G, Capunay C, Nazar M et al. Impact of pectus excavatum on cardiac morphology and function according to the site of maximum compression: effect of physical exertion and respiratory cycle. *Eur Heart J Cardiovasc Imaging* 2019;21:77-84.
3. Mocchegiani R, Badano L, Lestuzzi C, Nicolosi GL, Zanuttini D. Relation of right ventricular morphology and function in pectus excavatum to the severity of the chest wall deformity. *Am J Cardiol* 1995;76:941-6.
4. Oezcan S, Attenhofer Jost CH, Pfyffer M, Kellenberger C, Jenni R, Binggeli C et al. Pectus excavatum: echocardiography and cardiac MRI reveal frequent pericardial effusion and right-sided heart anomalies. *Eur Heart J Cardiovasc Imaging* 2012;13:673-9.
5. Lesbo M, Tang M, Nielsen HH, Frøkiær J, Lundorf E, Pilegaard HK et al. Compromised cardiac function in exercising teenagers with pectus excavatum. *Interact Cardiovasc Thorac Surg* 2011;13:377-80.
6. Malek MH, Fonkalsrud EW, Cooper CB. Ventilatory and cardiovascular responses to exercise in patients with pectus excavatum. *Chest* 2003;124:870-82.
7. Malek MH, Berger DE, Housh TJ, Marelich WD, Coburn JW, Beck TW. Cardiovascular Function Following Surgical Repair of Pectus Excavatum. *Chest* 2006;130:506-16.
8. Martinez-Ferro M. Indexes for Pectus Deformities. In Kolvekar S, Pilegaard H (eds): *Chest Wall Deformities and Corrective Procedures*. Cham: Springer International Publishing 2016; 35-60.
9. Haller JA, Jr., Kramer SS, Lietman SA. Use of CT scans in selection of patients for pectus excavatum surgery: a preliminary report. *J Pediatr Surg* 1987;22:904-6.
10. Kelly RE, Jr. Pectus excavatum: historical background, clinical picture, preoperative evaluation and criteria for operation. *Semin Pediatr Surg* 2008;17:181-93.
11. Don S. Radiosensitivity of children: potential for overexposure in CR and DR and magnitude of doses in ordinary radiographic examinations. *Pediatr Radiol* 2004;34 Suppl 3:S167-72; discussion S234-41.
12. Miglioretti DL, Johnson E, Williams A, Greenlee RT, Weinmann S, Solberg LI et al. The use of computed tomography in pediatrics and the associated radiation exposure and estimated cancer risk. *JAMA Pediatr* 2013;167:700-7.
13. Glinkowski W, Sitnik R, Witkowski M, Kocoń H, Bolewicki P, Górecki A. Method of pectus excavatum measurement based on structured light technique. *J Biomed Opt* 2009;14:044041.
14. Hebal F, Port E, Hunter CJ, Malas B, Green J, Reynolds M. A novel technique to measure severity of pediatric pectus excavatum using white light scanning. *J Pediatr Surg* 2019;54:656-62.
15. Taylor JS, Madhavan S, Szafer D, Pei A, Koppolu R, Barnaby K et al. Three-Dimensional Optical Imaging for Pectus Excavatum Assessment. *Ann Thorac Surg* 2019;108:1065-71.
16. Cartoski MJ, Nuss D, Goretsky MJ, Proud VK, Croitoru DP, Gustin T et al. Classification of the dysmorphology of pectus excavatum. *J Pediatr Surg* 2006;41:1573-81.

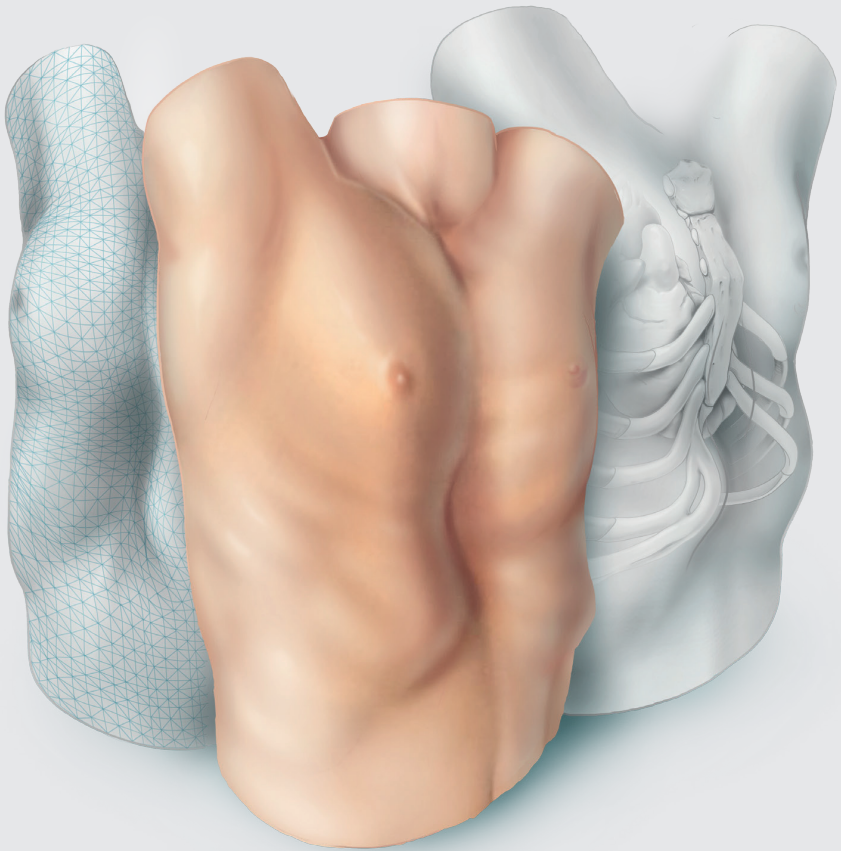
17. Collins GS, Reitsma JB, Altman DG, Moons KG. Transparent reporting of a multivariable prediction model for individual prognosis or diagnosis (TRIPOD) the TRIPOD statement. *Circulation* 2015;131:211-9.
18. Deviggiano A, Carrascosa P, Vallejos J, Bellia-Munzon G, Vina N, Rodríguez-Granillo GA et al. Relationship between cardiac MR compression classification and CT chest wall indexes in patients with pectus excavatum. *J Pediatr Surg* 2018;53:2294-8.
19. Kim M, Lee KY, Park HJ, Kim HY, Kang EY, Oh YW et al. Development of new cardiac deformity indexes for pectus excavatum on computed tomography: feasibility for pre- and post-operative evaluation. *Yonsei Med J* 2009;50:385-90.
20. Poston PM, Patel SS, Rajput M, Rossi NO, Chanamah MS, Davis JE et al. The correction index: setting the standard for recommending operative repair of pectus excavatum. *Ann Thorac Surg* 2014;97:1176-9; discussion 9-80.
21. Daemen JHT, Loonen TGJ, Coorens NA, Maessen JG, Maal TJJ, Hulsewé KWE et al. Photographic documentation and severity quantification of pectus excavatum through three-dimensional optical surface imaging. *J Vis Commun Med* 2020;43:190-7.
22. Daemen JHT, Loonen TGJ, Lozekoot PWJ, Maessen JG, Maal TJJ, Hulsewé KWE et al. Optical imaging versus CT and plain radiography to quantify pectus severity: a systematic review and meta-analysis. *J Thorac Dis* 2020;12:1475-87.
23. Coorens NA, Daemen JHT, Slump CH, Loonen TGJ, Vissers YLJ, Hulsewé KWE et al. The Automatic Quantification of Morphological Features of Pectus Excavatum Based on Three-Dimensional Images. *Semin Thorac Cardiovasc Surg* 2021.
24. Hair J, Anderson R, Babin B, Black W. Multivariate data analysis: A global perspective (Vol. 7): Pearson Upper Saddle River. In. NJ 2010.
25. Cook RD, Weisberg S. Residuals and influence in regression. New York: Chapman and Hall,1982.
26. Steyerberg EW, Harrell FE, Jr., Borsboom GJ, Eijkemans MJ, Vergouwe Y, Habbema JD. Internal validation of predictive models: efficiency of some procedures for logistic regression analysis. *J Clin Epidemiol* 2001;54:774-81.
27. Hosmer Jr DW, Lemeshow S, Sturdivant RX. Applied logistic regression. John Wiley & Sons,2013.
28. Bellemare F, Jeanneret A, Couture J. Sex Differences in Thoracic Dimensions and Configuration. *Am J Respir Crit Care Med* 2003;168:305-12.
29. Ewert F, Syed J, Kern S, Besendörfer M, Carbon RT, Schulz-Drost S. Symptoms in Pectus Deformities: A Scoring System for Subjective Physical Complaints. *Thorac Cardiovasc Surg* 2017;65:43-9.
30. Acosta J, Bradley A, Raja V, Aliverti A, Badiyani S, Motta A et al. Exercise improvement after pectus excavatum repair is not related to chest wall function. *Eur J Cardiothorac Surg* 2014;45:544-8.
31. Rattan AS, Laor T, Ryckman FC, Brody AS. Pectus excavatum imaging: enough but not too much. *Pediatr Radiol* 2010;40:168-72.
32. Kelly RE, Goretsky MJ, Obermeyer R, Kuhn MA, Redlinger R, Haney TS et al. Twenty-one years of experience with minimally invasive repair of pectus excavatum by the Nuss procedure in 1215 patients. *Ann Surg* 2010;252:1072-81.
33. Pilegaard HK, Licht PB. Early results following the Nuss operation for pectus excavatum – a single-institution experience of 383 patients. *Interact Cardiovasc Thorac Surg* 2008;7:54-7.

34. Hosie S, Sitkiewicz T, Petersen C, Göbel P, Schaarschmidt K, Till H et al. Minimally invasive repair of pectus excavatum--the Nuss procedure. A European multicentre experience. *Eur J Pediatr Surg* 2002;12:235-8.
35. Birkemeier KL, Podberesky DJ, Salisbury S, Serai S. Limited, fast magnetic resonance imaging as an alternative for preoperative evaluation of pectus excavatum: a feasibility study. *J Thorac Imaging* 2012;27:393-7.
36. Lo Piccolo R, Bongini U, Basile M, Savelli S, Morelli C, Cerra C et al. Chest fast MRI: an imaging alternative on pre-operative evaluation of Pectus Excavatum. *J Pediatr Surg* 2012;47:485-9.
37. Peduzzi P, Concato J, Kemper E, Holford TR, Feinstein AR. A simulation study of the number of events per variable in logistic regression analysis. *J Clin Epidemiol* 1996;49:1373-9.
38. Daemen JHT, Loonen TGJ, Verhulst AC, Maal TJJ, Maessen JG, Vissers YLJ et al. Three-Dimensional Imaging of the Chest Wall: A Comparison Between Three Different Imaging Systems. *J Surg Res* 2020;259:332-41.
39. Birkemeier KL, Podberesky DJ, Salisbury S, Serai S. Breathe in... breathe out... stop breathing: does phase of respiration affect the Haller index in patients with pectus excavatum? *Am J Roentgenol* 2011;197:W934-9.
40. Guillot MS, Rouchaud A, Mounayer C, Tricard J, Belgacem A, Auditeau E et al. X-ray-free protocol for pectus deformities based on magnetic resonance imaging and a low-cost portable three-dimensional scanning device: a preliminary study. *Interact Cardiovasc Thorac Surg* 2021;33:110-8.

Supplementary Table 1: Results from the multivariate logistic regression model of three-dimensional image derived measures and clinical characteristics.

Predictors & intercept	Multivariate logistic regression model 1 ^a					Multivariate logistic regression model 2 ^c				
	Males and females					Males only				
	B	B [†]	P value	OR	95% CI	B	B ^{††}	P value	OR	95% CI
Age (years)	-	-	0.37	-	-	-	-	0.32	-	-
BMI (kg/m ²)	-	-	0.31	-	-	-	-	0.51	-	-
Palpitations (yes/no)	-	-	0.49	-	-	-	-	0.31	-	-
Thoracic pain/tightness (yes/no)	-	-	0.57	-	-	-	-	0.66	-	-
Exercise intolerance (yes/no)	-	-	0.20	-	-	-	-	0.15	-	-
Dyspnea (yes/no)	-	-	0.66	-	-	-	-	0.54	-	-
Body image disturbance (yes/no)	-	-	0.17	-	-	-	-	0.18	-	-
Pectus depth (mm)	0.273	0.249	0.003 ^b	1.31	1.10-1.57	0.489	0.461	0.002 ^b	1.63	1.19-2.23
Pectus length (mm)	-	-	0.076	-	-	-	-	0.83	-	-
Craniocaudal position (%)	-	-	0.097	-	-	-	-	0.20	-	-
Cranial slope (degrees)	-	-	0.13	-	-	-	-	0.99	-	-
Asymmetry (%)	-	-	0.19	-	-	-	-	0.35	-	-
Anteroposterior distance (mm)	-0.050	-0.046	0.027 ^b	0.95	0.91-0.99	-	-	0.39	-	-
Transverse width (mm)	-	-	0.50	-	-	-	-	0.37	-	-
Intercept	5.728	5.231	-	-	-	-7.362	-6.938	-	-	-
	AUROC (95% CI): 0.935 (0.878-0.992) ^b					AUROC (95% CI): 0.947 (0.892-1.000) ^b				
	Bootstrap optimism corrected AUROC: 0.929					Bootstrap optimism corrected AUROC: 0.947				

^aNote on the multivariate logistic regression model: R²=0.678 (Nagelkerke), 0.487 (Cox-Snell); model: $\chi^2=40.69$, P<0.001. ^bStatistically significant at P≤0.05. ^cNote on the multivariate logistic regression model: R²=0.730 (Nagelkerke), 0.537 (Cox-Snell); model: $\chi^2=40.06$, P<0.001. [†]Regression coefficients multiplied by a shrinkage factor of 0.913. ^{††}Regression coefficients multiplied by a shrinkage factor of 0.942. Model 1 formula: $P(\text{cardiac compression}) = 1/(1+\exp(-(5.231+(0.249*\text{pectus depth})-(0.046*\text{anteroposterior distance}))))$. Model 2 formula: $P(\text{cardiac compression}) = 1/(1+\exp(-(-6.398+(0.461*\text{pectus depth}))))$. OR, odds ratio; CI, confidence interval; mm, millimeter; AUROC, area under the receiver operating characteristic





Visual diagnosis of pectus excavatum: an inter-observer and intra-observer agreement analysis

Jean H.T. Daemen, Erik R. de Loos, Tessa C.M. Geraedts, Hans Van Veer, Pieter Jan van Huijstee, Ted W.O. Elenbaas, Karel W.E. Hulsewé, Yvonne L.J. Vissers

Adapted from: J Ped Surg 2022;57;526-31.

Abstract

Background

Among patients suspected of pectus excavatum, visual examination is a key aspect of diagnosis and, moreover, guides work-up and treatment strategy. This study evaluated the inter-observer and intra-observer agreement of visual examination and diagnosis of pectus excavatum among experts.

Methods

Three-dimensional surface images of consecutive patients suspected of pectus excavatum were reviewed in a multi-center setting. Interactive three-dimensional images were evaluated for the presence of pectus excavatum, asymmetry, flaring, depth of deformity, cranial onset, overall severity and morphological subtype through a questionnaire. Observers were blinded to all clinical patient information, completing the questionnaire twice per subject. Agreement was analyzed by kappa statistics.

Results

Fifty-eight subjects with a median age of 15.5 years (interquartile range: 14.1-18.2) were evaluated by 5 (cardio)thoracic surgeons. Pectus excavatum was visually diagnosed in 55% to 95% of cases by different surgeons, revealing considerable inter-observer differences (kappa: 0.50; 95%-confidence interval [CI]: 0.41-0.58). All other items demonstrated inter-observer kappa's of 0.25-0.37. Intra-observer analyses evaluating the presence of pectus excavatum demonstrated a kappa of 0.81 (95%-CI: 0.72-0.91), while all other items showed intra-observer kappa's of 0.36-0.68.

Conclusions

Visual examination and diagnosis of pectus excavatum yields considerable inter-observer and intra-observer disagreements. As this variation in judgement could impact work-up and treatment strategy, objective standardization is urged.

Introduction

Among congenital anterior chest wall anomalies, pectus excavatum is the most common in the Western world. The condition is characterized by an inward displacement of the sternum and adjacent costal cartilage with a worldwide incidence of 1 to 8 per 1000 persons [1]. Patients may suffer from a wide variety of symptoms. This most commonly involves physical complaints, such as exercise intolerance, dyspnea and chest pain, but also psychological distress due to body image disturbances [2-5]. The morphological presentation of pectus excavatum is as diverse as its symptomatology, resulting from the combination and degree of phenotypical features present. Attempts to cluster morphological variations have led to categorization in descriptive subtypes, as proposed by Cartoski and colleagues [6]. For example, the most common type is a cup-shaped pectus excavatum, describing a localized depression with limited peripheral effects (i.e., usually deep with steep sides) [7]. Other features generally considered include the presence and degree of asymmetry and flaring, as well as the position of the deepest point. Key point in the diagnosis of pectus excavatum is the initial assessment through visual examination and subsequent qualitative description of phenotypical features. However, this is prone to inter-observer and intra-observer differences and could potentially influence clinical decision making in terms of work-up and treatment strategy. In extremis, patients may be offered or withheld from further analyses and treatment by different observers. To date, no studies have methodologically evaluated inter-observer and intra-observer agreement regarding the visual examination and diagnosis of pectus excavatum.

The aim of this study is to evaluate the inter-observer and intra-observer agreement of visual examination and diagnosis of pectus excavatum among experts. Assessments were based on interactive three-dimensional (3D) images of patients suspected of pectus excavatum.

Materials and Methods

Study design

We conducted a prospective cohort study wherein 3D images from a single center were reviewed in a multi-center setting. Prior to start, the study was approved by the local ethics and clinical research committee (Medical Ethics Review Committee Zuyderland, ID: METCZ20200089, approval date: May 8th, 2020). The need for informed

consent was waived. This report was written in compliance with the Strengthening the Reporting of Observational Studies in Epidemiology guidelines [8].

Participants

Subjects

We reviewed all consecutive patients who were referred for suspected pectus excavatum to one of the tertiary referral centers for chest wall disorders (Department of Surgery, Division of General Thoracic surgery, Zuyderland Medical Center, Heerlen, the Netherlands), and who received a thoracic 3D image between August 2019 and August 2020. Patients who underwent prior chest wall surgery or suffered from any form of light hypersensitivity were excluded. The latter was due to the flickering light emitted during 3D image acquisition that could provoke seizures.

Observers

Three-dimensional images of patients suspected of pectus excavatum were visually reviewed by 5 experienced pectus surgeons (4 general thoracic surgeons and one cardiothoracic surgeon) from 4 different tertiary referral centers in 2 countries (two surgeons from Zuyderland Medical Center, Heerlen, the Netherlands; and one surgeon from: University Hospitals Leuven, Leuven, Belgium; Catharina Hospital, Eindhoven, the Netherlands; and Haga Hospital, The Hague, the Netherlands). Single surgeon experience in consulting and surgical treatment of pectus excavatum ranged from 4 to 12 years with a mean annual surgical volume of 50 to 70 cases.

Sample size estimation

Since this is the first study to analyze observer agreement regarding the visual examination and diagnosis of pectus excavatum, it was not possible to determine the number of subjects and observers required. However, in order to provide a representative cohort, we chose to include all single institution patients consulting for suspected excavatum over a 1-year time period. In addition, the number of 5 observers was chosen arbitrarily.

Measurements and variables

Patient charts were reviewed for baseline patient characteristics including sex, age, body mass index and preoperative Haller index derived from either computed tomography or two-view plain chest radiographies [9, 10].

Three-dimensional images (see example Figure 1) were acquired by the Artec Leo (Artec3D, Luxembourg, Luxembourg) according to the imaging protocol described elsewhere [11]. Interactive (i.e., rotatable and translatable) 3D images were utilized to assess observer agreement since repeated live patient examinations by experts from different centers over a one-year time-period was not practically feasible.

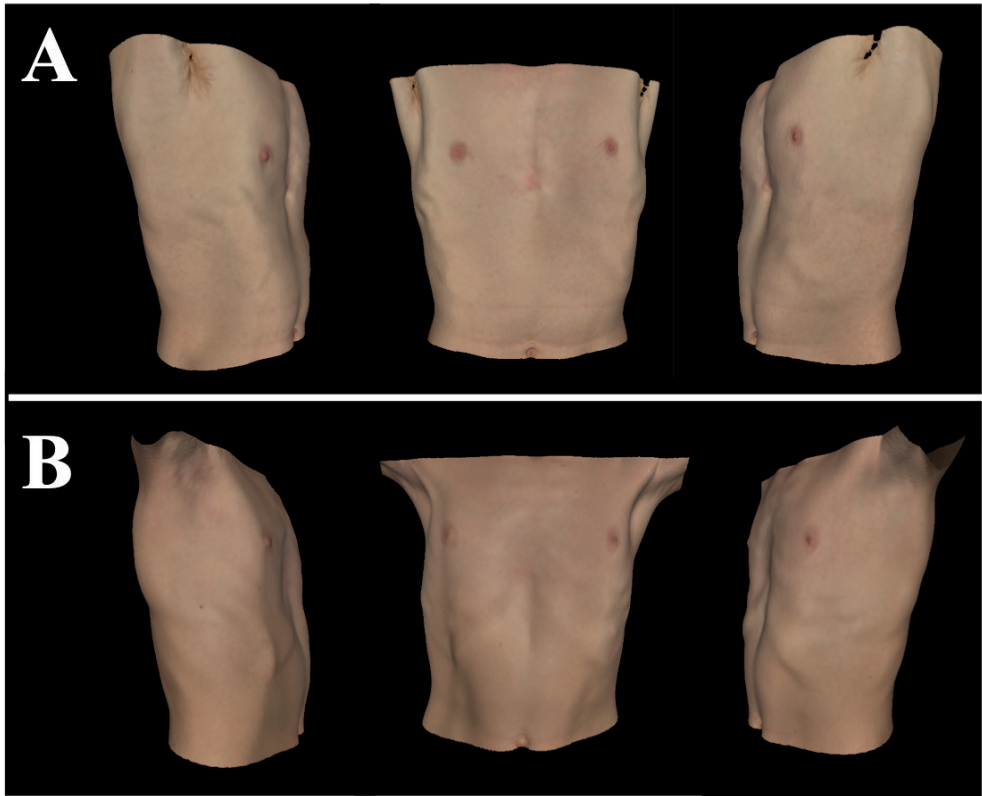


Figure 1: Three-dimensional images of (A-B) two distinct subjects that were judged to suffer from pectus excavatum by 3 of 5 observers, demonstrating inter-observer differences.

Observers were asked to visually examine 3D images on the basis of a 7-item questionnaire composed by the researchers (see Table 1). Observers were blinded to all clinical information (e.g., symptomatology and Haller index), as well as to the results of other observers and prior evaluations. The first question addressed whether the patient had pectus excavatum. If yes, agreement to 5 statements concerning the presence and severity of phenotypical pectus excavatum features was evaluated through binominal judgement (i.e., agree or disagree). Evaluated features were based

on the pectus characteristics described by Cartoski et al., [6] and encompassed the depth of deformity, its cranial onset point, the presence of asymmetry, flaring and overall severity. The use of these characteristics was further rationalized by Kelly [12] who emphasized that their preoperative notion affects surgical strategy. In addition, evaluation of the overall severity was rationalized by the fact that clinical evaluation algorithms, such as those described by Nuss and Kelly [13] and Frantz et al., [14] stratify patients based on the subjective overall severity of their deformity. Both the depth of the deformity and overall severity were evaluated with the difference being that severity was used as a comprehensive judgement of the pectus excavatum (including its disfiguring aspect) while depth solely referred to the visual depth of the excavation. We deliberately chose to, if possible, use binominal judgement options since offering more options would inevitably lead to a reduction in agreement. The last item to score encompassed the subtype of dysmorphology (i.e., cup-shaped, saucer-shaped, trench-like or other), according to the most common subtypes described by Kelly and colleagues [7]. Observers were not asked to judge surgical treatment eligibility or candidacy as this is a multifactorial decision, often and not solely based on visual examination alone. All observers completed the questionnaire twice per subject, the second time in a random order compared to the first run-through, while bearing at least one week in between.

Table 1: The 7-item questionnaire used to structure visual examination of interactive 3D images of patients suspected of pectus excavatum.

Item	Question	Answer options
1	Does the presented patient suffer from pectus excavatum?	Yes / No
2	Would you describe the deformity as deep?	Yes / No
3	Does the deformity exhibit a high cranial onset point?	Yes / No
4	Is the deformity asymmetric?	Yes / No
5	Is flaring present?	Yes / No
6	Would you judge the overall severity as severe?	Yes / No
7	How would you categorize the deformity?	Cup-shaped / Saucer-shaped / Trench-like / Any other

Statistical analysis

Statistical analyses were performed by SPSS statistics (IBM Corp. IBM SPSS Statistics for MacOS, Version 27.0, Armonk, NY, USA). Normally distributed continuous

variables were depicted as mean and standard deviation (SD). If skewed, the median, interquartile range (IQR) and range were used. Categorical variables were denoted as frequencies and percentages.

To evaluate inter-observer agreement, nominal questionnaire ratings from the first assessment round were submitted to Cohen's kappa statistics for all observer pairs. The weighted (i.e., based on the number of subjects evaluated) arithmetic mean of all observer pairs was, according to Light [15], employed as measure of overall agreement. Additionally, the inter-observer agreement per observer was based on the weighted arithmetic mean of all observer pairs encompassing the observer of interest. Two-sided 95% confidence intervals (CI) were calculated. Since further work-through of the questionnaire (after the first question) was halted in the absence of pectus excavatum, inter-observer agreement concerning the remaining statements could only be determined on the basis of patients identified as pectus excavatum by both observers of the observer pair. Intra-observer agreement was evaluated in a similar fashion but using repeated assessments by the same surgeon.

Post-hoc sensitivity analyses were performed to evaluate potential agreement differences based on the quantitative severity of pectus excavatum, measured through the Haller index. Patients were stratified applying a Haller index threshold of 3.25, that is generally considered indicative for treatment [9, 10]. In the case where both answer options were not represented in the comparison (e.g., if one of the two surgeons judges all patients as pectus excavatum), the variable was treated as constant and as such, it was not possible to determine Cohen's kappa. If so, the percentage of agreement was applied.

Kappa coefficients were interpreted as follows: a coefficient between 0.00-0.20, 0.21-0.40, 0.41-0.60, 0.61-0.80 and 0.81-1.00 respectively corresponded to slight, fair, moderate, substantial and almost perfect agreement [16].

Results

Three-dimensional images of 58 consecutive patients referred for suspected pectus excavatum were judged by 5 experienced chest wall surgeons. During the accrual period, only 1 patient denied participation. Included patients were predominantly male (86%) with an overall median age of 15.5 years (IQR: 14.1-18.2; range: 9.1-59.9)

and a mean BMI of 19.3 kg/m² (SD: 2.5). The median Haller index was 3.36 (IQR: 2.82-4.04; range: 2.12-10.21). No missing data was present.

Inter-observer agreement

During the first assessment round, patients were judged to suffer from pectus excavatum in 55% (n=32/58) to 95% (n=55/58) of cases by different surgeons, demonstrating considerable inter-observer differences. The overall inter-observer coefficient of agreement regarding the presence of pectus excavatum was 0.50 (95% CI: 0.41-0.58; see Table 2). This indicates a moderate level of agreement. Figure 1 shows two examples of subjects that were judged to suffer from pectus excavatum by 3 out of 5 observers. The largest share in disagreement was produced by observer E, revealing a kappa of 0.25 (95% CI: 0.16-0.33). In contrast, observer A to observer D demonstrated an inter-observer agreement between 0.47 and 0.61 (see Table 2), evaluating the presence of pectus excavatum.

Judgements regarding the depth of deformity, cranial onset point, and overall severity yielded fair to moderate agreement among raters with an overall kappa of respectively 0.37 (95% CI: 0.30-0.44), 0.37 (95% CI: 0.30-0.45) and 0.37 (95% CI: 0.30-0.44). In addition, slight to fair concordance (kappa: 0.25; 95% CI: 0.16-0.34) was observed among observers when evaluating the presence of thoracic asymmetry. Similar to the visual diagnosis of pectus excavatum, observer E yielded the lowest inter-observer agreement for the depth of deformity (0.23; 95% CI: 0.10-0.35), overall severity (kappa: 0.14; 95% CI: 0.01-0.26), as well as the presence of asymmetry (0.16; 95% CI: 0.00-0.32) and flaring (kappa: 0.31; 95% CI: 0.08-0.53).

Among patients judged to have pectus excavatum observers classified the subtype of morphology yielding an overall kappa of 0.34 (95% CI: 0.28-0.40), expressing fair agreement.

Inter-observer agreement between the two thoracic surgeons from the same center (i.e., observer A and observer D) ranged from 0.41 to 0.73 across all items scored. Despite these kappa levels demonstrated to be above average for all items scored (see Table 2), they were not superior to all individual observer pairs. For example, regarding the diagnosis of pectus excavatum, observer A and observer D demonstrated an inter-observer kappa of 0.73, while observer A and observer B (both from another center) demonstrated a kappa of 0.82.

Table 2: Inter-observer agreement regarding the visual assessment and diagnosis of patients suspected of pectus excavatum.

	Overall, kappa (95% CI)	Observer A vs B-E, kappa (95% CI)	Observer B vs A & C-E, kappa (95% CI)	Observer C vs A-B & D-E, kappa (95% CI)	Observer D vs A-C & E, kappa (95% CI)	Observer E vs A-D, kappa (95% CI)
Pectus excavatum	0.50 (0.41-0.58)	0.61 (0.47-0.74)	0.60 (0.46-0.73)	0.55 (0.41-0.69)	0.47 (0.31-0.63)	0.25 (0.16-0.33)
Deep deformity	0.37 (0.30-0.44)	0.45 (0.34-0.57)	0.27 (0.18-0.37)	0.43 (0.32-0.55)	0.40 (0.29-0.52)	0.23 (0.10-0.35)
High cranial onset	0.37 (0.30-0.45)	0.40 (0.29-0.52)	0.40 (0.28-0.53)	0.28 (0.17-0.39)	0.46 (0.34-0.57)	0.29 (0.15-0.44)
Asymmetry	0.25 (0.16-0.34)	0.31 (0.19-0.43)	0.21 (0.07-0.35)	0.20 (0.05-0.34)	0.34 (0.20-0.49)	0.16 (0.00-0.32)
Flaring	0.41 (0.30-0.52)	0.47 (0.31-0.64)	0.45 (0.30-0.60)	0.37 (0.20-0.54)	0.41 (0.26-0.56)	0.31 (0.08-0.53)
Severe	0.37 (0.30-0.44)	0.45 (0.34-0.56)	0.25 (0.15-0.35)	0.49 (0.38-0.60)	0.45 (0.34-0.55)	0.14 (0.01-0.26)
Subtype	0.34 (0.28-0.40)	0.39 (0.29-0.48)	0.28 (0.19-0.36)	0.31 (0.21-0.42)	0.37 (0.27-0.47)	0.33 (0.23-0.44)

CI, confidence interval.

Intra-observer agreement

The time between repeated assessments ranged from 7 to 26 days per observer. The overall intra-observer agreement regarding the presence of pectus excavatum was 0.81 (95% CI: 0.72-0.91; see Table 3), indicating substantial to almost perfect agreement. The kappa was lowest for observer B and E, who respectively gave 4 and 8 subjects an opposite judgement during the second compared to the first assessment round. For observer E this meant judging 41% as pectus excavatum, compared to 55% during the first round of assessment. Examples of patients for whom this was the case are shown in Figure 2.

Moderate intra-observer agreement was observed for judgements regarding the cranial onset point, the presence of flaring (0.41; 95% CI: 0.25-0.58) and the classification in morphological subtypes (0.55; 95% CI: 0.46-0.64). In addition, the repeated assessment of severity and depth of deformity yielded an overall agreement of respectively 0.65 (95% CI: 0.55-0.75) and 0.68 (95% CI: 0.59-0.78), both depicting substantial agreement.

Post-hoc sensitivity analysis

Among included patients, 52% (n=30/58) had a Haller index larger than or equal to 3.25. Scoring these patients, a higher median inter-observer agreement percentage of 97% (IQR: 77-100) was observed compared to patients with a Haller index <3.25 (median: 84%; IQR: 55-90), indicating improved inter-observer agreement among patients with a Haller index ≥ 3.25 . This trend was also observed for all other items except the classification of pectus morphology (Table 4).

A similar increased percentage of intra-observer agreement was observed judging the presence of pectus excavatum among patients with a Haller index ≥ 3.25 (median: 100%; IQR: 92-100) compared to patients with a Haller index <3.25 (median: 93%; IQR: 86-98). However, this was not uniformly reproduced since only 3 out of 6 items demonstrated superior kappa coefficients judging patients with a Haller index ≥ 3.25 (Table 4).

Table 3: Intra-observer agreement regarding the visual assessment and visual diagnosis of patients suspected of pectus excavatum.

	Overall, kappa (95% CI)	Observer A vs A, kappa (95% CI)	Observer B vs B, kappa (95% CI)	Observer C vs C, kappa (95% CI)	Observer D vs D, kappa (95% CI)	Observer E vs E, kappa (95% CI)
Pectus excavatum	0.81 (0.72-0.91)	0.88 (0.65-1.00)	0.68 (0.38-0.97)	0.77 (0.53-1.00)	1.00 (1.00-1.00)	0.73 (0.56-0.90)
Deep deformity	0.68 (0.59-0.78)	0.62 (0.40-0.84)	0.56 (0.32-0.79)	0.79 (0.62-0.96)	0.88 (0.71-1.00)	0.43 (0.11-0.76)
High cranial onset	0.51 (0.39-0.62)	0.46 (0.21-0.72)	0.49 (0.25-0.74)	0.50 (0.23-0.77)	0.43 (0.18-0.67)	0.82 (0.59-1.00)
Asymmetry	0.36 (0.23-0.48)	0.41 (0.18-0.63)	0.33 (0.02-0.65)	0.26 (-0.01-0.52)	0.33 (0.05-0.61)	0.56 (0.18-0.94)
Flaring	0.41 (0.25-0.58)	0.35 (0.00-0.70)	0.37 (0.05-0.69)	0.29 (-0.21-0.78)	0.54 (0.29-0.79)	0.62 (0.14-1.00)
Severe	0.65 (0.55-0.75)	0.76 (0.58-0.94)	0.47 (0.22-0.73)	0.76 (0.57-0.94)	0.60 (0.36-0.84)	0.68 (0.40-0.95)
Subtype	0.55 (0.46-0.64)	0.47 (0.29-0.65)	0.47 (0.27-0.66)	0.54 (0.34-0.73)	0.66 (0.50-0.82)	0.67 (0.43-0.91)

CI, confidence interval.

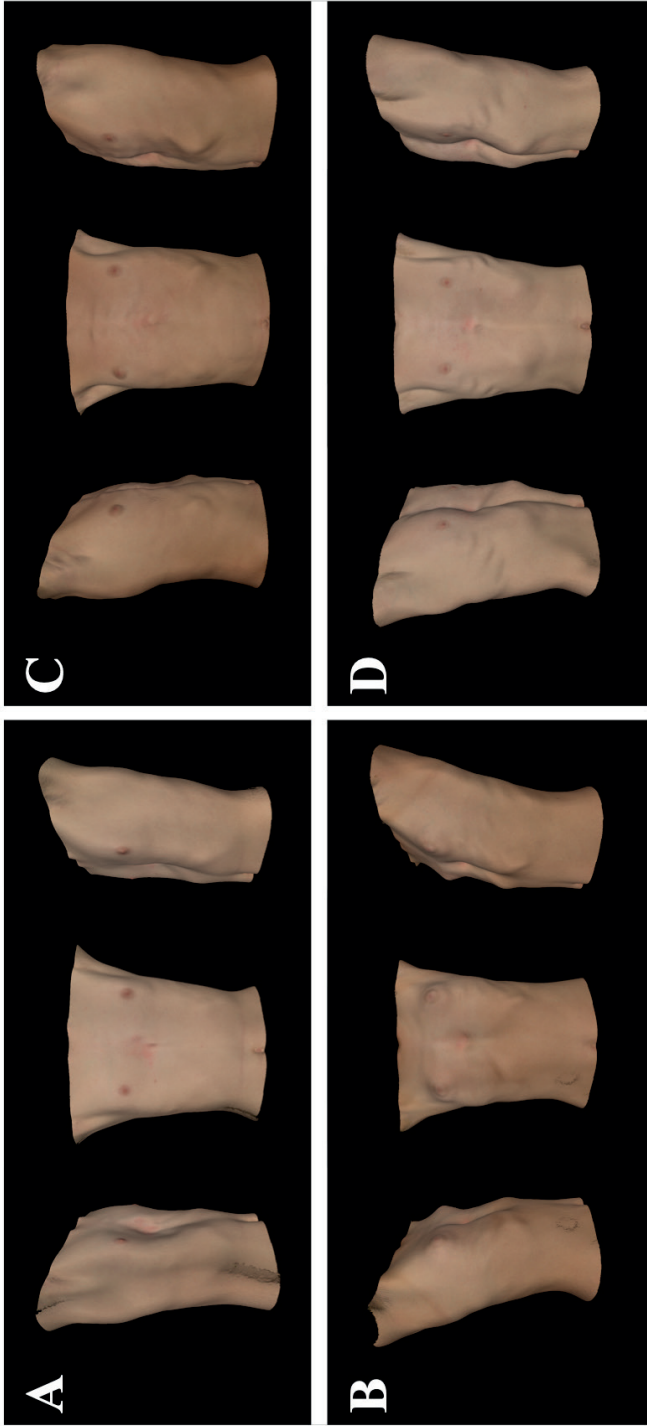


Figure 2: Three-dimensional images of (A-D) four distinct subjects that showed conflicting judgements regarding the presence of pectus excavatum upon repeated assessment (i.e., intra-observer disagreement) by observer E.

Table 4: Intra-observer and inter-observer agreement regarding the visual assessment and visual diagnosis of patients suspected of pectus excavatum, stratified by the preoperative Haller index.

	Inter-observer agreement		Intra-observer agreement	
	Haller index ≥ 3.25 (n=30)	Haller index < 3.25 (n=28)	Haller index ≥ 3.25 (n=30)	Haller index < 3.25 (n=28)
Pectus excavatum, percentage of agreement, median (IQR)	97 (77-100)	84 (55-90)	100 (92-100)	93 (86-98)
Deep deformity, kappa (95% CI)	0.36 (0.27-0.45)	0.24 (0.12-0.36)	0.67 (0.40-0.95)	0.50 (0.29-0.72) ^a
High cranial onset, kappa (95% CI)	0.41 (0.30-0.51)	0.28 (0.16-0.40)	0.44 (0.30-0.59)	0.39 (0.19-0.59)
Asymmetry, kappa (95% CI)	0.36 (0.23-0.49)	0.04 (-0.08-0.17) ^b	0.22 (0.05-0.38)	0.30 (0.11-0.48)
Flaring, kappa (95% CI)	0.47 (0.34-0.60)	0.32 (0.17-0.47)	0.49 (0.28-0.70)	0.29 (0.08-0.49)
Severe, kappa (95% CI)	0.35 (0.26-0.44)	0.28 (0.16-0.41) ^b	0.58 (0.44-0.72)	0.71 (0.54-0.89) ^a
Subtype, kappa (95% CI)	0.30 (0.22-0.37)	0.36 (0.26-0.46)	0.53 (0.41-0.64)	0.56 (0.42-0.69)

IQR, interquartile range; CI, confidence interval. ^aThe intra-observer kappa regarding the depth of deformity and severity were not incorporated for observer D while kappa could not be determined due to not all answer options being represented. ^bThe inter-observer kappa regarding the presence of asymmetry and severity was not incorporated for a single observer pair (observer B vs observer E) while kappa could not be determined due to not all answer options being represented.

Discussion

In the current study we evaluated the inter-observer and intra-observer agreement of visual examination and diagnosis of pectus excavatum. Experienced (cardio) thoracic pectus surgeons from different referral centers assessed interactive 3D images of patients suspected of pectus excavatum in a blinded and standardized manner through a 7-item questionnaire.

Three-dimensional images were utilized since live and repeated visual examination of 58 patients over a 1-year time period, by observers from different centers, was practically unfeasible. Evaluability of the 3D images was subjectively rated as fair to excellent by the observers. Three-dimensional images were made by the Artec Leo imaging system that has previously been validated for anterior chest wall images, demonstrating sub-millimeter accuracy and reproducibility [17]. In past years, the role of 3D imaging in the work-up and follow-up of pectus excavatum is expanding

progressively. It is being employed to determine pectus severity, through a derivative of the gold standard Haller index, without exposure to potentially harmful ionizing radiation [18], but also to visually document the deformity [11] and follow-up after both conservative and surgical treatment [19].

Overall, judgements among 5 distinct surgeons demonstrated slight to moderate agreement across all items addressed by the questionnaire. Despite these considerable inter-observer differences across all items, disagreements regarding the presence of pectus excavatum were deemed clinically most significant and demonstrated moderate agreement (κ : 0.50). Pectus excavatum was diagnosed in 55% of cases by observer E and 95% of cases by observer D, while the frequency of diagnosis ranged from 85% to 91% for observer A to observer C.

Inter-observer differences were observed to be less pronounced among patients with a Haller index ≥ 3.25 compared to those with a Haller index < 3.25 . Still, (during first run-through) between 32% and 89% of patients with a Haller index < 3.25 were diagnosed as having pectus excavatum. Moreover, pectus excavatum was defined as absent in up to 23% of cases with a Haller index ≥ 3.25 . Visual examination thus seems not able to uniformly differentiate between disease and no disease.

In the Netherlands and Belgium, where this study was conducted, as well as globally, a strict definition of pectus excavatum other than an inward depression of the sternum and adjacent costal cartilage is lacking. Moreover, strict criteria for clinical significance are not available. Furthermore, there are no definitions nor general consensus to define pectus features. For example, when should one define a pectus as deep and which degree of asymmetry and flaring must be classified as aberrant? On the other hand, even a mild pectus excavatum may require diagnosis to enter a follow-up program designated to evaluate progression with age, since a history of progression is drafted as one of the criteria for treatment [12].

Both Nuss and Kelly [13] and Frantz [14] reported a similar clinical evaluation algorithm of pectus excavatum. The primary assessment includes physical examination, whereafter patients are stratified based on severity. Patients judged to have severe pectus excavatum undergo chest computed tomography, pulmonary function testing and cardiac evaluation while those with mild or moderate deformities are enrolled into an exercise and posture program with follow-up every 6 to 12 months [13, 14]. Therefore, the primary evaluation of severity by the observer is key and determines subsequent proceedings. However, since the

overall assessment of severity only demonstrated fair to moderate inter-observer agreement (kappa: 0.37; 95% CI: 0.30-0.44), the work-up appears to be susceptible to observer subjectivity and may result in different strategies for the same patient being evaluated. In addition, given the overall substantial though imperfect intra-observer agreement (kappa: 0.65; 95% CI: 0.55-0.75) regarding severity, patients evaluated repeatedly by the same observer may be offered a different work-up.

Other phenotypical pectus excavatum features assessed for agreement encompass the depth of deformity, its cranial onset point, as well as the presence of asymmetry and flaring. Since all of these features demonstrated considerable inter-observer and intra-observer disagreement in conjunction with

the fact that they affect surgical strategy rather than diagnosis, strategies are likely to differ between observers and upon repeated evaluation. The importance of preoperative notion of the presence of asymmetry, flaring, asymmetry and extent of depression is also stressed by Kelly and colleagues and emphasized to affect surgical strategy [12]. For example, extremely deep pectus excavatum may necessitate the use of sternal elevation techniques and multiple bars during the Nuss procedure. Park and colleagues, moreover, advocate for the use of patient-specific, morphology-tailored Nuss bars, whereby disagreements regarding the presence or absence of asymmetry could also result in different treatment strategies [20]. In addition, flaring may prompt concomitant correctional procedures, such as cartilage resection [21] or retraction by the flare-buster technique [22].

Given the presented substantial inter-observer and intra-observer disagreement regarding the visual evaluation of patients suspected of pectus excavatum, objective parameters, definitions, and standardization in diagnosing pectus excavatum are urged. The Haller index is a quantitative measure that is routinely employed by 80% of experts to determine severity. However, its use is limited by the fact that it is, as a sole two-dimensional measure, not able to comprehensively reflect the extent of deformity (e.g., a wide chest with relative shallow pectus exhibits a similar Haller index as a barrel-shaped chest with focal deep pectus) as well as the different features assessed by the observers. This issue has also been stressed by Martinez-Ferro [23]. He emphasized the need for more comprehensive methods to quantify pectus excavatum and proposed the perfect index to be a combination of different pectus excavatum aspects. Quantification of these aspects, as evaluated by the observers in the current study (e.g., depth, asymmetry, flaring and so on), could provide the basis for such an index.

Three-dimensional images acquired of the patient's chest could provide a future way to standardization and objectively evaluate the morphology of pectus excavatum. Since 3D images are digital objects and encompass all information on the external pectus morphology, they can be used to quantify characteristics of pectus excavatum in an automated and standardized manner, eliminating inter-observer and intra-observer bias. However, for these quantitative measures to be used in the clinical setting, they require a meaning. This could be achieved by evaluating a large cohort of pectus excavatum patients and determining a "mean pectus excavatum". Like the idea of birth-weight-curves one can subsequently determine whether a patient has a below average (e.g., mild) or above average (e.g., severe) pectus. The number of standard deviations from the mean can, moreover, be used to further distinguish between for example severe and extremely severe deformities.

Limitations

The current study is limited by the fact that it is unknown how the involved surgeons, who may in theory be under- or overperformers, performed with respect to peers. Another limitation is that we were not able to determine the sample size required prior to start. In addition, given that patients were recruited from a tertiary referral center for chest wall disorders, the included cohort may not be representative for other centers.

The utilized questionnaire was not validated and did solely provide binominal answer options for the first 6 items. Yet, to date, no validated questionnaires exist to visually examine and score pectus excavatum severity.

The utilized 3D images are not fully comparable to live examination, where palpation, pose alterations and movement may potentially improve judgement. Nevertheless, their evaluability was rated as fair to excellent by the observers. In addition, the light position of the rendering software might influence the interpretation of the images and as such severity. In addition, 3D images were acquired during breath hold in the end-inspiratory phase. As a consequence, visual assessment may yield a less intrusive presentation of the pectus excavatum deformity, because the Haller index is known to be significantly lower during inspiration compared to expiration [24].

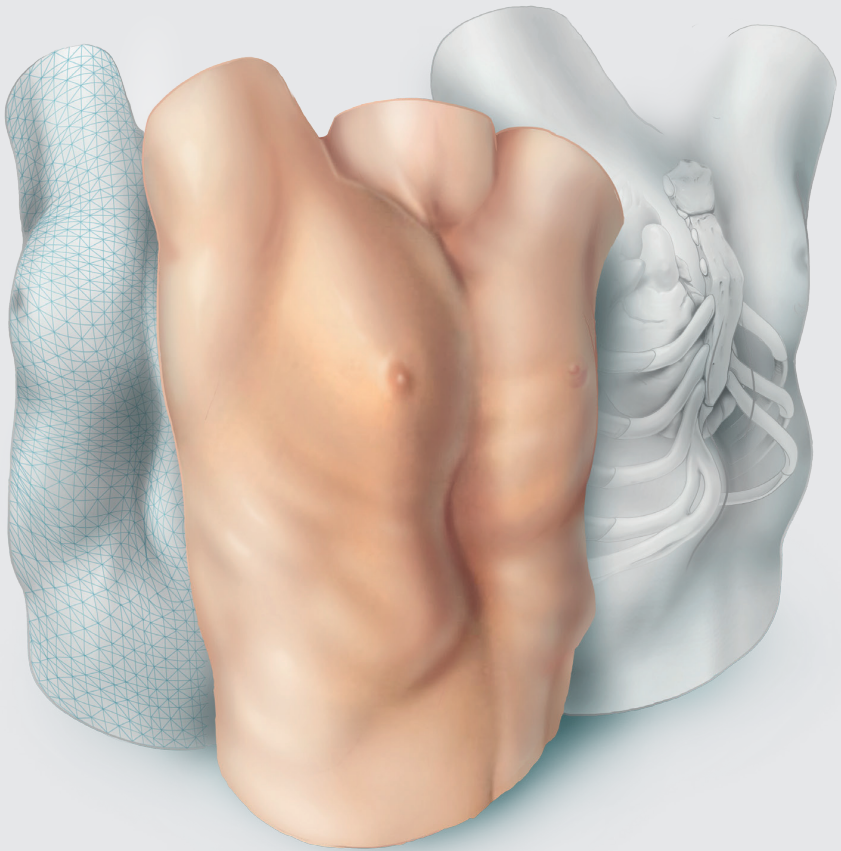
Conclusion

Visual examination and diagnosis of pectus excavatum by experienced (cardio) thoracic pectus surgeons yields considerable inter-observer and intra-observer disagreements. As this variation in judgement could impact work-up and treatment strategy, objective standardization of visual assessment is urged. Three-dimensional images could play a role in this process.

References

1. Brochhausen C, Tural S, Müller FK, Schmitt VH, Coerdts W, Wihlm JM et al. Pectus excavatum: history, hypotheses and treatment options. *Interact Cardiovasc Thorac Surg* 2012;14:801-6.
2. Ewert F, Syed J, Kern S, Besendörfer M, Carbon RT, Schulz-Drost S. Symptoms in Pectus Deformities: A Scoring System for Subjective Physical Complaints. *Thorac Cardiovasc Surg* 2017;65:43-9.
3. Fonkalsrud EW, Dunn JC, Atkinson JB. Repair of pectus excavatum deformities: 30 years of experience with 375 patients. *Ann Surg* 2000;231:443-8.
4. Kelly RE, Jr., Shamberger RC, Mellins RB, Mitchell KK, Lawson ML, Oldham K et al. Prospective multicenter study of surgical correction of pectus excavatum: design, perioperative complications, pain, and baseline pulmonary function facilitated by internet-based data collection. *J Am Coll Surg* 2007;205:205-16.
5. Miller KA, Woods RK, Sharp RJ, Gittes GK, Wade K, Ashcraft KW et al. Minimally invasive repair of pectus excavatum: A single institution's experience. *Surgery* 2001;130:652-9.
6. Cartoski MJ, Nuss D, Goretsky MJ, Proud VK, Croitoru DP, Gustin T et al. Classification of the dysmorphology of pectus excavatum. *J Pediatr Surg* 2006;41:1573-81.
7. Kelly RE, Quinn A, Varela P, Redlinger RE, Nuss D. Dysmorphology of Chest Wall Deformities: Frequency Distribution of Subtypes of Typical Pectus Excavatum and Rare Subtypes. *Arch Bronconeumol* 2013;49:196-200.
8. von Elm E, Altman DG, Egger M, Pocock SJ, Gøtzsche PC, Vandenbroucke JP. The Strengthening the Reporting of Observational Studies in Epidemiology (STROBE) statement: guidelines for reporting observational studies. *Lancet* 2007;370:1453-7.
9. Khanna G, Jaju A, Don S, Keys T, Hildebolt CF. Comparison of Haller index values calculated with chest radiographs versus CT for pectus excavatum evaluation. *Pediatr Radiol* 2010;40:1763-7.
10. Haller JA, Jr., Kramer SS, Lietman SA. Use of CT scans in selection of patients for pectus excavatum surgery: a preliminary report. *J Pediatr Surg* 1987;22:904-6.
11. Daemen JHT, Loonen TGJ, Coorens NA, Maessen JG, Maal TJJ, Hulsewé KWE et al. Photographic documentation and severity quantification of pectus excavatum through three-dimensional optical surface imaging. *J Vis Commun Med* 2020;43:190-7.
12. Kelly RE, Jr. Pectus excavatum: historical background, clinical picture, preoperative evaluation and criteria for operation. *Semin Pediatr Surg* 2008;17:181-93.
13. Nuss D, Kelly RE, Jr. Indications and technique of Nuss procedure for pectus excavatum. *Thorac Surg Clin* 2010;20:583-97.
14. Frantz FW. Indications and guidelines for pectus excavatum repair. *Curr Opin Pediatr* 2011;23:486-91.
15. Light RJ. Measures of response agreement for qualitative data: Some generalizations and alternatives. *Psychol Bull* 1971;76:365-77.
16. Landis JR, Koch GG. The measurement of observer agreement for categorical data. *Biometrics* 1977;33:159-74.
17. Daemen JHT, Loonen TGJ, Verhulst AC, Maal TJJ, Maessen JG, Vissers YLJ et al. Three-Dimensional Imaging of the Chest Wall: A Comparison Between Three Different Imaging Systems. *J Surg Res* 2020;259:332-41.

18. Daemen JHT, Loonen TGJ, Lozekoot PWJ, Maessen JG, Maal TJJ, Hulsewé KWE et al. Optical imaging versus CT and plain radiography to quantify pectus severity: a systematic review and meta-analysis. *J Thorac Dis* 2020;12:1475-87.
19. Lain A, Garcia L, Gine C, Tiffet O, Lopez M. New Methods for Imaging Evaluation of Chest Wall Deformities. *Front Pediatr* 2017;5:257.
20. Park HJ, Lee SY, Lee CS, Youm W, Lee KR. The Nuss procedure for pectus excavatum: evolution of techniques and early results on 322 patients. *Ann Thorac Surg* 2004;77:289-95.
21. Bosgraaf RP, Aronson DC. Treatment of flaring of the costal arch after the minimally invasive pectus excavatum repair (Nuss procedure) in children. *J Pediatr Surg* 2010;45:1904-6.
22. Park HJ, Kim KS. The sandwich technique for repair of pectus carinatum and excavatum/carinatum complex. *Ann Cardiothorac Surg* 2016;5:434-9.
23. Martinez-Ferro M. Indexes for Pectus Deformities. In Kolvekar S, Pilegaard H (eds): *Chest Wall Deformities and Corrective Procedures*. Cham: Springer International Publishing 2016; 35-60.
24. Birkemeier KL, Podberesky DJ, Salisbury S, Serai S. Breathe in... breathe out... stop breathing: does phase of respiration affect the Haller index in patients with pectus excavatum? *Am J Roentgenol* 2011;197:W934-9.





General discussion

The present thesis addresses the use of three-dimensional (3D) surface imaging as radiation-free alternative to current diagnostic procedures in pectus excavatum. A stepwise approach was applied to supplant commonly used radiologic diagnostic procedures by 3D imaging. We have developed a 3D image acquisition and processing protocol, validated the clinical use of multiple 3D imaging systems, determined cut-off values for 3D image derived severity measures which are applied as objective criteria for surgical candidacy, and developed a model to predict the probability of cardiac compression from 3D images. Furthermore, we evaluated observer differences regarding the visual examination and diagnosis of pectus excavatum from 3D images.

This general discussion is intended to put their rationale and findings into a broader perspective, address their implications, reflect on the lessons learned and choices made, as well as provide direction for future perspectives.

The rationale in perspective

The preeminent rationale for this thesis was the routine exposure to potentially harmful ionizing radiation, associated with current diagnostic procedures in the work-up of pectus excavatum.

Although computed tomography (CT) is the most frequently employed imaging technique [1] and gold standard [2] to evaluate pectus excavatum, the associated ionizing radiation is an established carcinogen. Every single acquisition attributes for an average effective dose of 7.0mSv (range: 4.0-18.0) [3], compared to an annual average dose of 2.9mSv in the Netherlands [4]. This is especially of concern for pediatric patients due to their relatively long life-time risk to develop associated pathologies [5-7]. Miglioretti and colleagues studied the risk of solid cancer and leukemia among pediatric patients (<15 years of age) who received a chest CT scan. They observed a life-time attributable risk of 18 per 10,000 (0.2%) patients [8].

If all Dutch newborns (approximately 170-thousand in 2017 [9]) with pectus excavatum were to be evaluated once before the age of 15 years, 425 patients would be exposed to a CT per year (based on a birth prevalence of 1 in 400 [10]). Provided that approximately 200 patients underwent surgical repair in 2017 (results from 77 of 95 Dutch hospitals) [9] in conjunction with the fact that roughly half of patients are eligible for surgery [11], 425 patients seem a plausible representation of the

annual number of patients evaluated for pectus excavatum in the Netherlands. Of these patients, one would develop a solid cancer or leukemia attributable to radiation exposure every year [8]. In contrast, for the United States of America this even concerns 17 cases per year (based on the number of births in 2017; 3.86 million [12]) who would develop a preventable solid cancer or leukemia.

Pediatric ionizing radiation thus remains of continuous global matter. This is best demonstrated by the different reports on this topic [13-16] and by up to half of international chest wall experts who employ plain radiographs as primary imaging modality instead of CT, in order to contain exposure [1, 17]. Moreover, one is obliged to always comply with the principles of justification and ALARA (as low as reasonably acceptable) when considering the use of radiation imaging.

Clinical implications

Preoperative work-up

In reliance of the present thesis, 3D imaging can like CT and plain radiographs be used as first-line diagnostic to evaluate the severity of pectus excavatum. However, employment of 3D imaging could result in additional diagnostic studies given its relatively lower diagnostic performance. Additional investigations will primarily be required in cases of negative 3D imaging in conjunction with a high clinical suspicion of surgical suitability, which is underscored by the relatively lower sensitivity of the external Haller index and cardiac compression prediction model based on 3D imaging. In such cases, one may intuitively be inclined to obtain an additional CT since it is still considered as gold standard for pectus evaluation. However, dynamic function tests like echocardiography, cardiac magnetic resonance imaging (MRI) and cardiopulmonary exercise testing may yield superior diagnostic value over static evaluation by CT and should therefore be advised as a second step. This moreover prevents radiation exposure further down the work-up.

Three-dimensional imaging can also substitute the use of conventional photography for visual documentation of pectus excavatum which is additionally performed by part of chest wall centers [18]. These photographs are used for preoperative planning purposes, to create patient awareness, to evaluate monitoring of conservative treatment, as well as to evaluate and compare over time postoperative results. In comparison, three-dimensional images are less time-consuming to acquire and moreover promote visuospatial understanding of

the deformity through addition of the third dimension which may translate into improved surgical planning. However, the latter is yet to be investigated.

Postoperative follow-up

Following surgical correction of pectus excavatum, a plain radiograph is routinely obtained to rule out the presence of a pneumothorax or hemothorax. Since 3D imaging only captures the chest wall surface, it is not suitable to supplant this postoperative plain radiograph. Though, routine postoperative follow-up could be facilitated by 3D imaging, using objective measures like the external pectus excavatum depth and external Haller index. Consecutive assessment of these measures allows caregivers to thoroughly assess evolution of the deformity and timely detect any deviations, such as overcorrection or recurrence. The advantage of 3D images compared to conventional follow-up by plain radiographs is that they can be repeated without limits since they elicit no negative effect on the patient's health.

Infrastructural and economic implications

Adopting 3D imaging as first-line diagnostic in the work-up and follow-up of pectus excavatum yields considerable implications for the present infrastructure which must be reconsidered. Where patients used to routinely visit the radiology department it should be thought of where 3D imaging can best be housed. Potential operators must be technically proficient and able to adequately deal with problems that arise during acquisition and processing, but also detect flaws in computerized measurements. For example, medical photographers may suffice. However, proficiency could also be obtained by dedicated training.

In addition, since 3D imaging systems are currently not featured by most centers, a one-time investment is involved. Depending on the imaging system's specifications, prices range from several hundred euros to over one hundred thousand euros. Furthermore, given that the resulting 3D images are stored under a new extension (e.g., .stl or .obj) which is often not supported by the readily available information and communication technology infrastructure, additional financial injections are needed to implement these new images into electronic patient files.

Despite these associated costs, it is conceivable that 3D imaging is more cost-effective than CT and plain radiographs for the purpose of pectus excavatum,

provided the base costs of the radiological imaging systems, the necessity for shielded rooms, as well as a consultant radiologist. Yet, the global cost effectiveness also depends on the general employability for purposes other than pectus excavatum. Here, 3D imaging is at a disadvantage because it concerns a new technique which is, despite its high potential, still mostly in the research phase. To corroborate the presumed superior cost-effectiveness of 3D imaging over current diagnostic procedures, future research is warranted which should incorporate all associated costs made alongside the entire work-up and postoperative follow-up.

In retrospect

A crucial part of research design is determination of the sample size, considering it significantly affects the validity and clinical relevance of the study's findings. Nevertheless, sample size determination is not always possible due to a lack of prior data or that such a large sample is required that the study becomes unfeasible.

It is equally important that the study cohort is representative for the population for whom the approach is intended. For example, in this thesis we included patients referred to secondary care for pectus excavatum, making our results less applicable to countries with a different referral policy.

What if we had to start over?

The accuracy and reproducibility of the 3D imaging system used in the present thesis, was evaluated by comparison of chest wall images obtained from healthy volunteers. Despite from a technical stand of view, there is no difference in accuracy and reproducibility between healthy volunteers and patients with a chest wall deformity, it would have been more appropriate to include actual patients with a chest wall deformity. Simply because one should aim to study the patients for whom the results are intended, as previously emphasized. Though, as also mentioned, sometimes it is necessary to make concessions for the sake of feasibility which trumps no data at all.

To this day, the Haller index is considered as gold standard severity measure for pectus excavatum, both in the field of research and in clinical practice. It is used as an objective criterium in the multifactorial process of surgical decision making and even determines reimbursement rates of surgical intervention in several countries such as the USA. Although the Haller index poses considerable limitations, its

routine use is primarily motivated by the absence of a superior alternative. For the same reasons we chose to investigate the performance of a 3D image based equivalent of the Haller index to determine surgical candidacy.

In Chapter 7 we evaluated observer differences regarding the visual examination and diagnosis of pectus excavatum through a questionnaire which addressed morphological pectus features. Combination of such features could potentially overcome the limitations of the Haller index by allowing for a comprehensive description of the pectus deformity. This is in concordance with the report of Martinez-Ferro who emphasized that the perfect alternative index would be a combination of different pectus excavatum features [1]. Consequently, it may have been more appropriate to first develop a new 3D image based index which is able to comprehensively describe the pectus deformity and subsequently evaluate its performance, instead of using the 3D image based external Haller index which poses similar limitations as the conventional Haller index. However, the problem faced with such an approach would be to select an appropriate reference method. Alternatively, using expert opinions would also be inappropriate given the observed subjectivity in Chapter 7.

Continuing on the use of reference standards, we utilized CT as reference to develop a 3D image based prediction model for cardiac compression in pectus excavatum. However, since CT is limited by producing static images in conjunction with the fact that chest and cardiac dimensions change along the respiratory and cardiac cycle, the presence of cardiac compression may be affected by the timing of acquisition. Therefore, it would have been better to use dynamic cardiac function tests (e.g., echocardiography and cardiac MRI) as reference standard to confirm the presence or absence of compression with improved certainty. For the same reasons it would be best to acquire a 3D image during both the inspiratory and expiratory phase. Yet, in this thesis, all images were acquired during the end inspiratory phase since CTs and plain radiographs were acquired during the similar phase. Moreover, in theory measurements are posture dependent.

Acquisition of a chest MRI in patients evaluated for pectus excavatum would provide more clinically useful information compared to a chest CT, however, is not routinely employed given its reduced availability due to capacity issues as well as increased costs and time-consumption.

Future perspectives

Pectus excavatum remains an underdiagnosed deformity. Even by experts, the deformity has long been considered as merely aesthetic. However, with the increasing amount of research on associated functional impairment and the substantial role of cardiac compression, emphasis has shifted, and surgical correction has become more widely accepted.

Taking into consideration the inter-observer and intra-observer differences in visual examination and diagnosis of pectus excavatum that are reported in this thesis, the need for standardization is urged. Here, there could be a major role for 3D imaging as it provides objective quantification of pectus excavatum and its morphological features [19], thus providing a common language among experts. To ensure identical interpretation of these values, a concept like growth curves where deviations from the mean are identified might be suitable but still needs development. For example, a severity, two standard deviations below the average, could be provided the label of a non-severe pectus excavatum.

During the Nuss procedure, a retrosternal metal bar is implanted that instantly corrects the deformity. Immediately after surgery, patients often expect an entirely anatomical chest wall, causing concern and dissatisfaction in the presence of a prominent cartilage ring or aggravated flaring. Remodeling of the chest wall is thought to take place over the following years. However, the process of remodeling has never been thoroughly investigated. Three-dimensional images could be used to objectively evaluate over time chest wall changes following surgery and gaining more insight into the process of remodeling.

In addition, after removal of the Nuss bar, patients sometimes report that the inward deformity returns. Although the sternum is believed to always show a minor degree of collapse after bar removal, the extent is not known. Here, 3D imaging could also be of aid. First to investigate and objectify the presumed normal chest wall changes after Nuss bar removal and secondly to provide objective guidance on the identification of recurrent cases.

Apart from the quantification of chest wall changes, the utilities of 3D imaging are broader. Using preoperative and postoperative images of preceding patients, a prediction model can be developed for future patients. This could improve patients' expectations during preoperative consultation and postoperative satisfaction with

the aesthetic result. Three-dimensional images could moreover be employed for preoperative surgical planning by determining the number of bars required and their position to obtain an optimal correction.

With the rapid improvement of camera systems incorporated in mobile devices, 3D imaging is even anticipated to be completely achievable through videoconferencing with the patient.

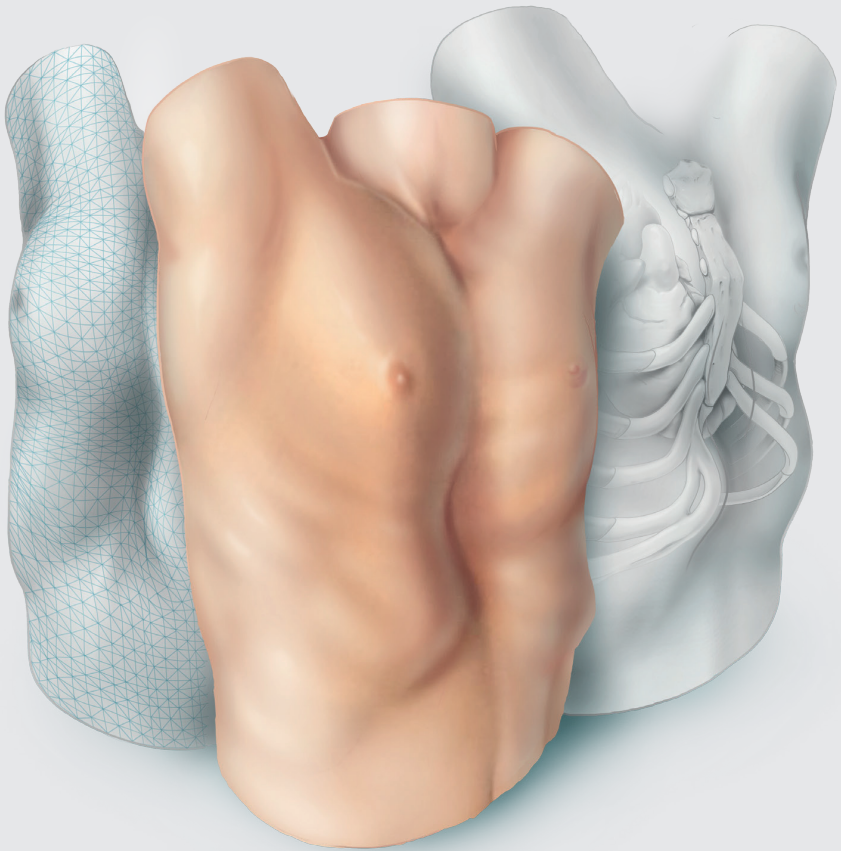
The validity of prediction models is assessed by both internal and external validation. In the present thesis, we internally validated the cardiac compression prediction model by bootstrapping. Future studies should focus on external validation to ascertain validity for prediction in other centers.

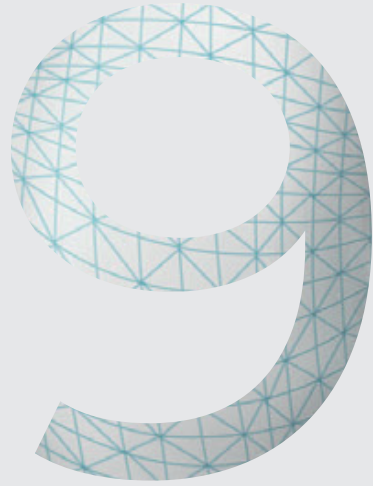
The primary aim of pectus evaluation has always been to determine its severity and assess whether it qualifies for treatment. The role of aesthetic complaints in surgical decision making is still a much-debated topic. Though, aesthetic complaints may well be of significance since they can elicit a severe psychosocial burden of disease and considerably compromise quality of life.

References

1. Martinez-Ferro M. Indexes for Pectus Deformities. In Kolvekar S, Pilegaard H (eds): *Chest Wall Deformities and Corrective Procedures*. Cham: Springer International Publishing 2016; 35-60.
2. Haller JA, Jr., Kramer SS, Lietman SA. Use of CT scans in selection of patients for pectus excavatum surgery: a preliminary report. *J Pediatr Surg* 1987;22:904-6.
3. Mettler FA, Jr., Huda W, Yoshizumi TT, Mahesh M. Effective doses in radiology and diagnostic nuclear medicine: a catalog. *Radiology* 2008;248:254-63.
4. Blootstelling aan ioniserende straling samengevat. Rijksinstituut voor Volksgezondheid en Milieu 2017. Available from: <https://www.rivm.nl/straling-en-radioactiviteit/blootstelling-en-gezondheidsrisico/blootstelling-aan-ioniserende-straling-samengevat>: Date last accessed: 19-02-2021.
5. Kleinerman RA. Cancer risks following diagnostic and therapeutic radiation exposure in children. *Pediatr Radiol* 2006;36:121-5.
6. Brenner D, Elliston C, Hall E, Berdon W. Estimated risks of radiation-induced fatal cancer from pediatric CT. *AJR Am J Roentgenol* 2001;176:289-96.
7. Don S. Radiosensitivity of children: potential for overexposure in CR and DR and magnitude of doses in ordinary radiographic examinations. *Pediatr Radiol* 2004;34 Suppl 3:S167-72; discussion S234-41.
8. Miglioretti DL, Johnson E, Williams A, Greenlee RT, Weinmann S, Solberg LI et al. The use of computed tomography in pediatrics and the associated radiation exposure and estimated cancer risk. *JAMA Pediatr* 2013;167:700-7.
9. Zuidema WP, van der Steeg AFW, Oosterhuis JWA, van Heurn E. Trends in the Treatment of Pectus Excavatum in the Netherlands. *Eur J Pediatr Surg* 2020.
10. Chung CS, Myrianthopoulos NC. Factors affecting risks of congenital malformations. I. Analysis of epidemiologic factors in congenital malformations. Report from the Collaborative Perinatal Project. *Birth Defects Orig Artic Ser* 1975;11:1-22.
11. Kelly RE, Goretsky MJ, Obermeyer R, Kuhn MA, Redlinger R, Haney TS et al. Twenty-one years of experience with minimally invasive repair of pectus excavatum by the Nuss procedure in 1215 patients. *Ann Surg* 2010;252:1072-81.
12. Number of births in the United States 1990-2018. Statista Research Department 2021. Available from: <https://www.statista.com/statistics/195908/number-of-births-in-the-united-states-since-1990/>: Date last accessed: 19-02-2021.
13. Mulvihill DJ, Jhawar S, Kostis JB, Goyal S. Diagnostic Medical Imaging in Pediatric Patients and Subsequent Cancer Risk. *Acad Radiol* 2017;24:1456-62.
14. Rattan AS, Laor T, Ryckman FC, Brody AS. Pectus excavatum imaging: enough but not too much. *Pediatr Radiol* 2010;40:168-72.
15. Goodman TR, Mustafa A, Rowe E. Pediatric CT radiation exposure: where we were, and where we are now. *Pediatr Radiol* 2019;49:469-78.
16. Brenner DJ, Hall EJ. Computed tomography—an increasing source of radiation exposure. *N Engl J Med* 2007;357:2277-84.
17. Khanna G, Jaju A, Don S, Keys T, Hildebolt CF. Comparison of Haller index values calculated with chest radiographs versus CT for pectus excavatum evaluation. *Pediatr Radiol* 2010;40:1763-7.

18. van Dijk H, Höppener PF, Siebenga J, Kragten HA. Medical photography: a reliable and objective method for documenting the results of reconstructive surgery of pectus excavatum. *J Vis Commun Med* 2011;34:14-21.
19. Coorens NA, Daemen JHT, Slump CH, Loonen TGJ, Vissers YLJ, Hulsewé KWE et al. The Automatic Quantification of Morphological Features of Pectus Excavatum Based on Three-Dimensional Images. *Semin Thorac Cardiovasc Surg* 2021.





Summary

Samenvatting

Summary

The **main objective of this thesis** has been to eliminate the exposure to ionizing radiation in the preoperative evaluation of pectus excavatum by introduction of three-dimensional (3D) surface imaging. It was hypothesized that 3D surface images can be used interchangeably with current diagnostic procedures as a valid and accurate diagnostic tool in the preoperative work-up of patients suffering from pectus excavatum. To test this hypothesis, individual chapters can be distinguished forming the basis of this thesis.

The general background and introduction to the different chapters are provided in **Chapter 1**.

In **Chapter 2** we started by evaluating the current role of three-dimensional imaging as a diagnostic tool to determine pectus excavatum severity compared to computed tomography (CT) and plain radiographs through a systematic review of the available literature. Based on this review we determined the different aspects to be studied to achieve the above-mentioned main objective of the present thesis.

Three-dimensional imaging was found to be an attractive, feasible and promising imaging technique to determine the severity of pectus excavatum without exposure to ionizing radiation. Although a pooled correlation of 0.89 between the computed tomography (CT) derived Haller Index and its 3D image equivalent based on external measures was found, further research was concluded to be imperative for 3D image to be used in the clinical process of decision making and help determine surgical candidacy. This included, amidst other aspects, the determination of cut-off values for 3D image based severity measures.

To be able to obtain 3D images in a reproducible manner, a dedicated protocol was developed in **Chapter 3**. Individual steps included patient positioning and instructions, data acquisition, and data processing. As a subsidiary aim, it was evaluated whether anthropometric measurements recorded using conventional two-dimensional photography can be equally obtained from 3D images. Based on 19 consecutive pectus excavatum patients who were imaged using the developed protocol, feasibility was demonstrated. In addition, 3D imaging was found to be interchangeably usable with anthropometric measurements to determine the severity of pectus excavatum (intraclass correlation coefficient: 0.97; 95%-confidence interval: 0.88 to 0.99; $P < 0.001$).

Building on the developed protocol (**Chapter 3**) we evaluated the accuracy and reproducibility of three commercially available 3D imaging systems that can be used to obtain images of the anterior chest wall in **Chapter 4**. The devices concerned one static (3dMD system [3dMD, Atlanta, GA, USA]) and two hand-held imaging systems (Artec Leo [Artec3D, Luxembourg, Luxembourg] and the Einscan Pro 2X Plus [Shining 3D, Hangzhou, China]) of which the former is currently considered as gold standard. Among 15 healthy volunteers, 3D images of the anterior chest wall were acquired twice per imaging device. All devices demonstrated statistically comparable reproducibility with a mean absolute difference between consecutive images ranging from 0.48 to 0.59mm. The accuracy was best for the Artec Leo imaging system (0.81mm.), as also employed in the different studies incorporated in the present thesis.

Having developed a dedicated imaging and processing protocol (**Chapter 3**), as well as determined the accuracy and reproducibility of the imaging system of our choice (**Chapter 4**), we proceeded to determine cut-off values for the 3D image based alternative severity measures, such that 3D image can be used in the clinical process of decision making and help determine surgical candidacy. Using the Haller index and correction index derived from conventional imaging modalities (i.e., CT and two-view plain radiographs) as reference, the 3D image derived external Haller index and external correction index were found to be accurate radiation-free alternatives to facilitate surgical decision-making among patients suspected of pectus excavatum with values of ≥ 1.83 and $\geq 15.2\%$ indicative for surgery (**Chapter 5**).

Next to severity measures, such as the external Haller index and external correction index, intrathoracic information on cardiac status also aids in the process of surgical decision making. Cardiac compression is considered as one of the indications for corrective surgery. Yet, since 3D images solely contain information regarding the surface topography, cardiac evaluation is not conceivable with 3D images as it is with CT. **Chapter 6** therefore aimed to develop a 3D image-based prediction model for cardiac compression in patients evaluated for pectus excavatum. Exploring 3D image derived pectus measurements and baseline patient characteristics (including subjective symptoms), a combination of the external pectus depth and external anteroposterior distance was identified as predictive for cardiac compression. In a second model for males alone, solely the external pectus depth was identified as predictor. Both models provided an outstanding discriminatory performance (area under the receiver-operating characteristic curve of 0.935 and

0.947, respectively) between the presence and absence of cardiac compression with negligible optimism.

Exploiting the potential of 3D images, **Chapter 7** evaluated the inter-observer and intra-observer agreement of visual examination and diagnosis of pectus excavatum among experts from different centers. Interactive three-dimensional images were evaluated for the presence of pectus excavatum, asymmetry, flaring, depth of deformity, cranial onset, overall severity, and morphological subtype through a questionnaire. Fifty-eight interactive 3D images of pectus excavatum patients were evaluated twice by 5 (cardio)thoracic surgeons, yielding considerable inter-observer and intra-observer differences. For example, 55% (n=32/58) to 95% (n=55/58) patients were judged to suffer from pectus excavatum by different experts. As this variation in judgement could significantly impact work-up and treatment strategy, objective standardization is urged.

To conclude, a general discussion on the results and findings of this thesis, as well as an elaboration on its scientific and societal impact are to be read in **Chapter 8**.

Returning to the hypothesis, this thesis demonstrated that 3D images can be used interchangeably with current diagnostic procedures as a valid and accurate diagnostic tool in the preoperative work-up of patients suffering from pectus excavatum. Still, future studies should aim to address the limitations, ensuring its solid scientific embedding.

Samenvatting

Pectus excavatum, ook wel bekend als trechterborst of schoenmakersborst, is de meest voorkomende aandoening van de borstwand. De exacte ontstaanswijze is vooralsnog onbekend. De huidige theorieën beschrijven een afwijking van het ribkraakbeen, waardoor een typische indeuking van de borstwand ontstaat met verplaatsing van het borstbeen naar achteren. Dit kan schaamte en cosmetische klachten veroorzaken, maar ook fysieke klachten door compressie van het hart. Door deze verscheidenheid aan mogelijke klachten is het belangrijk een gedegen preoperatieve evaluatie uit te voeren. Onderdeel van deze evaluatie is beeldvorming. In de huidige praktijk behelst dit vaak beeldvormingsmethoden die de patiënt blootstellen aan ioniserende röntgenstraling, zoals een röntgenfoto of computertomografie (CT)-scan. Deze straling heeft op termijn negatieve gezondheidseffecten, met name bij relatief jonge patiënten, die het grootste deel uitmaken van de populatie met pectus excavatum.

Doel van dit proefschrift is het elimineren van de blootstelling aan röntgenstraling bij de preoperatieve evaluatie van pectus excavatum door toepassing van driedimensionale (3D) oppervlaktebeeldvorming. De hypothese is dat deze 3D-beelden kunnen worden gebruikt als een betrouwbaar en nauwkeurig diagnostisch instrument in de preoperatieve evaluatie van patiënten met een pectus excavatum. Om deze hypothese te testen worden afzonderlijke hoofdstukken onderscheiden.

Dit proefschrift begint met een algemene inleiding over pectus excavatum in **Hoofdstuk 1**.

Hoofdstuk 2 is een inventarisatie van beschikbare kennis over 3D-beeldvorming om de ernst van pectus excavatum te bepalen in vergelijking met röntgenfoto's en CT. Hiervoor werd een systematische review verricht. Er werd aangetoond dat de mate van ernst van de pectus excavatum op basis van 3D-beeldvorming (externe Haller index) positief gecorreleerd was aan de mate van ernst op basis van de CT (Haller index). Verder onderzoek werd noodzakelijk geacht voor het gebruik van 3D-beelden in het klinische besluitvormingsproces en voor het selecteren van patiënten geschikt voor chirurgische behandeling. Dit omvatte onder meer de bepaling van afkapwaarden voor op 3D-beelden gebaseerde maten voor de ernst van pectus excavatum om patiënten te selecteren voor chirurgie.

Om op reproduceerbare wijze 3D-beelden te kunnen verkrijgen, werd in **Hoofdstuk 3** een beeldvormingsprotocol ontwikkeld specifiek voor borstwandaandoeningen. De afzonderlijke stappen omvatten de positionering van en instructies aan de patiënt, het verkrijgen van de beelden, en het verwerken en bewerken hiervan. Hierbij werd tevens duidelijk dat de manuele externe dieptemeting van pectus excavatum middels schuifmaat vergelijkbaar is met de dieptemeting op basis van de 3D-beelden.

Voortbouwend op het ontwikkelde beeldvormingsprotocol in **Hoofdstuk 3**, werd in **Hoofdstuk 4** de nauwkeurigheid en reproduceerbaarheid van een drietal commercieel verkrijgbare 3D-beeldvormingssystemen geëvalueerd. Deze systemen omvatten één statisch (3dMD systeem [3dMD, Atlanta, GA, USA]) en twee handbediende beeldvormingssystemen (Artec Leo [Artec3D, Luxemburg, Luxemburg] en de Einscan Pro 2X Plus [Shining 3D, Hangzhou, China]) waarvan eerstgenoemde de geaccepteerde gouden standaard is. Bij 15 gezonde vrijwilligers werden 3D-beelden van de voorste borstwand vervaardigd, twee opnames per beeldvormingssysteem. Alle systemen vertoonden een statistisch vergelijkbare reproduceerbaarheid. De Artec Leo vertoonde de beste (sub-millimeter) nauwkeurigheid en werd om deze reden gekozen. Dit beeldvormingssysteem is daarom ook gebruikt in de opvolgende studies.

In **Hoofdstuk 5** is er na probleemstelling in **Hoofdstuk 2** gezocht naar afkapwaarden van objectieve indices op basis van 3D-beelden die kunnen worden gebruikt om een operatie-indicatie te stellen. Gebruikmakend van de Haller-index en de correctie-index op basis van conventionele beeldvormingsmethoden (d.w.z. CT en röntgenfoto's in twee richtingen), bleken de externe Haller-index en externe correctie-index op basis van de 3D-beelden een nauwkeurig stralingsvrij alternatief te zijn, waarbij waarden van respectievelijk $\geq 1,83$ en $\geq 15,2\%$ indicatief zijn voor chirurgische behandeling van pectus excavatum.

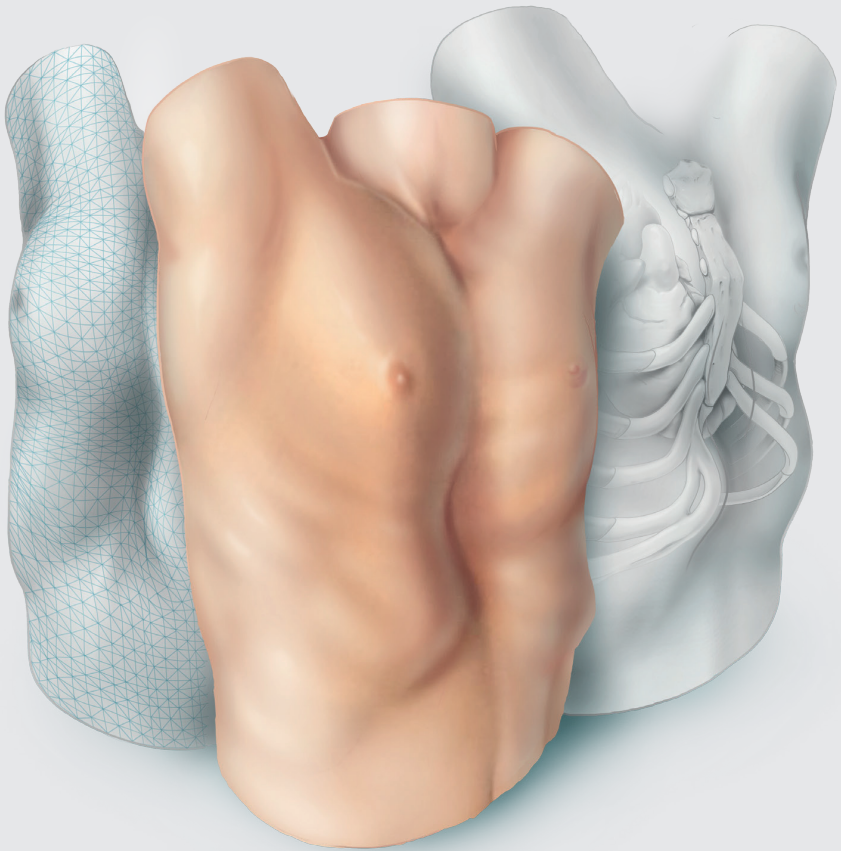
Naast objectieve metingen van de ernst van pectus excavatum, zoals de externe Haller-index en de externe correctie-index (**Hoofdstuk 5**), is ook compressie van het hart door pectus excavatum een van de indicaties voor chirurgische behandeling van pectus excavatum. Aangezien 3D-beelden echter alleen informatie over de oppervlaktetopografie (lees: buitenzijde van de borstwand) bevatten, is een directe evaluatie van eventuele compressie van het hart niet mogelijk, zoals dit met bijvoorbeeld CT wel is. Het doel van **Hoofdstuk 6** was

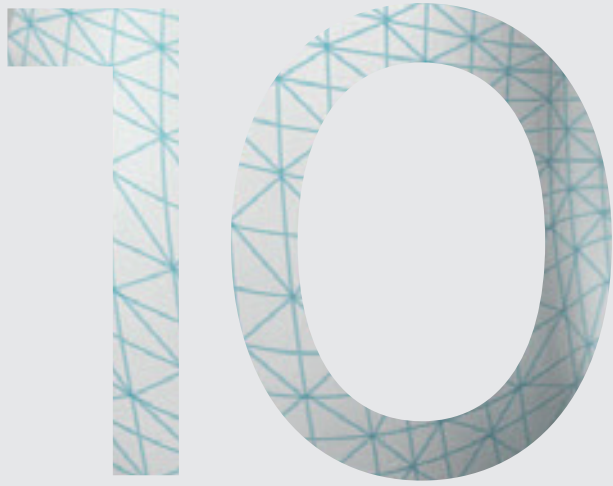
daarom een voorspellingsmodel te ontwikkelen voor compressie van het hart op basis van 3D-beelden. Een combinatie van de externe pectusdiepte en de voor-achterwaartse afstand (van voorzijde borstbeen tot achterzijde ruggengraat) werden hierbij geïdentificeerd als voorspellend voor compressie van het hart. In een tweede model dat louter gebaseerd was op mannelijke patiënten, werd alleen de externe pectusdiepte als voorspellend geïdentificeerd. Beide modellen gaven een uitstekend onderscheidend vermogen tussen de aan- en afwezigheid van compressie van het hart.

In **Hoofdstuk 7** werd de overeenstemming in de visuele beoordeling van 3D-beelden door verschillende experts geëvalueerd, en ook de overeenstemming bij herhaalde beoordeling door eenzelfde expert. Door middel van een vragenlijst werden interactieve 3D-beelden digitaal beoordeeld op de aanwezigheid van pectus excavatum, asymmetrie, flaring, diepte, beginpunt, algemene ernst en morfologisch subtype van pectus excavatum. Achtenvijftig interactieve unieke 3D-beelden werden tweemaal beoordeeld door 5 (cardio)thoracale chirurgen. Er bleek een aanzienlijk verschil te bestaan in de beoordeling tussen experts en herhaalde beoordeling van eenzelfde expert. Zo werden 55% tot 95% van de patiënten door verschillende experts beoordeeld als lijdend aan pectus excavatum. Aangezien deze variatie in beoordeling van grote invloed kan zijn op de uiteindelijke behandelingsstrategie, werd aangedrongen op vervolgstudies naar standaardisatie, onder andere middels het opstellen van definities.

Een algemene discussie over de resultaten en bevindingen van dit proefschrift, evenals een uitwerking van de wetenschappelijke en maatschappelijke impact ervan, is te lezen in **Hoofdstuk 8**.

Dit proefschrift toont aan dat 3D-beelden kunnen worden gebruikt als een betrouwbaar en nauwkeurig diagnostisch hulpmiddel in de preoperatieve evaluatie van patiënten met pectus excavatum.





Impact paragraph

The aim of this chapter is to describe and elaborate on the scientific and societal impact achieved and anticipated by the current thesis.

Relevance for patients

The fundamental rationale for this thesis has been the routine exposure to potentially harmful ionizing radiation associated with current diagnostic procedures in the work-up of pectus excavatum. In the consecutive chapters, scientific basis was provided allowing the use of three-dimensional (3D) imaging as primary diagnostic modality in pectus excavatum with appropriate accuracy compared to current modalities.

Most patients seeking consultation for pectus excavatum concern those of pediatric age. Especially these patients are at risk to develop radiation associated pathologies due to their relatively long life-time risk, therefore pediatric patients are the ones who benefit most from the anticipated transition towards the use of 3D imaging as primary diagnostic modality in pectus excavatum. Yet, as radiation exposure is potentially hazardous for all age groups, adults benefit likewise.

Based on local preferences, pectus centers have up until now used either computed tomography (CT) or plain radiographs as primary screening modality. The global ratio is about 50:50. Considering this, it must be said that patients referred to a pectus center that already dispensed CT and employs plain radiographs instead still benefit, albeit to a lesser extent because the associated effective radiation dosage of plain radiography is lower than CT. Nevertheless, 3D imaging is strengthened by its potential use for follow-up, mitigating the cumulative radiation dose exposed to during the entire treatment course. On the other hand, a disadvantage of 3D imaging is its contraindication in patients with any form of light hypersensitivity.

As mentioned, about half of all pectus centers primarily employ plain chest radiographs during work-up. These centers and their patients benefit from the possibility to predict cardiac compression from 3D images which would otherwise require additional diagnostics. Yet, in the presence of a patient presenting with a story of impairing cardiac symptoms and a low model-predicted probability for compression, the patient may need further analysis.

Currently, 3D images are obtained by dedicated imaging systems for which a hospital visit is required. Although these investigations are often clustered to

reduce the number of outpatient visits, it is anticipated that follow-up and even primary consultation including 3D imaging can be done completely through videoconferencing. Tablets and mobile phones already come with a light detection and ranging scanner allowing the acquisition of 3D images, with intuitive software and applications allowing easy utilization at home. This is specifically valuable given the relatively large adherence area of tertiary pectus referral centers. In addition, the possibility may be created for patients to send a 3D image of their chest to obtain a preliminary advice, aiming to overcome the general unawareness on pectus excavatum among first-line caregivers. Currently, patients are often referred to a pectus specialist center rather late, after conducting their own search through web-based sources.

Relevance for clinical practices

Adopting 3D imaging is, as with all technical novelties, forecasted to unfold rather slowly due to the necessary infrastructural changes, monetary investments, the general viscosity of changes in medicine, and the primary initiative which must often be taken by local pectus experts who recognize its potential. On the other hand, after renowned pectus centers worldwide begin using 3D imaging, a snowball effect may be expected. To advance this effect, the scientific evidence for 3D imaging should be expanded, to which this thesis contributes.

Three-dimensional imaging requires restrained operators for acquisition and processing of the acquired raw data. The most logical step would be to educate medical photographers to do so (as done in our center) since they understand the basic principles of digital imaging and are housed in most centers. Moreover, 3D imaging is often regarded as a step-up from conventional two-dimensional photography. However, first the 3D imaging system of choice needs to be purchased, alongside the required information communication technology upgrades, including storage, software and so on. Potentially, this is a major barrier to medical centers since the cost-effectiveness compared to current diagnostic procedures remains unknown. One way to cut costs would be to centralize pectus care in tertiary referral centers, which has already naturally occurred in the Netherlands. In addition, 3D imaging can be employed in other fields than thoracic surgery, such as plastic surgery and oral and maxillofacial surgery where its medical use originated. Moreover, given its inexhaustible potential of applications in analysis, follow-up and surgical planning,

the burden of investment may be diluted among various departments. Besides, 3D imaging systems are readily commercially available for less than \$1000. In short, adopting 3D imaging requires careful weighing and subsequent planning with inclusion of all stakeholders. Three-dimensional imaging is not superior to current diagnostic procedures in terms of accuracy but primarily aims to shield patients from potentially harmful ionizing radiation. Although scientifically proven, significant unawareness on associated risks of radiation exposure remains globally, resulting in its inconsiderate use.

Relevance for pectus society

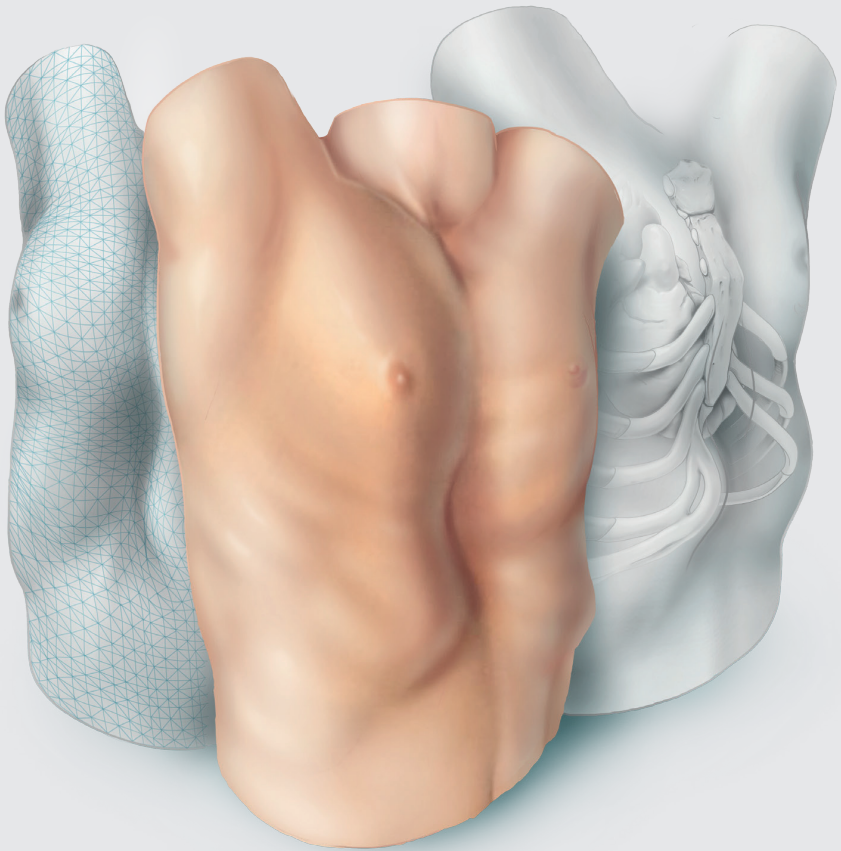
In the past decades, research on pectus excavatum exponentially grew. However, relatively little is still known about the deformity itself whereby visual examination and diagnosis remains rather subjective, henceforth urging the need for standardization. Here is a major role for 3D imaging as it allows objective quantification of pectus excavatum and its morphological features. Using such objective measures is anticipated to provide a common language among experts. However, interpretation of these numeric values could mutually be subject to observer differences since their severity is judged according to the expert's reference frame. This could be overcome by using a concept like growth curves where deviations from the mean are identified. For example, a severity several standard deviations below the mean, could be labeled as a non-severe pectus excavatum.

Another issue that may be overcome is the subjective recurrence of pectus excavatum reported by patients during follow-up after bar removal which is often not recognized or acknowledged by experts. In these cases, 3D imaging can provide objective measures.

In addition, part of cases who undergo repair of pectus excavatum are dissatisfied by the postoperative aesthetic result. Three-dimensional imaging could also be employed to provide a patient-specific prediction of the postoperative outcome, aligning expectations during preoperative consultation, and thereby reducing the likelihood for postoperative dissatisfaction about the aesthetic result.

In conclusion, although the use of three-dimensional imaging in pectus excavatum is still in its infancy, its usefulness is already apparent in daily practice by pioneering

centers. The present thesis demonstrated the feasibility, validity and accuracy of three-dimensional imaging and evaluated several of its applications. We expect the share of three-dimensional imaging to only increase, especially in the objectification of pectus excavatum which remains a rather subjective diagnosis. Still, future studies should aim to address the limitations and future directions elaborated on, ensuring its solid scientific embedding.





Dankwoord

Het huidige proefschrift staat niet alleen symbool voor mijn wetenschappelijke ontwikkeling, maar ook centraal in de persoonlijke ontwikkeling die ik heb doorgemaakt tijdens mijn relatief korte promotietraject. Zonder de begeleiding van, en samenwerking met ondergenoemden was het nooit mogelijk geweest om deze ontwikkeling door te maken en dit proefschrift te voltooien. Hierbij verdient iedereen die, op welke manier dan ook, aan dit proefschrift heeft meegewerkt eenzelfde mate van waardering en erkenning.

Allereerst zou ik graag alle patiënten willen bedanken voor hun deelname aan de verschillende studies, uitgevoerd ten behoeve van dit proefschrift. Zonder uw welwillendheid en gebrek aan zelfzucht zou het onmogelijk zijn om gedegen wetenschappelijk onderzoek uit te voeren en tot nieuwe inzichten te komen die veelal enkel baat hebben voor toekomstige patiënten.

De beoordelingscommissie, bestaande uit: Prof. dr. L.P.S. Stassen, Prof. dr. W. Morshuis, Prof. dr. S.G.F. Robben, Prof. dr. C. Slump en Dr. P. Sardari Nia, bedankt voor uw beoordeling van dit proefschrift. Het positieve oordeel van een commissie met een dergelijke statuus geeft dit proefschrift een extra dimensie. Eveneens wil ik de aanvullende leden van de promotiecommissie bedanken.

Mijn promotor, Prof. dr. Maessen, beste Jos, wij kenden elkaar initieel slechts van gezicht vanuit mijn voorgaande onderzoek bij de cardiothoracale chirurgie in het Maastrichtse. Naar gelang ons contact tijdens het promotietraject intensiverde heb ik de vruchten mogen plukken van uw ongeëvenaarde kennis en passie. Uw academische instelling en kritische noot hebben gezorgd voor een solide en doordachte basis van de verscheidene artikelen. Hierbij heb ik bewondering voor het feit dat u ondanks uw academische en klinische taken, en ook uw taak als afdelingshoofd, toch altijd tijd hebt weten te vinden voor overleg en input. Ik wil u graag bedanken voor uw exceptionele enthousiasme en begeleiding. Ik hoop dat we de samenwerking tussen het Heerlense en Maastrichtse nog lang mogen voortzetten.

Mijn co-promotor, Dr. de Loos, beste Erik, mijn dagelijkse toen-nog-niet-gepromoveerde-promotor. Ik vergeet nooit meer de dag dat ik op de long-operatiekamer stond tijdens mijn co-schap snijdend en toch wel enigszins verbaasd was over de relaxte sfeer waarin er tijdens het opereren met keiharde techno-muziek meer dan genoeg ruimte was voor grappen en grollen. Gezien sfeer voor mij een groot gedeelte van het werkplezier bepaalt, hoopte ik dan ook

dat je zou vragen of ik heil zag in onderzoek bij de thoraxchirurgie. Terugkijkend is mijn keuze voor dit onderzoek, denk ik, een van de beste keuzes geweest waarbij ik grote bewondering heb voor het feit dat het jouw persoonlijke doel is om de carrière van een ander vooruit te helpen in plaats van te denken aan je eigen toekomst. Daarnaast ben ik door jouw onuitputbare enthousiasme en je geloof in het vormen van een geolied team waarbij iedereen zijn kwaliteiten in optima forma benut, nog meer gaan inzien dat het team belangrijker is dan het individu. Jouw motto: "ik ben niet je begeleider, we doen het samen" zal ik daarom ook nooit vergeten en meenemen in mijn eigen carrière. Het mooiste voorbeeld van dit "samen" is wellicht ons gezamenlijk promotietraject. Naast het feit dat we elkaar elk uur van de dag bestoken met belletjes (een dag niet gebeld met Loosje is een dag niet geleefd), ideeën voor onderzoek, afspraken en deadlines heb ik naast het wetenschappelijke, ook op klinisch, operatief, maar bovenal ook op persoonlijk vlak veel van je geleerd. Ik waardeer onze grenzeloze eerlijkheid naar elkaar toe tijdens onze dagelijkse gesprekken; zowel met betrekking tot werk als privé. Kortom, je hebt mij echt op alle mogelijke vlakken proberen te betrekken (en nog steeds!). Voor deze kansen en ervaringen, maar bovenal voor hetgeen dat ik van je geleerd heb, zal ik je eeuwig dankbaar blijven. Ik hoop dat we nog vele jaren mogen samenwerken. P.s. ik zal plechtig zweren de AIS-codes nooit te vergeten tijdens de overdracht!

Mijn co-promotor, dr. Vissers, beste Yvonne, ons verhaal start eveneens op OK Q03. Ik weet nog goed dat ik na die eerste longoperatie profylactisch excuus heb aangeboden voor mijn amicale gedrag. Gelukkig bleek dit achteraf niet nodig. Enfin, tijdens de periode waarin dit proefschrift tot stand is gekomen ben jij met name de stabiele en beheerste factor geweest die de tijd nam om samen te zitten voor uitleg en uitgebreide doch gerechtvaardigde revisies. Daarnaast was jij diegene die juist op moeilijke momenten geriefelijk de knopen doorhakte en recht door zee was. Voor al deze aspecten bewonder ik jou ten zeerste. Ik wil je tevens bedanken voor het onuitputbare enthousiasme en de exceptionele begeleiding. Ik hoop dat we in de toekomst nog veel mogen samenwerken.

Wanten en Reza, (studie)maten, gedurende de gehele opleiding een hechte groep en ondanks dat we elkaar niet meer dagelijks zien, kunnen we altijd op elkaar terugvallen. Ik ben zeer vereerd om jullie mijn paranimfen te mogen noemen. De drie musketiers terug in de gelederen. Ondanks dat eenieder zijn eigen ideeën en persoonlijk instelling heeft, blijven we een mooie combinatie die elkaar het vuur

aan de schenen kan leggen. Ik kan hier veel herinneringen ophalen maar hetgeen waar ik met name naar uitkijk is dat wij elkaar in de toekomst nog vaak mogen blijven zien! Kusjes aan de A-KO vrouwen.

Dr. Hulsewé, beste Karel, natuurlijk niet weg te denken uit de thoraxclub. Hetgeen ik aan onze samenwerking altijd het meeste gewaardeerd heb zijn de grondige revisies van, en kritische vragen op elk manuscript. Dit betrof vaak aspecten die eerder bij niemand ter gedachte kwamen en derhalve resulteerden in een solide verantwoording en interpretatie van de uitgevoerde studie. Ik hoop onze fijne samenwerking in de toekomst te mogen voortzetten, zowel op onderzoeks- als operatief gebied.

Eerst stond je later in het dankwoord onder de zeker niet minder belangrijke noemer van “assistenten”. Maar als nieuwste maat van de thoraxclub ben je, net zoals op de hiërarchische ladder, in dit proefschrift naar voren geschoven. Dr. van Roozendaal, Lori, nogmaals van harte met deze mijlpaal als differentiant; dit doen weinigen je na. Ondanks onze relatief korte gezamenlijke periode in het Zuyderland is het er een om niet te vergeten; vanwege de gezelligheid, alsmede het leren opereren en de (onbedoelde) adviezen. Ik hoop nog lang met je te mogen samenwerken en wie weet over 5 jaar....

Meneer Loonen, Tommie, wij gaan samen al heel wat jaartjes mee. Van beste maten tijdens de studie Technische Geneeskunde tot samenwonen tijdens onze stages. Van drie maanden samen vertoeven in Oeganda tot het samen uitvoeren van verschillende wetenschappelijke studies. Door met jou te sparren en de facilitering vanuit het 3D Lab, heb jij mede de basis gelegd voor dit proefschrift, alsook voor verschillende katertjes. Hiervoor ben ik je dankbaar. Ik weet alleen niet of de studenten die een slecht cijfer kregen dit ook waren. Naast dit alles: nog waardevoller is onze vriendschap en het feit dat jij mij hebt leren relativeren en laten inzien dat er nog iets anders is dan werken alleen. Ik hoop dat wij nog heel wat jaren meegaan, maar daar twijfel ik niet aan!

Als ik het over het 3D Lab van het Radboud UMC heb, dan mag een dankwoord aan Prof. Dr. Maal niet ontbreken. Beste Thomas, dank voor alle (technische) ondersteuning tijdens de initiële fase van het promotietraject.

Zonder de een te roemen en de ander tekort te doen wil ik ook alle chirurgen van de Maatschap Heelkunde Zuid-Limburg bedanken. Ik heb tot nu toe veel geleerd

en hoop ook in de toekomst veel van jullie te leren, ook al zullen jullie vast af en toe denken: komt die gek weer op zijn vrije dag leren opereren. Ozan, ik help met liefde mee met onderzoek; ruilen voor de benadering bij een liesdesobstructie?

Dr. Sardari Nia, beste Peyman, onder uw begeleiding heb ik als jonge studentonderzoeker de eerste stappen mogen zetten in de wetenschappelijke wereld. Ik ben dankbaar dat ik een steentje heb mogen bijdragen aan het verwezenlijken van uw innovatieve ideeën en vooruitstrevende inzichten op het gebied van perioperatieve simulatie en training. Ondanks dat onze wegen zich hebben gescheiden hoop ik dat wij in de toekomst nogmaals mogen samenwerken op wetenschappelijk dan wel chirurgisch vlak. Ik wil u bedanken voor uw onuitputtelijke enthousiasme welke mijn wetenschappelijke interesse heeft aangewakkerd, alsmede voor alle leermomenten en geboden kansen.

Dr. Heuts, beste Sam, onder jouw hoede en de hoede van Peyman ben ik ooit begonnen als groentje bij de cardiothoracale chirurgie in het Maastrichtse. Je hebt mij echt opgevangen en geïntroduceerd, maar met name vaak naar een verlaagd bewustzijn geholpen. Naast het veelvoud aan versnaperingen heb ik veel van je geleerd en stond je, maar sta je ook nog steeds altijd klaar om te helpen waar nodig. We hebben samen een mooi aantal publicaties gerealiseerd en dit zijn we, ondanks onze andere richtingen, nog steeds aan het uitbreiden. Ik zal onze memorabele congressen en avonden nooit vergeten. Daar laat ik het bij; wij moeten allebei ooit nog een stafplek krijgen. Idiopathische brandwonden in New York?! Grachten Leiden?! Duim breken?! Blauwe lichten?! Gent?! Ik hoop samen nog veel mooie momenten met je mee te maken!

Als ik het over New York heb, dan moet ik het ook zeker over drs. Jules Olsthoorn hebben. Ik wil je bedanken voor alle gezellige avonden samen bij de CTC. Al liepen deze op het conto van de Heuts toch wel vaak uit de hand.

Dr. Lozekoot, beste Pieter, post clinicus van het jaar, maatje, als er iemand is die ervoor zorgt dat jonge honden zoals ik genoeg exposure krijgen dan ben jij het wel. Elk belletje over een abces dat nog gedraineerd moest worden, of een POK die jij liever superviseerde dan zelf deed, zal ik nooit vergeten en tot in der eeuwigheid waarderen. Daarnaast ben ik dankbaar voor alle discrete gesprekken en tips, maar met name voor het veelvoud aan wederzijdse afbrekende feedback zonder dat dit ooit heeft geleid tot één boze blik. Zelfs niet toen je opeens underdressed was op

weg naar de WBS. I'm guilty as charged. Dat we maar lang maten mogen blijven, ook in tegenspoed!

Prof. Slump, beste Kees, of is het nu Cees (?), u vormt een rode draad door een groot gedeelte van mijn relatief korte carrière. Initieel was u met name geïnteresseerd in wie de potjes Monopoly aan het winnen was achter in de collegezaal. Echter, naar gelang de tijd vorderde, hebben wij gelukkig ook serieus samengewerkt. Ik heb veel van u geleerd en pas dit nog dagelijks toe in het begeleiden van andere studenten. Zo gaat het niet altijd om het eindproduct maar is de weg ernaartoe en hetgeen dat je op deze weg leert veelal belangrijker. Bedankt voor alles dat ik van u heb mogen leren en ik wil u alvast veel plezier toewensen met uw pensioen. Het gaat u goed!

Ernst, Mirianne en Juul, jullie waren en zijn nog steeds het kloppend hart van vele wetenschappelijke studies binnen de thoraxchirurgie. Zonder jullie onuitputtelijke inzet en enthousiasme binnen het 3DPECTUS-project was dit project nooit een succes geworden. Bedankt voor alle inclusies, gemaakte 3D-foto's en uitermate fijne samenwerking. Ik hoop nog lange tijd met jullie te mogen blijven samenwerken.

De behandeling van pectus-patiënten geschiedt in een multidisciplinaire setting, hetgeen betekent dat dit een teamsport is. Daarom wil ik, naast hierboven genoemde medisch fotografen, ook de kinderartsen, cardiologen en oud-huisartsen bedanken voor hun specifieke bijdragen.

Toch moet ik hier ook het operatieteam van de thoraxchirurgie benoemen waar ik mij in de loop van de tijd een deel van ben gaan voelen. Jullie zijn vanaf het begin een warm bad geweest, ook als ik weer aankwam met de vraag of ik (ALWEER!) een 3D foto mocht maken bij de zoveelste pectuspatiënt. Tegenwoordig zijn jullie meer geïnteresseerd in mijn liefdesleven. Als ik tips nodig heb weet ik jullie te vinden.

HJC Vedette, "eye of the tiger, **** like a shrimp", Bussink, Einstein, Fitski, Haas, Hollie, Koers, Luc, Snurre, jullie hebben als jaarclub mijn studentenleven in Enschede gekleurd met witgele versnaperingen, raketjes en af en toe een beetje brokkelen. Jullie beschikken over iets té veel belastend materiaal om mijn leven tot een hel te kunnen maken (daarom ook de censuur voor het promotiefeest), dus ik zal hier louter aardig zijn. Ik wil jullie bedanken voor alle turbulente avonden en littekens, maar vooral voor het feit dat we altijd een collectief zijn geweest en bovenal nog steeds zijn. Ook al gingen we midden in Groningen in een volle kroeg

met Vin****-leden strijdend en worstelend ten onder in ons clubtenu, we gaan nog elk jaar samen op (nu gelukkig een buitenlandse) stedenstrip en zouden deze Groningen-ervaring zonder enige twijfel herhalen. Ik hou van jullie!

Meneer Janssen, René, vriend van het eerste uur, enneuh, wat heb jij eigenlijk aan dit proefschrift bijgedragen? Tsja, in ieder geval stond je aan de basis: samen doorstonden we onze iets te lange middelbare schoolcarrière met vooral ontspanning en lol hoog in het vaandel. Gedurende mijn promotietraject heb jij gezorgd voor de (on)nodige gezelligheid. Hierdoor was ik in staat om op gezette tijden af te schakelen om daarna met een frisse blik weer verder te werken; al dan niet met kater. Ik hoop dat onze vriendschap nog lang mag blijven bestaan!

Ondanks dat wij niet meer de hechte drie-eenheid zijn kan ik Daan Berends natuurlijk niet vergeten. Ooit samen een kookclub opgericht, veel mooie momenten beleefd en bovenal goede gesprekken.

Drs. Daemen, beste Karin, wellicht dat je het zelf nooit zo ervaren hebt, maar mede dankzij jouw adviezen en nuchtere blik heb ik twee belangrijke keuzes gemaakt: starten met de opleiding arts-klinisch onderzoeker, alsmede switchen van onderzoek plek. Ondanks dat wij beiden nooit zullen weten hoe het zonder deze keuzes gelopen was, ben ik je hiervoor buitengewoon dankbaar.

Drs. Elenbaas, Drs. Van Huijstee en Drs. Van Veer, alle drie gerenommeerde thoraxwand-chirurgen. Ik wil u bedanken voor de productieve maar bovenal prettige samenwerking bij de OBJECTIFY-studie. Zonder uw welwillendheid en kritische blik was er nooit een dergelijk mooi eindresultaat geweest. Mijn voorstel: laten wij deze bundeling van krachten ook in de toekomst voortzetten.

Als ik het over het UZ Leuven heb, dan mag ik Dr. Yanina Jansen natuurlijk niet vergeten. Of beter gezegd: Sjaninake. Vanaf dag één heb ik jou proberen te choqueren, maar dat is tot op de dag van vandaag nooit gelukt. Dank voor alle gezelligheid en je wetenschappelijke input. Ik kijk uit naar onze toekomstige samenwerking.

Beste Nadine, jij was de eerste student die ons vanuit Twente kwam vergezellen op het 3DPECTUS-project. Het werk dat jij hiervoor verzet hebt, met name op het gebied van automatisering en kwantificering, heeft tot op de dag van vandaag een enorme toegevoegde waarde. Onze (bijna dagelijkse) overlegmomenten heb ik zeer gewaardeerd en hebben keer op keer geleid tot een doordachte klinisch-

technische basis van onze onderzoeken. Bedankt voor alles en veel succes met het afronden van je eigen promotietraject, en ook je tweede master in de natuurkunde.

Ook Renée Hovenier, Kim van der Tak en Mart Wubbels, studenten van de master Technische Geneeskunde wil ik bedanken voor hun bijdrage aan de pectus onderzoekslijn tijdens hun drie maanden durende stages.

De kracht van onderzoek binnen de thorax onderzoeksgroep van het Zuyderland is dat de kwaliteiten van iedereen in optima forma benut worden om zo efficiënt mogelijk tot een solide wetenschappelijk eindproduct te komen. Hier valt ook koffiedrinken en uitbrakken op de tussenverdieping onder. Ongeacht de grootte van de bijdrage blijft onderzoek simpelweg een team effort waar geen plek is voor me, myself and I. Daarom wil ik zeker niet vergeten om Drs. Paul Hollering, Dr. Matthijs Van Gool, Dr. David Van Dijk, Dr. Lori van Roozendaal, Drs. Maxim Peeters, Drs. Ine Rochus, Dr. Jan Stoot, Drs. Nicky Janssen, Drs. Alexander Pennings, Drs. Paul Andel, Drs. Tessa Geraedts, Omar Ashour, Elise van Polen, Iris Laven, Linda Crapels, Dr. Aimée Franssen, Drs. Arlette Angelica Ramos Gonzalez (de Vamos de Ribas de Campos), Anna Hofstra, Tim Peeters, Sven Verdonschot, Pelle van der Hoven, Inez Cortenraad, Iris Michels, Drs. Robert van den Broek, en Iris Kamps te bedanken.

Daarnaast wil ik ook Anke Neyens, Prof. dr. Lee Bouwman en Noémi van Nie bedanken voor de dagelijkse ondersteuning en goedkeuring van de verschillende studies. Hierbij hoort natuurlijk ook de financiële ondersteuning door het Research en Innovatiefonds van het Zuyderland, en ook RVE 4. Laatstgenoemde ten tijde geleid door Anke Neyens welke ik nogmaals wil bedanken als, hoe het toen voelde, mede-voorvechter van het pectus-onderzoek zonder wiens steun het gedane nooit gerealiseerd had kunnen worden.

Jens (Marijn Jense of Jens Marijne) en Misha, ondanks dat onze gezamenlijke promotie periode bijna helemaal uit een lockdown en avondklok heeft bestaan wil ik jullie bedanken voor alle gezelligheid (tot 21:00 uur en erna), alsmede voor het doorstaan van mijn aanwezigheid. Ondanks dat ze al genoemd zijn, mogen Tessje en Paulus ook hier natuurlijk niet ontbreken. Of weet je niet meer dat je hierbij was Tess?

Als ik het dan over mijn tijd op de T1 in Heerlen heb, dan moet ik Simone natuurlijk ook bedanken. Simone bedankt voor alle praatjes, adviezen en hulp bij het plannen van onmogelijke afspraken.

Zonder een enkele collega(-assistent) tekort te doen, wil ik in het bijzonder Koentje, Merol, Gabs, Diebs, Markie, Robbie en Cassie bedanken voor alle doordeweekse etentjes, felle discussies en veel-te-veel wijn avonden (JA, we hebben een probleem). Daar horen natuurlijk ook Lori, Poodtje en (nogmaals) Diebs bij; dank voor de gezellige avondjes, ook al voelde ik mij elke ochtend nadien verschrikkelijk slecht (zou het toch weer die limoncello zijn; hoeveel procent zit daar nu in?) Waarom ik dit hier benoem weet ik niet maar ik wil ook de Mees-gegadigden bedanken, gewoon omdat het een heerlijke magische nacht was. To the moon and back. Maar wanneer gaan we weer? Wie reist via Eindhoven?

Merel, Floor en Es(ter), koffietjes, cappuccino of takkenthee? Bedankt voor alle fijne momenten en (onbedoeld) (liefdes)advies. Een dag Zuyderland Sittard staat voor mij altijd garant voor gezelligheid met jullie! Zonder Floor en Es tekort te doen moet ik natuurlijk Merel in het bijzonder ook nog bedanken voor het bewaken van mijn nachtrust met elk bericht of belletje: "ben je nou nog steeds aan het werken, ga eens slapen joh!". Dat er vervolgens nog een uur over van alles en niks gebabbeld werd hebben we het verder niet over.

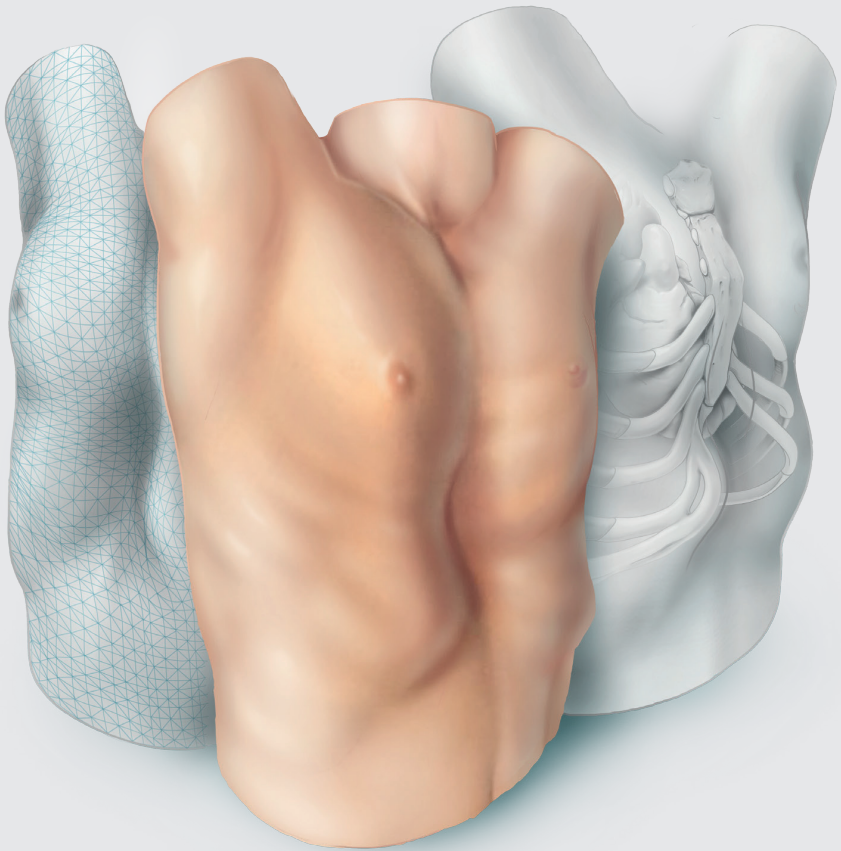
Koen(tje) Verkoelen of was het toch Verkoulen? Mooie man, chirurgiemaat van het eerste uur en sinds kort promovendus bij de longchirurgie. Bedankt voor alle mooie momenten, gedeelde naïviteit, gezellige avonden en vooral veel gelach! Ondanks onze relatief korte carrière hoop ik dat onze vriendschap nog lang mag blijven bestaan!

Juultje, Caesar, mevrouw Roelofs, ondanks dat wij niet meer samen zijn kan en wil ik jouw naam hier onder geen enkele voorwaarde weglaten. De woorden zijn wel iets aangepast anders worden anderen nog jaloers. Nu zonder flauwekul. Jij hebt mijn promotietraject meegemaakt van begin tot (bijna) einde en ik ben je enorm dankbaar voor het feit dat jij daar deel van hebt uitgemaakt. Zonder jouw opofferingen (zelfs ten tijde van ziekte) die jij glimlachend en zonder enige twijfel deed om mij op elke denkbare wijze te ondersteunen zal ik nooit vergeten en tot in de eeuwigheid waarderen. Het ga je goed, lieve Juul! Kump goad.

Luc, broertje, veel woorden hebben wij twee niet nodig. Wij gedijen goed zonder elkaar maar zijn tegelijkertijd heel hecht met elkaar. Ik ben supertrots op wie je bent en op hoe ver je het al hebt geschopt in je nog jonge carrière. Helaas valt er in de medische wereld weinig te onderhandelen over salaris anders nam ik jou mee naar P&O! Ik wens je alle geluk toe met Nick! Ik hou van je broertje!

Moeder en Vader, Marian en Benjo, ondanks alle voorgaande dankwoorden: jullie hebben mijn basis gevormd. Jullie hebben mij geleerd om keihard te werken en geleerd dat je altijd 10 stappen harder moet lopen dan anderen. Zo kom je waar je wilt zijn en bereik je hetgeen je ambieert. Desondanks was ik nergens geweest zonder jullie als stabiele thuishaven met allround steun, zowel mentaal als emotioneel, maar ook op praktisch gebied. De kinder-en jeugdijaren waren soms wat hobbelig maar sieren tot op heden de verhalen die onbedoeld de aardbodem bereiken en welke nu met humor ontvangen worden. Ik ben nu al bang voor mijn eigen nageslacht. Ondanks dat we goed zonder elkaar kunnen, zou ik nooit zonder jullie kunnen. Ik bewonder jullie enorm, ben trots op onze intieme grenzeloze band, en zie jullie als mijn idolen bij wie ik altijd mijn relaas mag doen; zowel in goede als in slechte tijden. Bedankt voor alles en voor jullie onvoorwaardelijke liefde en steun! Ik hou van jullie!

Helaas is vergeten menselijk, daarom wil ik tot slot iedereen die in het voorgaande dankwoord niet geroemd is, alsnog bedanken voor alle enthousiasme, inzet en samenwerking in de totstandkoming van dit proefschrift.





Curriculum vitae
List of publications

Curriculum vitae

Jean Hubertus Theresia Daemen was born on April 18th, 1992, in Puth, the Netherlands. He graduated from secondary school (Atheneum, Trevianum, Sittard, the Netherlands) in 2011. Immediately thereafter he started a bachelor program in Technical Medicine at the University of Twente (Enschede, the Netherlands). Following graduation in 2014, he began a master's program in Technical Medicine with focus on Medical Imaging and Interventions. During this period, he obtained an additional degree as radiation expert (Radiation Expertise Level 3). However, after his second master's year, which comprised of clinical internships in different medical centers and an appended three-month volunteering period in rural Uganda (Nakaseke General Hospital, Nakaseke, Uganda), he decided to become a physician in his desire to care for the diseased. In 2016 he started with Medical school (Master Medicine and Clinical Research) at the University of Maastricht (Maastricht, the Netherlands). He combined his Medical school with research at the Department of Cardiothoracic Surgery at Maastricht University Medical Center (Maastricht, the Netherlands) under supervision of Dr. P. Sardari Nia and Dr. S. Heuts. After a fruitful period (2016-2018), resulting in multiple publications and congress meetings, Jean relocated to the department of General Thoracic Surgery at Zuyderland Medical Center (Heerlen, the Netherlands) where he, during his internships, focused on research with regards to pectus excavatum and received a research grant (Research and Innovation Fund, Zuyderland Medical Center, Heerlen, the Netherlands). In 2020 he completed his master in Technical Medicine with honors, as well as his masters in Medicine and Clinical Research. He continued his PhD program on three-dimensional imaging in pectus excavatum under supervision of Dr. E.R. de Loos, Dr. Y.L.J. Vissers and Prof. dr. J.G. Maessen, accomplishing the present thesis. During this period, he was one of the invited guest editors for a special series on the minimally invasive treatment of pectus deformities as well as a special series on chest wall resections and reconstructions. In the same center, he commenced his medical career at the department of General Surgery as a resident not in training in April 2021. In July 2022, he started as General Surgical resident.



List of publications

This thesis (in order of appearance)

Daemen JHT, Loonen TGJ, Lozekoot PWJ, Maessen JG, Maal TJJ, Hulsewé KWE, Vissers YLJ, de Loos ER. Optical imaging versus CT and plain radiography to quantify pectus severity: a systematic review and meta-analysis. *J Thorac Dis* 2020;12:1475-87.

Daemen JHT, Loonen TGJ, Coorens NA, Maessen JG, Maal TJJ, Hulsewé KWE, Vissers YLJ, de Loos ER. Photographic documentation and severity quantification of pectus excavatum through three-dimensional optical surface imaging. *J Vis Commun Med* 2020;43:190-7.

Daemen JHT, Loonen TGJ, Verhulst AC, Maal TJJ, Maessen JG, Vissers YLJ, Hulsewé KWE, de Loos ER. Three-dimensional imaging of the chest wall: a comparison between three different imaging systems. *J Surg Res* 2020;259:332-41.

Daemen JHT, Coorens NA, Hulsewé KWE, Maal TJJ, Maessen JG, Vissers YLJ, de Loos ER. Three-dimensional surface imaging for clinical decision making in pectus excavatum. *Semin Thorac Cardiovasc Surg* 2022;34:1364-73.

Daemen JHT, Heuts S, Rezazadah Ardabili A, Maessen JG, Hulsewé KWE, Vissers YLJ, de Loos ER. Development of prediction models for cardiac compression in pectus excavatum based on three-dimensional surface images. *Semin Thorac Cardiovasc Surg* 2023;35:202-12.

Daemen JHT[†], de Loos ER[†], Geraedts TCM, Van Veer H, Van Huijstee PJ, Elenbaas TWO, Hulsewé KWE, Vissers YLJ. Visual diagnosis of pectus excavatum: an inter-observer and intra-observer agreement analysis. *J Ped Surg* 2022;57:526-31.

[†] *Equal contribution status.*

Other

Laven IEWG, Franssen AJPM, **Daemen JHT**, Hulsewé KWE, Vissers YLJ, de Loos ER. Thinking outside the “Enhanced Recovery After Surgery” box: would a more progressive, patient-tailored approach in chest tube management be next?. *J Thorac Dis* 2023.

Janssen N, **Daemen JHT**, Michels IL, Franssen AJPM, Maessen JG, Hulsewé KWE, Vissers YLJ, de Loos ER. Preoperative imaging of clinically relevant intrathoracic abnormalities in pectus excavatum. *Quant Imaging Med Surg* 2023.

Daemen JHT, Haecker FM, de Loos ER. Special series: minimally invasive treatment of pectus deformities. *J Thorac Dis* 2023.

Janssen N†, **Daemen JHT**†, van Polen EJ, Coorens NA, Jansen YJL, Franssen AJPM, Hulsewé KWE, Vissers YLJ, Haecker FM, de Campos JRM, de Loos ER. Pectus excavatum: consensus and controversies in clinical practice. *Ann Thorac Surg* 2023.

Franssen AJPM, Degens JHRJ, **Daemen JHT**, Laven IEWG, Hulsewé KWE, Vissers YLJ, de Loos ER. Mediastinal staging by thoracic surgeons: are we close to a paradigm shift?. *J Thorac Dis* 2022.

Denessen EJ, Heuts S, **Daemen JHT**, van Doorn WP, Vroemen WH, Snels JW, Segers P, Van 't Hof AW, Maessen JG, Bekers O, Van Der Horst IC, Mingels AM. High-sensitivity cardiac troponin I and T kinetics differ following coronary bypass surgery: a systematic review and meta-analysis. *Clin Chem* 2022.

Janssen N†, **Daemen JHT**†, Ashour O, van Hulst L, Hulsewé KWE, Vissers YLJ, de Loos ER. Nuss bar removal without straightening is a safe technique: a single center experience. *J Thorac Dis* 2022;14:3335-42.

† *Equal contribution status.*

Jansen YJL, **Daemen JHT**, Hulsewé KWE, Vissers YLJ, de Loos ER. Tracheal and cricotracheal resections: see one, do none, centralize? *J Thorac Dis* 2022;14:2735-7.

Laven IE, **Daemen JHT**, Jansen YLJ, Janssen N, Franssen AJPM, Heuts S, Maessen JG, van den Broek FJC, Hulsewé KWE, Viseers YLJ, de Loos ER. Thoracic surgery in the Netherlands. *J Thorac Dis* 2022.

Huang J, Bian C, Zhang W, Mu G, Chen Z, Xia Y, Yuan M, Ujie H, **Daemen JHT**, de Loos ER, Zhu Q, Wu W, Chen L, Wang J. Partitioning the lung field based on the depth ratio in three-dimensional space. *Trans Lung Cancer Res* 2022;11:165-75.

Coorens NA, **Daemen JHT**, Slump CH, Jansen Y, Maessen JG, Vissers YLJ, Hulsewé KWE, de Loos ER. Predicting aesthetic outcome of the Nuss procedure in patients with pectus excavatum. *Semin Thorac Cardiovasc Surg* 2022.

Janssen N, **Daemen JHT**, van Polen EJ, Jansen YJL, Hulsewé KWE, Vissers YLJ, de Loos ER. Dutch translation, cultural adaptation and linguistic validation of the pectus excavatum evaluation questionnaire. *J Thorac Dis* 2022;14:2556-64.

Laven IEWG, Franssen AJPM, van Dijk DPJ, **Daemen JHT**, Gronenschild MHM, Hulsewé KWE, Vissers YLJ, de Loos ER. A no-chest drain policy after VATS wedge resection in selected patients: our 12-year experience. *Ann Thorac Surg* 2022.

Rochus I, **Daemen JHT**, van Vugt R, Hulsewé KWE, Vissers YLJ, de Loos ER. Delayed presentation of manubriosternal dislocation after thoracolumbal spondylodesis in a polytrauma patient – a case report. *Acta Chir Belg* 2022.

Willems S, **Daemen JHT**, Hulsewé KWE, Belgers EHJ, Sosef MN, Soufidi K, Vissers YLJ, de Loos ER. Outcomes after hybrid minimally invasive treatment of Boerhaave syndrome: a single-institution experience. *Acta Chir Belg* 2022.

Janssen N, Laven IEWG, **Daemen JHT**, Hulsewé KWE, Vissers YLJ, de Loos ER. Negative pressure wound therapy for massive subcutaneous emphysema: a systematic review and case series. *J Thorac Dis* 2022;14:43-53.

Heuts S, Adriaans BP, Kawczynski MJ, **Daemen JHT**, Natour E, Lorusso R, Schalla S, Maessen JG, Wildberger JE, Jacobs MJ, Rylski B, Bidar E. Extending aortic replacement beyond the proximal arch in acute type A aortic dissection: a meta-analysis of short-term outcomes and long-term actuarial survival. *Eur J Vasc Endovasc Surg* 2021;63:674-87.

Laven IEWG, **Daemen JHT**, Janssen N, Gronenschild MHM, Hulsewé KWE, Vissers YLJ de Loos ER. Risk of a pneumothorax requiring pleural drainage after drainless VATS pulmonary wedge resection: a systematic review and meta-analysis. *Innovations (Phila)* 2021;17:14-24.

Geraedts TCM, **Daemen JHT**, Visser YLJ, Hulsewé KWE, Van Veer HGL, Abramson H, de Loos ER. Minimally invasive repair of pectus carinatum by the Abramson method: a systematic review of six studies. *J Ped Surg* 2022;57:325-32.

Daemen JHT, Vissers YLJ, Hulsewé KWE, de Loos ER. Editorial commentary: A journey towards least invasive thoracic surgery? *Transl Lung Cancer Res* 2021;10:4027-8.

Heuts S, Denessen EJS, **Daemen JHT**, Vroemen WHM, Sels JW, Segers P, van 't Hof AWJ, Maessen JG, van der Horst ICC, Mingels AMA. Meta-analysis evaluating high-sensitivity troponin T kinetics after coronary artery bypass grafting in relation to the current definitions on myocardial infarction. *Am J Card* 2021;163:25-31.

Geraedts TCM, **Daemen JHT**, Vissers YLJ, de Loos ER. VATS-assisted surgical rib fixation for costochondral separation injury. *Innovations (Phila)* 2021;16:568-70.

Lozekoot PWJ[†], **Daemen JHT**[†], van den Broek RAM, Maessen JG, Gronenschild MHM, Vissers YLJ, Hulsewé KWE, de Loos ER. Surgical mediastinal lymph node staging for non-small-cell lung carcinoma. *Transl Lung Cancer Res* 2021;10:3645-58.

[†] *Equal contribution status.*

de Loos ER, **Daemen JHT**, Coorens NA, Maessen JG, Vissers YLJ, Hulsewé KWE. Sternal elevation by the crane technique during pectus excavatum repair: a quantitative analysis. *JTCVS Techniques* 2021;9:167-75.

Coorens NA[†], **Daemen JHT**[†], Slump CH, Loonen TGJ, Vissers YLJ, Hulsewé KWE, de Loos ER. The automatic quantification of morphological features of pectus excavatum based on three-dimensional images. *Semin Thorac Cardiovasc Surg* 2022;34:772-81.

[†] *Equal contribution status.*

de Loos ER, **Daemen JHT**, Janssen N, Hulsewé KWE, Vissers YLJ. Suture anchor repair of pectoralis major muscle dehiscence after modified Ravitch. *Innovations (Phila)* 2021;16:485-7.

Olsthoorn JR, **Daemen JHT**, de Loos ER, ter Woorst JF, van Straten AHM, Maessen JG, Sardari Nia P, Heuts S. A minimally invasive approach versus full sternotomy for resection of benign atrial masses: a systematic review and meta-analysis of observational studies. *Innovations (Phila)* 2021;16:426-33.

de Loos ER, Andel PCM, **Daemen JHT**, Maessen JG, Hulsewé KWE, Vissers YLJ. Safety and feasibility of rigid fixation by SternaLock Blu plates during the modified Ravitch procedure: a pilot study. *J Thorac Dis* 2021;13:2952-8.

Ji Y, Zhang T, Yang L, Wang X, Qi L, Tan F, **Daemen JHT**, de Loos ER, Qiu B, Gao S. The effectiveness of three-dimensional reconstruction in the localization of multiple nodules in lung specimens: a prospective cohort study. *Transl Lung Cancer Res* 2021;10:1474-83.

Bakens MJAM, Andel PCM, **Daemen JHT**, Hulsewé KWE, Vissers YLJ, de Loos ER. A case series: xiphoidectomy for xiphodynia, a rare thoracic wall disorder. *J Thorac Dis* 2021;13:2216-23.

de Loos ER[†], **Daemen JHT**[†], Pennings AJ, Heuts S, Maessen JG, Hulsewé KWE, Vissers YLJ. Minimally invasive repair of pectus excavatum by the Nuss procedure: The learning curve. *J Thorac Cardiovasc Surg* 2020;163:828-37.

[†]*Equal contribution status.*

de Loos ER, Pennings AJ, van Roozendaal LM, **Daemen JHT**, van Gool MH, Lenderink T, van Horck M, Hulsewé KWE, Vissers YLJ. Nuss procedure for pectus excavatum: a comparison of complications between young and adult patients. *Ann Thorac Surg* 2021;112:905-11.

Daemen JHT[†], de Loos ER[†], Vissers YLJ, Bakens M, Maessen JG, Hulsewé KWE. Intercostal nerve cryoablation versus thoracic epidural for postoperative analgesia following pectus excavatum repair: a systematic review and meta-analysis. *Interact Cardiovasc Thorac Surg* 2020;31:486-98.

[†]*Equal contribution status.*

Daemen JHT, van den Broek RAM, Lozekoot PWJ, Maessen JG, Hulsewé KWE, Vissers YLJ, de Loos ER. The learning curve of video-assisted mediastinoscopic lymphadenectomy for staging of non-small-cell lung carcinoma. *Interact Cardiovasc Thorac Surg* 2020;31:527-35.

Sardari Nia P, Heuts S, **Daemen JHT**, Olsthoorn JR, Chitwood WR, Maessen JG. The EACTS simulation-based training course for endoscopic mitral valve repair: an air-pilot training concept in action. *Interact Cardiovasc Thorac Surg* 2020;30:691-8.

Daemen JHT, Lozekoot PWJ, Maessen JG, Gronenschild MHM, Bootsma GP, Hulsewé KWE, Vissers YLJ, de Loos ER. Chest tube drainage versus video-assisted thoracoscopic surgery for a first episode of primary spontaneous pneumothorax: a systematic review and meta-analysis. *Eur J Cardiothorac Surg* 2019;56:819-29.

Daemen JHT, Deden LN, van den Ende A, Pijl MEJ, Slump CH, Berends FJ, Aarts EO. A novel abdominal wall entry suction device to increase Veress needle safety: A prospective cohort pilot study. *Ann Med Surg (Lond)* 2019;47:70-4.

Daemen JHT, Heuts S, Olsthoorn JR, Maessen JG, Sardari Nia P. Mitral valve modelling and three-dimensional printing for planning and simulation of mitral valve repair. *Eur J Cardiothorac Surg* 2019;55:543-51.

Sardari Nia P, **Daemen JHT**, Maessen JG. Development of a high-fidelity minimally invasive mitral valve surgery simulator. *J Thorac Cardiovasc Surg* 2019;157:1567-74.

Daemen JHT, Heuts S, Olsthoorn JR, Maessen JG, Sardari Nia P. Right minithoracotomy versus median sternotomy for reoperative mitral valve surgery: a systematic review and meta-analysis of observational studies. *Eur J Cardiothorac Surg* 2018;54:817-25.

Heuts S, **Daemen JHT**, Streukens SAF, Olsthoorn JR, Vainer J, Cheriex EC, Maessen JG, Sardari Nia P. Preoperative Planning of Transapical Beating Heart Mitral Valve Repair for Safe Adaptation in Clinical Practice. *Innovations (Phila)* 2018;13:200-6.

Sardari Nia P, Heuts S, **Daemen J**, Luyten P, Vainer J, Hoorntje J, Cheriex E, Maessen JG. Preoperative planning with three-dimensional reconstruction of patient's anatomy, rapid prototyping and simulation for endoscopic mitral valve repair. *Interact Cardiovasc Thorac Surg* 2017;24:163-8.

Peer-reviewed (non-PubMed/EMBASE-indexed)

Daemen JHT, Hulsewé KWE, Vissers YLJ, de Loos ER. Uniportal VATS right apical segmentectomy (S1): a case report and the surgical technique. *J Vis Surg* 2021;8.